

Angefertigt am
Institut für Medizinische Virologie
Nationales Referenzzentrum für Hepatitis-B- und D-Viren
der Justus-Liebig-Universität Gießen

Influence of Hepatitis B Virus Surface Protein Variants Associated with Antiviral Resistance on Viral Assembly and Secretion of Hepatitis B and Hepatitis D Viruses

Einfluss von Hepatitis B Virus Oberflächenproteinvarianten, die assoziiert sind mit antiviraler Resistenz, auf das virale Assembly und die Sekretion von Hepatitis B und Hepatitis D Viren

Inauguraldissertation
zur Erlangung des akademischen Grades
d o c t o r r e r u m n a t u r a l i u m
(Dr. rer. nat.)
des Fachbereiches 08-Biologie und Chemie
der Justus-Liebig Universität Gießen

vorgelegt von
Christina Mohr MSc.-Biol.

Gießen 2014

Dekan: **Prof. Dr. Holger Zorn**

Gutachter: **Prof. Dr. Michael Martin**
PD Dr. Dieter Glebe

Pour tous les petits héros,
qu'ils attendent dans l'ombre le retour du soleil

Zaz; Recto Verso, 2013

Für all die kleinen Helden,
die im Schatten darauf warten in die Sonne zurück zu kehren

Index

LIST OF ABBREVIATIONS	I
ABSTRACT	IV
ZUSAMMENFASSUNG	V
1. INTRODUCTION	1
1.1. Viral Hepatitis	1
1.1.1. Infection with the Hepatitis B Virus (HBV).....	1
1.1.2. HBV/HDV Co- and Super-Infection	1
1.1.3. Seroepidemiology and Transmission of the Hepatitis B and D Virus	2
1.1.4. Prevention of an HBV- and HDV-Infection.....	3
1.1.5. Therapy of Chronic HBV and HDV-Infection	3
1.2. Hepatitis B Virus (HBV)	4
1.2.1. Classification	4
1.2.2. Viral Properties.....	5
1.2.2.1. Morphology and Structure.....	5
1.2.2.2. Genomic Structure and Organization	6
1.2.2.3. Viral Surface Proteins.....	8
1.2.3. Viral Life Cycle and Replication.....	10
1.3. Hepatitis Delta Virus (HDV)	12
1.3.1. Classification	12
1.3.2. Morphology and Genomic Structure	13
1.3.3. Viral Life Cycle.....	14
1.4. Model Systems for HBV and HDV	16
1.5. Aim of the Work	18
2. MATERIALS AND METHODS	19
2.1. Materials	19
2.1.1. Antibiotics	19
2.1.2. Antibodies and Nuclear Staining.....	19
2.1.2.1. Primary Antibodies.....	19
2.1.2.2. Secondary Antibodies.....	19
2.1.2.3. Nuclear Staining	20
2.1.3. Peptide	20
2.1.4. Antivirals	20
2.1.5. Buffer, Media and Solutions.....	20
2.1.5.1. Buffers	20
2.1.5.2. Media.....	21

2.1.5.3. Solutions.....	22
2.1.6. Commercial Kits, Enzymes and Competent Bacteria	22
2.1.7. Cell Lines	23
2.1.8. Viruses Derived from Serum/Plasma of Chronically Infected Individuals	24
2.1.9. Plasmids.....	24
2.1.9.1. Standard Plasmids	24
2.1.9.2. HBV-Expression Plasmids for HBV Phenotypic Assay	24
2.1.9.3. Plasmids for Analyzing HBV Variants Harboring Stopmutants within the S-ORF....	25
2.1.9.4. Plasmids Encoding HBV Surface Proteins for Generating Recombinant HDV in Cell Culture	25
2.1.10. PCR, Primer, Probes and Mastermixes	25
2.1.10.1. Primer and TaqMan Probes for Quantitative Polymerase Chain Reaction (qPCR) ..	25
2.1.10.2. Primer for Generating an HDV-RNA Standard	26
2.1.10.3. Sequencing Primer for HDV-RNA-Standard.....	26
2.1.10.4. Mastermixes for Hot Start and Gradient PCR.....	26
2.1.10.5. qPCR Mastermixes.....	26
2.1.11. Equipment, Consumable Supplies and Software.....	27
2.2. Methods.....	29
2.2.1. Preparation of an RNA-Standard <i>in vitro</i> for HDV qPCR	29
2.2.1.1. Amplification of one HDV Genome out of the Plasmid pSVLD3.....	29
2.2.1.2. Isolation and Purification of the PCR Templates	29
2.2.1.3. Synthesis of RNA <i>in vitro</i> and Phenol/Chloroform Extraction	30
2.2.1.4. Formaldehyde Gel	31
2.2.1.5. Calculation of Genome Equivalent.....	31
2.2.2. Preparation of Competent Bacteria for Transformation ("chemical method").....	31
2.2.3. Transformation	32
2.2.3.1. Transformation of Plasmid-DNA into <i>E.coli</i>	32
2.2.3.2. Plasmid-Preparation with the Plasmid-Plus-Midi-Kit (Qiagen).....	32
2.2.4. Cultivation of Immortalized Cell Lines.....	32
2.2.4.1. Freezing and Thawing of Eukaryotic Cell Lines.....	32
2.2.4.2. Passaging of Immortalized Cell Lines.....	33
2.2.5. Phenotypic Resistance Assay for Characterization of Patient Isolates.....	33
2.2.5.1. Transfection.....	33
2.2.5.2. Phenotypic Assay	34
2.2.5.3. Calculation of Transfection-Efficiency by Secreted Alkaline Phosphatase- (SEAP)- Detection Assay.....	35
2.2.5.4. Statistical Analysis of the Data from Phenotypic Resistance Assay <i>in vitro</i>	35
2.2.6. Cell Viability Test with WST-1 (Roche).....	36
2.2.7. Isolation of Viral Genomes from Supernatant, Plasma or Cell Lysates	37
2.2.7.1. Isolation of Intracellular Viral RNA and DNA	37
2.2.7.2. Manual Isolation of Viral RNA and DNA in the Supernatant or in Serum.....	37
2.2.7.3. Automated isolation of viral DNA in the Supernatant with Freedom EVO.....	37
2.2.8. qPCR	38
2.2.8.1. SYBR-Green Based qPCR	38
2.2.8.2. TaqMan Probe Based qPCRs	38
2.2.9. Preparation of a Sucrose Gradient for Isolation and Purification of HBV and HDV.....	39
2.2.10. Preparation of a Linear Caesium-Chloride (CsCl)-Gradient	40
2.2.11. Isolation and Cultivation of Primary <i>Tupaia</i> Hepatocytes (PTHs)	40

2.2.12.	Infection of PTHs with HBV and HDV	41
2.2.13.	ELISA against Secreted HBV Surface Proteins	41
2.2.14.	UREA-Assay	42
2.2.15.	Staining for Immunofluorescence	42
3.	RESULTS.....	43
3.1.	Phenotypic Characterization of Isolates from Chronically Infected HBV-Patients.....	43
3.2.	Characterization of Known HBsAg-Mutations During Antiviral Therapy of Chronic Hepatitis B.....	45
3.2.1.	Secretion of Enveloped Virions and Subviral Particles.....	45
3.2.2.	Immunohistochemical Analysis of HBV Surface Protein Variants	48
3.2.3.	Comparison of Sedimentation Behavior for Purified HBV with Cell Culture Derived HBV in the CsCl-Gradient.....	53
3.2.4.	Analysis of a LHBs Deficient HBV Mutant Using the CsCl-Gradient	54
3.2.5.	Analysis of HBV Variants with Mutations at Position 172 into the SHBs Using the CsCl-Gradient	55
3.2.6.	Analysis of HBV Variants with Mutations at Position 196 into the SHBs Using the CsCl-Gradient	56
3.3.	Establishment of a Transfection and Infection System for HDV Pseudo-Particles	57
3.3.1.	Production and Establishment of an HDV RNA-standard for RT-qPCR.....	57
3.4.	Characterization of HDV from Human Plasma	60
3.4.1.	Characterization of HDV Derived from Human Plasma in a Linear CsCl-Gradient	60
3.4.2.	Purification of Plasma-Derived HDV with a Continuous Sucrose Gradient.....	60
3.4.3.	Infection of PTHs with Purified HDV Derived from Human Plasma.....	61
3.4.4.	Analysis of the Kinetic of Infectivity for HBV and HDV on PTH	62
3.4.5.	HBV/HDV Co- and Super-Infection of PTH	63
3.5.	Characterization of Recombinant HDV Pseudo-Particles from Cell Culture	65
3.5.1.	Production of HDV Pseudo-Particles in Cell Culture with Different Variants of HBV Surface Proteins	65
3.5.2.	Infection of PTHs with Recombinant HDV Pseudo-Particles.....	66
3.5.3.	Neutralization of Infection of Cell Culture-Derived and Plasma-Derived HDV Using Monoclonal Antibodies	67
3.6.	Production of Recombinant HDV with Mutations in the HBV Surface Proteins	68
4.	DISCUSSION.....	69
4.1.	Phenotypic Resistance Profile of Special Patient Isolates During Antiviral Therapy.....	69
4.2.	Influence of Mutations within the HBV S-ORF that Arise During Antiviral Therapy on the Viral Life Cycle of HBV	71
4.3.	Establishment of an RNA Standard for HDV RT-qPCR	76

4.4. Characterization of HDV Derived from Human Plasma of a Chronically Infected Patient.....	77
4.5. Infection of PTH with Purified HDV	77
4.6. Production and Detection of Recombinant HDV Enveloped with Different Combinations of HBsAg	79
4.7. Infection of PTH with Recombinant HDV in Comparison with Purified HDV	81
4.8. Influence of Mutations within the HBV S-ORF that Arise During Antiviral Therapy on the Viral Life Cycle of the Hepatitis D Virus.....	82
5. PERSPECTIVES	85
6. REFERENCES	86
7. LIST OF OF FIGURES	102
8. LIST OF TABLES.....	103
9. APPENDIX.....	104
10. PUBLICATIONS.....	113
11. DANKSAGUNG	114
12. ERKLÄRUNG	115

List of abbreviations

A		EtOH	ethanol
aa	amino acid	ETV	entecavir
ADAR-1	double-stranded RNA specific adenosine deaminase acting on RNA-1	F	
ADV	adefovir	f.c.	final concentration
ANOVA	analysis of variants	FCS	fetal calf serum
B		G	
bp	base pair	g	gram
C		GE	genome equivalent
°C	celsius	GRE	glucocorticoid-responsive element
cDNA	complementary DNA	H	
cccDNA	covalently closed circular DNA	h	hours
CsCl	cesium chloride	HBcAg	hepatitis B virus core antigen
C-terminus	carboxy terminus	HBeAg	hepatitis B e antigen
D		HBsAg	hepatitis B surface antigen
Da	Dalton	HBSS	Hank`s balanced salt solution
DHBV	duck hepatitis B virus	HBx	hepatitis B X protein
DMEM	Dulbecco`s Modified Eagle Medium	HBV	hepatitis B virus
DMSO	dimethyl sulfoxide	HCC	hepatocellular carcinoma
DNA	Deoxyribonucleic acid	HDV	Hepatitis Delta virus
DR1/2	direct repeats	HDAg	Hepatitis Delta antigen
ds DNA	double stranded DNA	hsp	heat-shock-protein
E		HSPGs	heparan-sulfate proteoglycans
<i>E.coli</i>	<i>Escherichia coli</i>	I	
EDTA	ethylenediaminetetraacetic acid	IC	inhibitory concentration
EGTA	ethylene glycol tetraacetic acid	IFN- α	interferon- α
ELISA	enzyme linked immunosorbent assay	L	
ER	endoplasmic reticulum	l	litre
EtBr	ethidium bromide	LB-medium	lysogeny broth medium
		LHBs	large hepatitis B virus surface antigen

List of abbreviations

L-HDAg	large hepatitis Delta virus antigen	PEG	polyethylene glycol
LMV	lamivudine	PFA	paraform aldehyde
		pgRNA	pregenomicRNA
M		PHH	primary human hepatocytes
μ	micro	p.i.	post infection
μl	micro litre	pol	polymerase
m	milli/meter	PRE	posttranscriptional regulation element
M	molar	PTHs	primary <i>Tupaia</i> hepatocytes
mABs	monoclonal antibodies		
MHBs	middle hepatitis B Virus antigen	Q	
min	minute	qPCR	quantitative PCR
mg	milligram		
ml	millilitre	R	
mRNA	messenger RNA	RF	resistance factor
MVB	multivesicular bodies	rcDNA	relaxed circular DNA
MxA-protein	human myxovirus resistance protein 1	RNA	ribonucleic acid
		RNP	ribonucleoprotein
N		rpm	revolutions per minute
NES	nuclear export signal	RT	reverse transcription
NLS	nuclear localization sequence	RT-qPCR	reverse transcription quantitative polymerase chain reaction
NP40	nonident P-40		
NPC	nuclear pore complex	S	
NRE	negative regulating element	SD	standard deviation
nt	nucleotide	SEAP	secreted alkaline phosphatase
NTCP	sodium taurocholate co- transporting polypeptide	SHBs	small hepatitis B virus surface antigen
N-terminus	amino-terminus	S-HDAg	small hepatitis Delta antigen
		ssRNA	single-stranded RNA
O		SV40	simian virus 40
OD	optical density		
ORF	open reading frame	T	
		TAE	Tris-acetate EDTA
P		TDV	tenofovir
PBS	phosphate buffered saline	TFB	transforming buffer
PCH	primary chimpanzee hepatocytes	TNE	Tris-Natrium(sodium)-ETDA
PCR	polymerase chain reaction		

V

v/v volume per volume

W

WHO world health organization

WHV woodchuck hepatitis B virus

WMHBV woolley monkey hepatitis B virus

WST water soluble tetrazolium salt

w/w weight per weight

Abstract

The viral hepatitis is one of the five most important infectious diseases worldwide and is caused by the hepatitis B virus (HBV). The development of a chronic HBV infection raises the risk to generate liver fibrosis, cirrhosis, and hepatocellular carcinoma. Two different therapy-concepts to treat a chronic HBV infection are used: the treatment with IFN- α and the therapy with nucleos(t)ide analogs. Due to the high variability of the HBV genome and the missing proofreading function of the viral polymerase, several drug-resistant mutants arise during the long term treatment with nucleos(t)ide analogs in chronically infected patients. Because of the strong overlapping open reading structure of the HBV genome, mutations in the viral polymerase also affect the genes of the other viral proteins especially the gene for the HBV surface proteins.

In the present work, a series of HBV surface protein variants were generated that can arise during the treatment with nucleos(t)ide analogs, bearing a stop mutation in the internal loop of the small hepatitis B surface antigen (SHBs) (sW172*, L176*, W182*, sW199*, W196*, L216*). These HBV variants show a strongly reduced secretion of HBV virions. The stop mutations in the SHBs of HBV probably lead to the loss of the internal loop between transmembrane domain III and IV resulting in a truncated SHBs variant. Surprisingly, a stop mutation at position 172 in the SHBs did not fully inhibit the secretion of HBV particles.

Mutations in the HBV surface proteins can also have strong consequences for the satellite virus of HBV: the hepatitis delta virus (HDV). This virus is dependent on the surface proteins of its helper virus HBV for virion assembly, secretion, and infectivity. The antiviral treatment with nucleos(t)ide analogs may have consequences for the clinical prognosis and treatment of a patient chronically infected with HBV as well as for HBV/HDV co-infected patients. For analyzing the implications of HBV surface protein mutations on the viral life cycle of HDV in the future, an *in vitro* transfection system to generate recombinant HDV pseudo-particles in the hepatoma cell line Huh7 was established. With the help of these recombinant HDV-like particles, an infection system on primary hepatocytes, derived from the asian treeshrew *Tupaia belangeri* was then established. In this context, a full genomic HDV RNA standard was generated *in vitro* to be able to quantify the newly synthesized HDV RNA absolutely. The production of HDV pseudo-particles in Huh7 cells could show that the SHBs is crucial for the viral assembly and secretion, whereas the large hepatitis B virus surface antigen (LHBs) is required for a successful infection of primary *Tupaia* hepatocytes. Using these methods, HDV pseudo-particles were generated, covered with HBV surface protein variants possessing characteristic mutations in the SHBs (sW172*, sW172L, sW196*, sW196S, sW196L) that can arise during antiviral therapy. The present study could show that a stop mutation at position 172 and 196 as well as an amino acid change from tryptophan to serine or leucine at position 196 in the SHBs blocks the viral assembly and secretion of HDV pseudo-particles.

Zusammenfassung

Die virale Hepatitis ist eine der fünf wichtigsten Infektionskrankheiten weltweit und wird verursacht durch das Hepatitis B Virus. Die Entwicklung einer chronischen HBV Infektion erhöht das Risiko, Leberfibrose, -zirrhose oder ein hepatozelluläres Karzinom zu bilden. Zwei unterschiedliche Therapiekonzepte werden verwendet, um eine chronische HBV Infektion zu therapieren: die Behandlung mit IFN- α und die Therapie mit Nucleos(t)id Analoga. Auf Grund der hohen Variabilität des HBV Genoms und der fehlenden Korrekturlesefunktion der viralen Polymerase, entstehen während der antiviralen Langzeittherapie mit Nucleos(t)id Analoga von chronisch HBV-infizierten Patienten verschiedene Medikamenten-resistente Mutanten. Durch die stark überlappende Struktur der offenen Leserahmen des HBV Genoms, beeinträchtigen Mutationen in der viralen Polymerase auch die Gene der anderen viralen Proteine, vor allem das Gen, welches für die HBV Oberflächenproteine kodiert.

In dieser Arbeit wurden eine Reihe von HBV Oberflächenproteinvarianten generiert, die charakteristisch während einer antiviralen Behandlung mit Nucleos(t)id Analoga auftreten können, welche eine Stoppmutation in der internen Schleife des kleinen Hepatitis B Virus Oberflächenproteins (SHBs) (sW172*, L176*, W182*, sW199*, W196*, L216*) besitzen. Diese HBV Varianten weisen eine stark reduzierte Sekretion von HBV Virionen auf. Die Stoppmutationen im SHBs von HBV führen vermutlich zu einem Verlust der internen Schleife zwischen der Transmembrandomäne III und IV, was in einer trunkeierten SHBs Variante resultiert. Überraschenderweise führt eine Stoppmutation an der Position 172 im SHBs nicht zur vollständigen Inhibition der Sekretion von HBV Partikeln.

Mutationen in den HBV Oberflächenproteinen können auch Konsequenzen für das Satellitenvirus von HBV haben: das Hepatitis Delta Virus (HDV). Dieses Virus ist abhängig von den Oberflächenproteinen seines Helfervirus HBV für dessen Zusammenbau, Sekretion und dessen Infektiosität. Die antivirale Therapie mit Nucleos(t)id Analoga kann Auswirkungen auf die klinische Prognose und die Behandlung von chronisch HBV-infizierten ebenso wie für HBV/HDV-koinfizierte Patienten haben. Um zukünftig die Auswirkungen von Mutationen in den HBV Oberflächenproteinen auf den viralen Lebenszyklus von HDV untersuchen zu können, wurde ein *in vitro* Transfektionssystem etabliert, um rekombinante HDV pseudo-Partikel in der Hepatomzelllinie Huh7 zu generieren. Mit der Hilfe dieser rekombinanten HDV ähnlichen-Partikel wurde dann ein Infektionssystem in primären Hepatozyten des asiatischen Spitzhörnchens *Tupaia belangeri* etabliert. In diesem Zusammenhang wurde ein voll-genomischer HDV-Standard *in vitro* generiert, um neu synthetisierte RNA absolut quantifizieren zu können. Die Generierung von HDV Pseudo-Partikeln in Huh7 Zellen hat gezeigt, dass das SHBs wichtig für das virale Assembly und die Sekretion ist, während das große Hepatitis B Virus Oberflächenantigen (LHBs) nötig ist, um primäre *Tupaia* Hepatozyten erfolgreich infizieren zu können. Mit Hilfe dieser Methoden wurden HDV Pseudo-Partikel generiert, die mit HBV Oberflächenproteinvarianten umhüllt wurden, welche charakteristische Mutationen im SHBs (sW172*, sW172L, sW196*, sW196S, sW196L) aufwiesen, die während einer antiviralen Therapie auftreten können. Die Untersuchungen haben gezeigt, dass eine Stoppmutation an der Position 172 und 196, ebenso wie ein Aminosäureaustausch von Tryptophan zu Serin oder Leucin an der Stelle 196 im SHBs das virale Assembly und die Sekretion von HDV Pseudo-Partikeln inhibiert.

1. Introduction

1.1. Viral Hepatitis

1.1.1. Infection with the Hepatitis B Virus (HBV)

Viral hepatitis is an inflammation of the liver and often caused by the infection with the hepatitis B virus (HBV). The course of infection is variable and depends on the dose of infection, the fitness of the virus, as well as the immune status, the gender, and age of the infected individual. Three stages of an HBV infection are known: acute, chronic and fulminant hepatitis B. Normally, if adults with a competent immune system are infected with a low dose, in 95 % of all cases, this leads to the elimination of the virus by the immune system and results in immunity. After inoculation of an immune competent individual with a high dose of HBV, this can result in an acute hepatitis B, which is characterized by flu-like symptoms, tiredness, abdominal pain, and jaundice (visible as yellowing of the eyes). Normally, the acute hepatitis heals after several weeks and patients recover and develop immunity. However, a severe course of the infection is the fulminant hepatitis which occurs in < 1 % of the infections. If untreated, fulminant hepatitis leads to death within a few days due to fatal liver failure. The establishment of a chronic infection with hepatitis B depends on the age of the infected person and is a major problem in high endemic regions. Newborns are often infected during childbirth, if the chronically HBV-infected mother harbours high titers of HBV. In 90 % of these cases, the infection results in chronic hepatitis B (Ganem and Prince 2004) leading to a higher risk to develop liver fibrosis and cirrhosis within 10-20 years. If untreated, this chronic viral infection may lead to the development of hepatocellular carcinoma (Beasley et al. 1981) that can result in death.

1.1.2. HBV/HDV Co- and Super-Infection

Hepatitis B virus surface proteins are essential for the assembly and release of HDV virions, therefore an HDV infection is always associated with an HBV infection (Chang et al. 1991; Jenna and Sureau 1998, 1999; Komla-Soukha and Sureau 2006). The course of the HDV infection also depends on the genotype, also called "clade", of the infecting virus. HDV clade-1 is the most common genotype worldwide and is associated with a wide spectrum of severe hepatitis (Niro et al. 1997). Clades 2 and 4 are known to induce milder forms of hepatitis (Wu 2006; Su et al. 2006), whereas for example HDV clade 3 is strongly associated with severe and fulminant hepatitis (Casey et al. 1993; Manock et al. 2000; Gomes-Gouvêa et al. 2009). Two infection patterns occur for HBV and HDV infection: the HBV/HDV co-infection and HBV/HDV super-infection.

A simultaneous infection of a healthy individual with HBV and HDV is called a "co-infection" resulting in an acute hepatitis B and hepatitis D (reviewed in Farci 2003). The acute co-infection cannot be distinguished clinically from an ordinary acute hepatitis B, although it can lead to a stronger

form of acute hepatitis B mono-infection. In more than 90 % of these cases the acute HBV/HDV co-infection leads to subsequent clearance and immunity of HDV, as already described for HBV (reviewed in Pascarella and Negro 2011).

The HBV/HDV super-infection describes the additional HDV infection of a patient already chronically infected with HBV. In contrast to the co-infection, this way of infection induces a stronger form of acute hepatitis. In up to 80 % of all cases, this infection pattern leads to the HDV-chronicity (Smedile et al. 1981, 1982). Once a chronic HDV infection is established, it can be observed that HDV suppresses HBV replication to low levels *in vivo* (Sagnelli et al. 2000; Heidrich et al. 2009). To do so, the hepatitis Delta antigens (HDAg) S-HDAg and L-HDAg (s = small and l = large isoform) interact with the interferon-inducible MxA-protein leading to a repression of the HBV enhancer activity. Thus the nuclear export of viral mRNA is prevented (Gordien et al. 2001, Williams et al. 2009). Liver diseases like liver cirrhosis (Rizzetto et al. 1983) and fibrosis (Fattovich et al. 1987) progress much faster in patients who are chronically infected with HDV than in patients who are infected with HBV, only (Fattovich et al. 2000, Taylor 2006). The prevalence to develop hepatocellular carcinoma in HBV/HDV super-infected patients remains a subject of controversial debates (Cross et al. 2008; Romeo et al. 2009).

1.1.3. Seroepidemiology and Transmission of the Hepatitis B and D Virus

Viral hepatitis is still a global health problem, although there is a safe and effective vaccine available since 1982 (Lavanchy 2004, 2005). According to the World Health Organization (WHO) two billion people show signs of past or present HBV infection (anti-HBc) including more than 240 million people as chronic carriers. Every year an estimated number of 600.000 people die because of the sequelae of an acute or chronic hepatitis B infection. This is why hepatitis B is one of the five most important infectious diseases worldwide (WHO 2013). Approximately 5 % of the global HBV-carriers are co-infected with HDV, leading to a total of 12 million HDV-carriers worldwide (Farci 2003a). The occurrence of HBV and HDV infection vary greatly throughout the world. High endemic regions for chronic HBV infections are, in particular, Third World regions such as parts of Africa and Asia, whereas Europe and North America have a low prevalence (reviewed in Lavanchy 2005). Similar to HBV, the different HDV-clades are distributed all over the world and are highly endemic to several African countries (Sub-Saharan region), the Amazonian region (Amazon basin), and in the Middle East. In industrialized countries, HDV was found preferentially in the Mediterranean region, for example Turkey and Italy (reviewed in Pascarella and Negro 2011). In high endemic areas with the risk of repeated exposure, multiple infections with several HDV-clades can occur (Wu et al. 1999). Since HDV particles are enveloped by the viral surface proteins of HBV, the transmission of HDV is related to that of HBV. In Europe and North America, HBV is transmitted via sexual contact, blood, or

blood products (parental). The most prominent infection pathway in Asia is from mother to child during childbirth (perinatal) (reviewed in Lavanchy 2005).

1.1.4. Prevention of an HBV and HDV Infection

The hepatitis B vaccination is an effective means against HBV infection. Due to the close link between HBV and HDV, HBV vaccination also prevents an HDV infection. The only components of the recombinant HBV vaccine are subviral particles, composed of the small hepatitis B surface proteins (SHBs) (genotype A) derived from recombinant yeast (Peterson et al. 1984; Szmuness et al. 1980). A proper immune response after successful vaccination results in neutralization of HBV *in vivo* and *in vitro* and protects against infection, but fails to protect against naturally occurring vaccine induced-escape mutants (Carman et al. 1990), and against mutants that can arise during antiviral therapy (Kamili et al. 2009). To avoid this problem, the preS1-domain of HBV should be additionally included.

1.1.5. Therapy of Chronic HBV and HDV Infection

In spite of the fact that there is a vaccine available, more than 240 million people are chronically infected with HBV (WHO 2013). They bear a high risk to develop liver cirrhosis and hepatocellular carcinoma (HCC) (Ganem and Prince 2004, Dienstag 2008). The antiviral treatment using interferon or nucleos(t)ide analogs is used to prevent these long-term effects and to bring the viral replication efficiently to the lowest level. One possibility for the treatment of HBV or HDV infection is the application of interferon- α (IFN- α). It stimulates the immune system and modulates the immune response against HBV and HDV (reviewed in Lavanchy 2004). Depending on the HBV genotype, 40 % of IFN- α treated hepatitis B patients can seroconvert to HBeAg negativity and in a limited number of cases, the treatment leads to a successful clearance of HBsAg (Korenman et al. 1991). However, the therapy with IFN- α implies a series of side effects (Perrillo et al. 1990; Pardo et al. 1995) but until today, it is the only antiviral therapy against chronic HDV infection available that promises healing.

The second treatment option is focused on the viral transcriptase. To this end nucleos(t)ide analogs are used to control the chronic HBV infection. The four common antiviral drugs, divided into nucleoside analogs (lamivudine and entecavir) and nucleotide analogs (tenofovir and adefovir), are derivatives of nucleotide triphosphates. They inhibit the HBV reverse transcriptase and therefore prevent viral replication and virion formation. The given nucleoside and nucleotide analogs are inactive precursors. They are taken orally. Within hepatocytes, they are converted into their activated forms by cellular kinases. Together with the naturally occurring nucleotide triphosphates, the active forms of the

nucleos(t)ide analogs are incorporated into the viral DNA during the reverse transcription process, leading to its premature termination. The treatment with nucleos(t)ide analogs has less side effects than the treatment with IFN- α , but during the antiviral therapy HBV resistance mutants often occur, leading to an antiviral breakthrough that represents a problem in antiviral treatment (Gish 2009, Dienstag 2009).

The hepatitis B virus is genetically relatively stable, but may develop at some gene regions high variability depending on the selective pressures, similar to HIV or several RNA viruses. The high adaptability results from several different factors. One of them is the error-prone activity of the viral polymerase that results in a high nucleotide-substitution rate during replication. Promoted by the fact that HBsAg-positive carriers exhibit high virus titers, various genetically different but closely related virus variants can occur in one patient. This mixture of different virus variants is named "quasi-species" and can additionally persist in the form of a mini-chromosome (this is the covalently closed circular (ccc)DNA form of the HBV genome) in infected liver cells. Due to the fact that this cccDNA within liver cells exhibits a long half-life period, several quasi-species can exist as "virological memory" in infected hepatocytes (Seeger and Mason 2000). If one of these variants has an essential mutation in one of the catalytic subdomains of the viral polymerase that is resistant against a used nucleos(t)ide analog, this mutation increases the selective advantage of this HBV variant and can promote the development of a full resistance to these antiviral inhibitors. Normally, the therapy with nucleos(t)ide analogs has proven to decrease the viral load of chronically infected HBV patients. But the treatment can exert a selective pressure and drug-resistant HBV mutants frequently arise during antiviral therapy leading to an antiviral breakthrough and resulting in treatment failure.

An additional promising antiviral approach could be the amino-terminal myristoylated peptide containing amino acid 2-48 of the preS1-domain of HBV (Glebe et al. 2005). It could be shown that this peptide is able to block the HBV-infection as well as HDV infection *in vitro*, effectively (Glebe et al. 2005, Gripon et al. 2005, Yan et al. 2012). At present, this inhibitor is being tested in clinical studies.

1.2. Hepatitis B Virus (HBV)

1.2.1. Classification

The hepatitis B virus, which belongs to the family of *Hepadnaviridae*, induces chronic and/or acute hepatitis (Feitelson et al 1986) and is characterized by a strong liver tropism and high host specificity. *Hepadnaviridae* replicate in differentiated liver cells only and show no cytopathogenicity (Chisari and Ferrari 1995). If they have entered their host cells, all *Hepadnaviridae* replicate via a reverse transcriptase and a pregenomic RNA (Summers and Mason 1982). A typical feature of the cells

infected with *Hepadnaviridae* is the synthesis and secretion of virions and a huge amount of subviral particles (Ganem 1991).

The mammalian hepatitis B virus is the prototype of the family of *Hepadnaviridae* (from hepa: liver; DNA: type of the genome) and belongs to the genus *Orthohepadnaviridae* (Robinson et al. 1984, King et al. 2012). *Orthohepadnaviridae* were discovered in humans (Dane et al. 1970) as well as in Old World primates, in New World primate as well as several rodents of the *Sciuridae* (squirrels) and in bats (Drexler et al. 2013). In addition to the *Orthohepadnaviridae*, some bird species serve as hosts, too. The avian viruses differ in their structure and because of that, they were separated into the genus of *Avihepadnaviridae*.

At present, nine mayor genotypes (A to I) were divided for human HBV, based on > 8 % nucleotide variation over the entire genome (Norder et al. 2004). Genotypes can be further distinguished in several subgenotypes (> 4 % nucleotide variation). The distribution of HBV genotypes over the world reflects the prevalent ethnical distribution (Bartholomeusz and Schaefer 2004) and the HBV genotype D is the most common genotype over the world.

1.2.2. Viral Properties

1.2.2.1. Morphology and Structure

HBV is an enveloped virus with a diameter of about 45 nm (Dane et al. 1970). In the negative contrast electron microscope, the virions appear as characteristic double-shelled particles (Figure 1). HBV is a DNA-virus with a partially double-stranded genome. The viral polymerase binds to the viral DNA as well as a protein kinase derived from the host cell. This complex is surrounded by the nucleocapsid (core protein, HBc) (32 nm-34 nm in diameter) (Almeida et al. 1971). The HBV core consists of 180 or 240 core protein subunits (HBc), which form dimers, which then again form an icosahedron with a T3 (180 subunits) or a T4 (240 subunits) symmetry (Crowther et al. 1994; Kenney et al. 1995). The core-capsid is enveloped by a lipid membrane, where three main types of surface proteins are embedded; the L(arge) (39 kDa, 42 kDa), the M(iddle) (31 kDa), and the S(mall) (24 kDa) HBV surface proteins. These three proteins form the hepatitis B virus surface antigen (HBsAg).

Compared to the amount of capsids, HBsAg is over-expressed (Ganem 1991; Gerlich et al. 2007) leading to the assembly of filamentous structures (variable length) and spheres (20 nm in diameter) which contain no viral DNA and therefore are not infectious. In serum of HBV infected patients, the subviral particles can be found in up to 1000-fold excess (Ganem 1991; Gerlich et al. 2007).

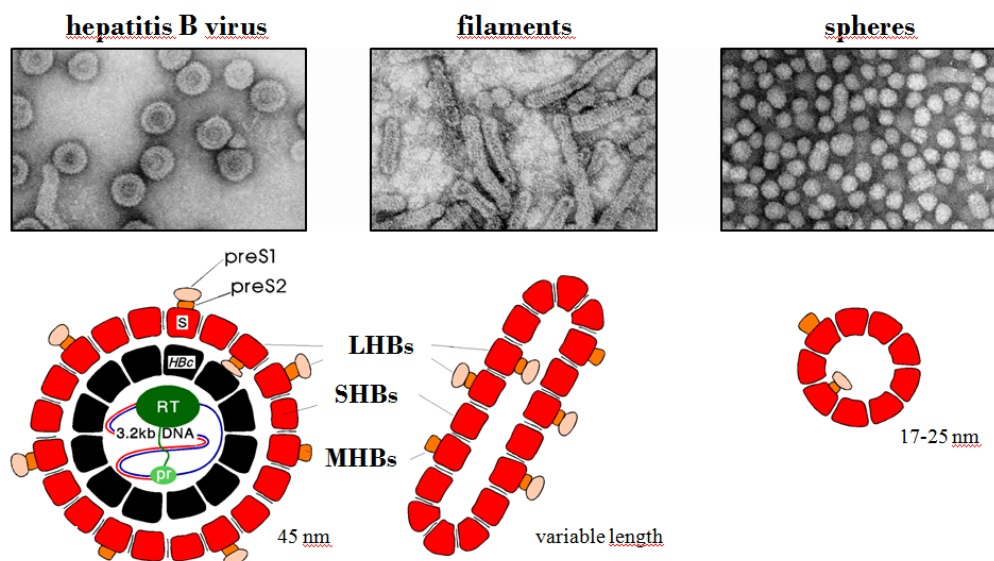


Figure 1: Structure of HBV and subviral particles. **A)** Negative contrasted electron microscopical picture of virions (left), filaments (middle), and spheres (right). **B)** Schematic model of virions and subviral particles. Virions (left) and subviral particles (middle and right) are covered with HBsAg consisting of s-domain (red), preS2-domain (orange) and preS1-domain (rose). Virions additionally include the viral core capsid (HBe, black) and viral polymerase (red and blue lines) linked to the reverse transcription (RT, dark green) and primer domain (pr, bright green). Modified after Gerlich 2013.

1.2.2.2. Genomic Structure and Organization

HBV is known to be one of the smallest mammalian DNA viruses. Despite the fact that the HBV DNA is small in genome-size, it is highly complex (Figure 2). The viral genome consists of a circular, partially double-stranded (ds) DNA exhibiting a plus and a negative strand. The longer, complete strand with negative polarity has a defined 5' and 3' end with a length of 3182-3248 nucleotides (nt), depending on the genotype (Summers et al. 1975). The ends of the negative strand are not closed and exhibit an overlength of 8-10 nt (terminal redundancy) to which the primer domain of the viral polymerase is covalently bound (Gerlich and Robinson 1980; Bartenschlager and Schaller 1988). The viral DNA has a small area with triplex formation in the region where the terminal redundancy of the minus strand is spanned by the plus strand (Will et al. 1987). The circular structure of the DNA is caused by base pairing between both strands. The complementary plus strand does not encode for viral proteins and is therefore not transcribed. The incomplete plus strand owns a defined 5' end and a variable 3' end (1100-2600 nt total length), depending on how far the viral polymerase can synthesize the plus strand before the virus is secreted (Hruska et al. 1977; Landers et al. 1977). Another characteristic of the viral genome are two direct repeats (DR1 and DR2) (Dejean et al. 1984) which have an important function during viral replication (Siddiqui et al. 1979; Will et al. 1987).

The negative strand encodes for four conserved, partially overlapping open reading frames (ORFs) (Schlicht and Schaller 1989) that differ in length (Tiollais et al. 1985) and encode for all viral proteins. Expression of mRNA encoding viral proteins is done by the alternative use of different start codons.

The ORFs encode for 1) HBV core protein (HBc) and its "soluble form" (HBe), 2) the viral polymerase including priming and spacer domain, reverse transcriptase- and RNase H-domain (80 % of the genome length), 3) the surface proteins (HBsAg) and the X-protein.

The expression of the ORFs is regulated by four promoters (core, preS1, preS2/2, X) and two enhancers, the glucocorticoid-responsive element (GRE) increasing transcription and a negative regulating element (NRE) that lowers the transcription from precore/core-promotor selectively (Tang et al. 2001). Liver- and differentiation-dependent factors bind to the enhancer, leading to a hepatocyte specific transcription and replication (reviewed in Glebe 2006). The termination of the transcription is accomplished by a polyadenylation signal, thus, every mRNA shares a common 3`end (Ganem and Varmus 1987). Additional regulatory elements at the messenger RNA (mRNA)-level are known, the posttranscriptional regulation element (PRE) that suppresses the splicing of transcribed viral RNAs and enables the transport of unspliced mRNAs into the cytoplasm (Huang and Liang 1993), or the encapsidation signal ϵ at the 5`end of the pregenomic RNA (Junker-Niepmann et al. 1990). In combination with the viral polymerase, the ϵ -signal is necessary for encapsidation of the virus (Hirsch et al. 1990, Bartenschlager and Schaller 1992)

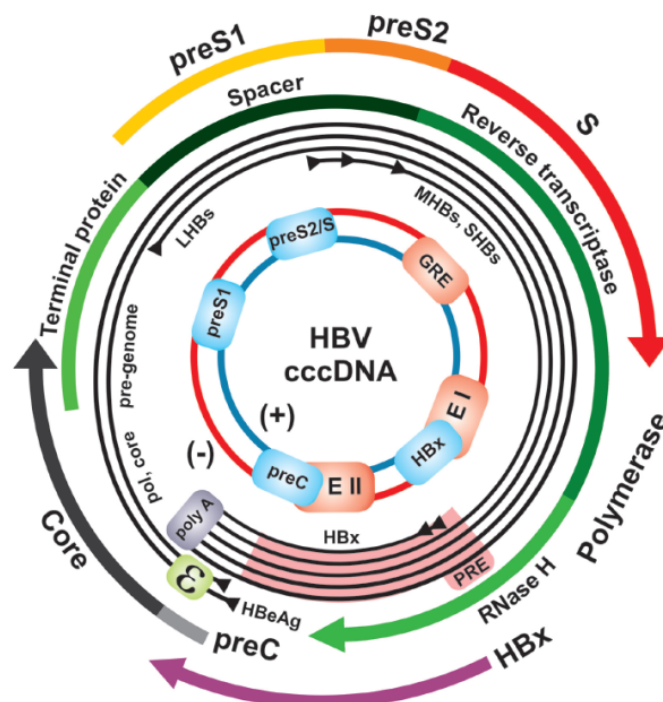


Figure 2: Genome structure of HBV. Multi-colored arrows at the outside present the four ORFs with their encoding proteins: the core-ORF (black), the S-ORF (color change from yellow to red) including the preS1-domain (yellow), the preS2-domain (orange), and the s-domain (red). Finally, the viral polymerase is depicted in green including the terminal protein (bright green), the spacer domain (deep dark green), the reverse transcriptase (dark green), and the RNase H-domain (bright green). Black lines show the diverse transcribed mRNAs for the viral proteins with their polyA-tail and the ϵ -signal sequence. mRNAs are described from inside out: X-protein, MHBs and SHBs, LHBs, pregenomic (pg) RNA, and HBeAg. The two cycles in the middle represent the cccDNA strands with negative (blue) and positive (red) polarity including their respective promoters (bright blue) and enhancers (apricot). E: enhancer, GRE: glucocorticoid-response-element, ϵ : epsilon, encapsidation signal (modified after Glebe and Bremer 2013).

1.2.2.3. Viral Surface Proteins

Three different viral surface proteins are embedded into the lipid membrane that surrounds hepatitis B virions and subviral particles (Almeida et al. 1971). They all are encoded by a unique ORF, the S-ORF. Because of the use of variable initiation codons, the proteins share the same C-terminus (same stop codon) but have different N-termini (Heermann et al. 1984). Two different mRNAs are transcribed for translating HBsAg; the LHBs encoding mRNA of 2.4 kilo bases (kb) and the mRNA of 2.1 kb encoding for MHBs and SHBs (Kaneko and Miller 1988). Thus, the HBV surface proteins differ in their N-termini sequence and also in their glycosylation status (Schmitt et al. 1999). The N-glycosylation starts co-translationally within the ER (Gavilanes et al. 1982) whereas O-glycosylation takes place post-translationally in the Golgi apparatus during secretion (Patzner et al. 1986, Huovila et al. 1992).

The Small Hepatitis B Virus Surface Antigen (SHBs)

The smallest HBV surface protein is the SHBs, consisting of the s-domain, only. Its sequence is found in MHBs and LHBs, too. The SHBs is the major component of virions and subviral particles with essential functions during morphogenesis, virion assembly, and secretion (Bruss et al. 1994). The s-domain exhibits at least two, probably four hydrophobic transmembrane spanning helices (Berting et al. 2000). This conformation leads to the formation of an internal loop (aa 28-79) and an external loop (aa 99-161) (Figure 3). A short linear sequence of the internal loop is involved in virion assembly and mediates the binding to matured nucleocapsids (Bruss 1997). The external loop carries the important HBsAg-determinants and is also known as antigenic loop (a-determinant) (Figure 3). At asparagine (Asn)-146, the antigenic loop carries an N-glycosylation site (Peterson 1981). The s-domain contains 14 cysteins, at least eight within the external antigenic loop are supposed to cross-link the envelope protein with each other. This is believed to stabilize the SHBs within the viral envelope and forms its tertiary structure (Mangold and Streeck 1993; Mangold et al. 1995). The antigenic loop bears important epitopes (Norder et al. 2004) essential for neutralizing antibodies, for example derived from the immune reaction towards the HBV vaccine (Peterson et al. 1984; Emini et al. 1986;). Interestingly, mutations into the SHBs, occurring during antiviral therapy of HBV, can lead to escape variants (Cooreman et al. 2001; Locarnini 2005).

The Middle Hepatitis B Virus Surface Antigen (MHBs)

The MHBs consists of the s-domain (226 amino acids (aa)) and a 55 aa long N-terminal addition that is called the preS2-domain. During synthesis, the preS2-domain is translocated into the ER-lumen and is N-glycosylated at asparagine (Asn)-4 (Stibbe and Gerlich 1982) and further (within the Golgi-apparatus) O-glycosylated at threonine (Thr)-37 in all genotypes, besides genotype A (Schmitt et al. 1999). In contrast to LHBs and SHBs, MHBs apparently is not necessary either for virion assembly or infectivity for HBV (Bruss and Ganem 1991, Le Seyec et al. 1998) as well as HDV (Sureau et al.

1994). Its function for the replication cycle of HBV still remains unclear, although it is highly conserved within all *Orthohepadnaviridae* (Heermann et al. 1984). When MHBs is expressed, a proper N-glycosylation site at Asn-4 is necessary for the virion secretion (Block et al. 1994; Sheu and Lo 1994; Lu et al. 1995).

The Large Hepatitis B Virus Surface Antigen (LHBs)

The largest HBV surface protein (LHBs) is formed by the s-domain, the preS2-domain, and the preS1-domain which contains 108, 118, or 119 aa (depending on the genotype). LHBs is an ingredient of the spheres and a major and important component of the virions. The LHBs exists in two topologies, either internally located into the lumen of the virion (Figure 3 B, left site), or externally located and exposed on the viral surface (Figure 3 B, right site) (Bruss et al. 1994; Lambert and Prange 2003). Both isoforms adopt essential functions in viral assembly of HBV and infectivity of HBV and HDV. The preS1-conformation exposed on the viral surface is essential for preS1-mediated binding to human hepatocytes via its potential receptor (NTCP) and therefore mediates viral entry and subsequent infection (Yan et al. 2012). In combination with the internal loop of SHBs (aa 28-79), the internal preS1-located conformation is essential for the binding of the viral envelope with the matured core-capsid containing the viral genome (Bruss 1997). About 50 % of the LHBs were reported to change its conformational state from internal to external isoforms (Bruss et al. 1994; Ostapchuk et al. 1994; Prange and Streeck 1995). How the LHBs passes the ER-membrane is still unclear. The LHBs contains an acylation site at glycine 2 with myristic acid at the N-terminus (Persing et al. 1987). This myristoylation might mediate, together with the preS1-domain, the specific attachment of HBV to hepatocytes.

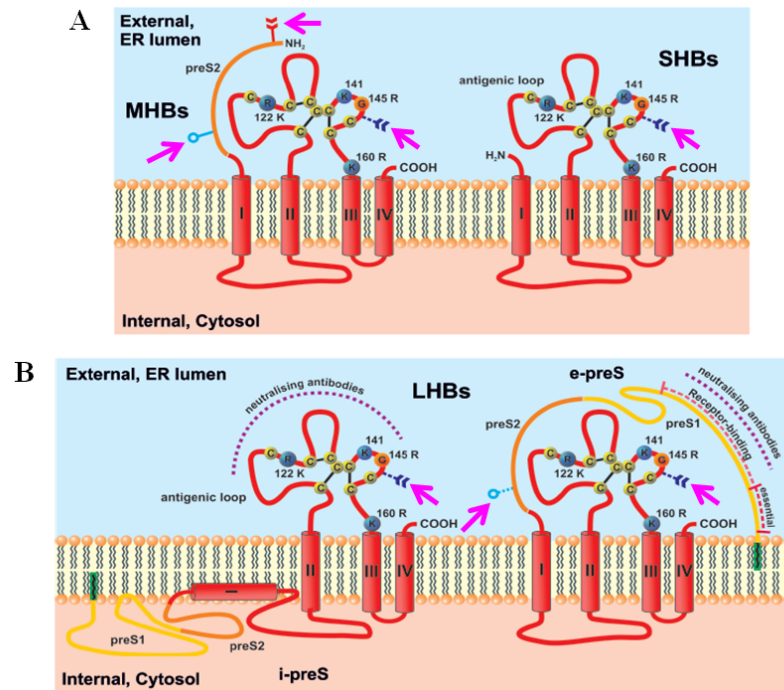


Figure 3: Hypothetical membrane topologies of HBsAg. **A)** MHBs (left) and SHBs (right) with their four transmembrane spanning domains (red) signed with Roman numerals. SHBs contains the antigenic loop (between transmembrane domain II and IV) including eight conserved cysteins linked via disulfide bridges (yellow dots connected to each other). **B)** Model of the LHBs topology. LHBs is depicted as its internally located isoform (i-preS, left) and its externally located isoform (e-preS, right). At the internally located isoform, the antigenic loop is exposed at the external side and is a binding site for neutralizing antibodies (lilac dotted line). At the externally located isoform, the preS1-domain is presenting its receptor-binding site (red dotted line). Yellow, blue, and lilac arrows and rings tagging the glycosylation site are highlighted with pink arrows. Blue background marks the external side of the virus as well as the ER-lumen. Rose marks the internal side of the virus or the cytosol of the cell (modified after Glebe and Bremer 2013).

1.2.3. Viral Life Cycle and Replication

After infection, HBV circulates within the blood stream and has to pass through small pores of the liver endothelium to reach the space of Dissé. There, initial low-affinity binding of HBV to hepatocytes is mediated by heparan-sulfate proteoglycans (HSPGs) (Schulze et al. 2007; Leistner et al. 2008, Sureau and Salisse 2013). Successful binding of HBV to the high-affinity receptor is necessary for the following uptake into its host cell. For a long time, the high-affinity receptor was unknown. In November 2012, a Chinese scientist group around Wenhui Li reported that the sodium taurocholate cotransporting polypeptide (NTCP) is a functional receptor for HBV and HDV (Yan et al. 2012). Binding of HBV to the NTCP is mediated by the preS1 region of the LHBs. Two sites of the preS1-domain (aa 9-18 (essential) and aa 29-48 (accessory)) and N-terminal myristic acid are believed to contribute to the binding event (Neurath et al. 1986a; Le Seyec et al. 1998; Glebe et al. 2005; Engelke et al. 2006; Leistner et al. 2008). Another binding region within the s-domain is probably also needed for virion uptake and fusion (Glebe et al. 2005; Jaoudé and Sureau 2005). After binding, HBV is taken up into an unknown compartment, by a still unknown endocytotic mechanism, where fusion of the

viral and cellular membranes might occur. The viral capsid is unpacked and actively transported to the nuclear pore complex (NPC) along microtubules because of the nuclear localization sequence (NLS) of the HBV core protein (Rabe et al. 2006). At the nuclear pore complex (NPC), the nucleocapsid binds via the α/β -importin mediated pathway to the nuclear basket and is transported into the karyoplasm (Kann et al. 1999; Rabe et al. 2003). Inside the karyoplasm, the relaxed circular (rc) DNA is completed to the plasmid-like covalently closed circular DNA (cccDNA) by a cellular DNA-polymerase (Köck and Schlicht 1993). Then cccDNA is associated with histones and exists as mini-chromosome besides the cellular DNA (Bock et al. 1994; Newbold et al. 1995). The formation of the cccDNA is the first marker of an effective infection. In contrast to retroviruses, HBV DNA does not require integration into the host genome to complete a replicative cycle. In contrast, a random integration of (sub)-genomic DNA fragments can occur leading to a dead end of the HBV viral replication. After formation of the cccDNA, the transcription of the minus strand takes place. Several sets of mRNAs (pregenomic (pg) RNAs and subgenomic RNAs) are transcribed (Rall et al. 1983) induced by the cellular polymerase II which starts upstream of the DR1. The skipping of the transcriptional stop-signals leads to the transcription of the pg-mRNA that exhibits an over-length of 3.5 kb. After export out of the nucleus, pg-mRNA is translated into the viral polymerase (pol) and the HBV core protein (HBcAg) and serves as template for reverse transcription. After forming a complex with cellular chaperons (heat-shock protein (hsp) 90 and hsp 23) (Hu and Seeger 1996, Hu et al. 1997), viral polymerase binds to the ϵ -signal at the 5'-end of the pg-mRNA (Junker-Niepmann et al. 1990; Bartenschlager and Schaller 1992). When a sufficient amount of viral core proteins is synthesized, the assembly of core-capsids happens spontaneously (Seifer et al. 1993). Then, core proteins encapsidate the pg-mRNA-polymerase-chaperon-complex into immature particles in the cytosol of the cell (Bartenschlager and Schaller 1992; Hu and Seeger 1996). Within the immature core-particles, the encapsidated pg-mRNA serves as template for the reverse transcription via the reverse transcriptase domain of the viral polymerase (Summers and Mason 1982). The following plus-strand synthesis is mediated by the DNA-dependent-DNA-polymerase activity of the viral polymerase and also takes place within the nucleocapsid (Lien et al. 1986; Seeger and Maragos 1989). Now, mature core-particles can re-migrate into the nucleus for a refill/accumulation of the intra-nuclear cccDNA pool (Tuttleman et al. 1986; Summers et al. 1990) or can interact with HBsAg-containing membranes at the ER (Miller et al. 1984; Gerelsaikhan et al. 1996), for envelopment. The other viral mRNAs are also exported in the cytoplasm and transcribed into HBsAg (2.4 kb and 2.1 kb) and the X-protein (0.9 kb) (Kaneko and Miller 1988). Enveloped virions bud and get secreted via multivesicular bodies (MVB) (Lambert et al. 2007). In contrast to that, the formation of subviral particles can occur autonomously at the ER. They are released via the common secretory pathway through ER and Golgi (Gavilanes et al. 1982; Patzer et al. 1986; Huovila et al. 1992).

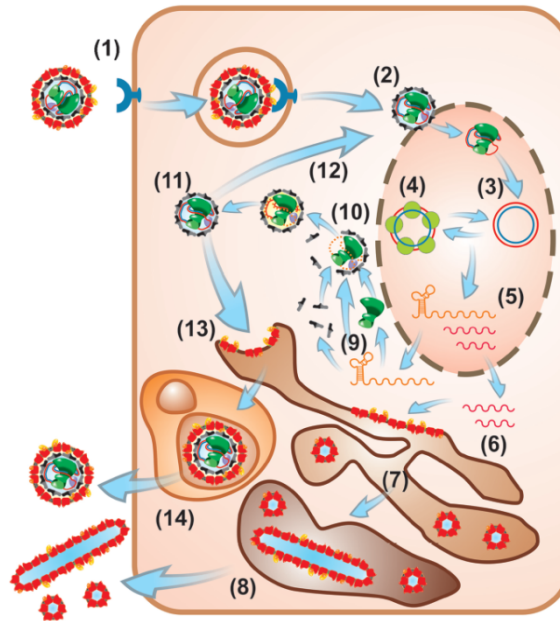


Figure 4: Schematic overview of viral life cycle. (1) Attachment and up-take via its high affinity receptor NTCP, (2) release of the viral DNA into the karyoplasm, (3) formation of cccDNA, (4) complex-formation with cellular histones, (5) transcription of pgRNA and mRNAs for LHBS and MHDs/SHBs, (6) transport of mRNAs into the cytoplasm, (7,8) formation and secretion of subviral particles via ER and Golgi, (9) translation of pgRNA into core-proteins and polymerase, (10) virion assembly, (11) genome maturation, (12) retransport of matured core-capsid to the nucleus, (13,14) envelopment and secretion of virions via MVB (modified after Glebe and Bremer 2013).

1.3. Hepatitis Delta Virus (HDV)

1.3.1. Classification

The hepatitis Delta virus was discovered by M. Rizzetto in 1977 while studying liver biopsies of patients chronically infected with HBV (Rizzetto et al. 1977). At the beginning it was regarded as a new antigen of HBV called Delta-antigen. Later it turned out to be a new virus with a single-stranded (ss) RNA genome. It belongs to the Genus *Deltavirus*, with HDV as its sole member (van Regenmortel et al. 2000). Recent studies have shown a high genetic diversity of HDV RNA over the world. Until now, eight major genotypes are described, classified as "clades". They are labeled as HDV-1 to HDV-8 (Le Gal et al. 2006). These clades show a high heterogeneity because of the missing proofreading function of the RNA polymerase (Imazeki et al. 1990; Fu and Taylor 1993) inducing a high mutation rate of the viral RNA. In a chronically infected patient, non-coding regions of the viral genome mutate up to $3 \times 10^{-2} - 3 \times 10^{-3}$ base substitutions per year (Lee et al. 1992). Due to this fact, the genetic variability differs up to 16 % within the same clade indicating that in one infected individual many quasispecies can be found. The genetic variability between genotypes varies between 20 %-40 % (Dény 2006; Le Gal et al. 2006).

1.3.2. Morphology and Genomic Structure

The virion of HDV is a spherical particle of about 36-45 nm (Figure 5 A). HDV contains a single-stranded circular RNA of approximately 1.7 kb. Because of the high GC content of the nucleotide sequence, the viral RNA can fold itself using 74 % intra-molecular base-pairing that results in an unbranched rod-like structure (Wang et al. 1986, Kuo et al. 1989, Branch et al. 1989). Viral replication occurs via the transcription of multimeric genomic and antigenomic intermediates (Figure 5 B) (Chen et al. 1986, Kuo et al. 1988). The viral RNA encodes for a single structural protein; the hepatitis Delta antigen (HDAg). This protein exists in a short isoform (small HDAg, S-HDAg, 24 kDa) and in a long isoform (long HDAg, L-HDAg, 27 kDa) (Weiner et al. 1988). L-HDAg is 19 amino acids longer than the S-HDAg and is produced by a RNA editing mechanism which changes the stop codon of the S-HDAg into a tryptophan (Taylor 1992, Zheng et al. 1992, Casey and Gerin 1995). The cellular enzyme double-stranded RNA specific adenosine deaminase acting on RNA-1 (ADAR-1), is responsible for this mechanism (Casey and Gerin 1995; Polson et al. 1996; Wong and Lazinski 2002). Both HDAg proteins enable distinct functions in the viral life cycle. While the S-HDAg is essential for viral replication (Kuo et al. 1989) and secretion (Wang et al. 1991), the L-HDAg is required for packaging (Chang et al. 1991; Ryu et al. 1992) and for direct binding with the HBV surface proteins (Chang et al. 1991; Lee et al. 1995). It has another relevant function in the repression of viral replication (Chao et al. 1990). The viral replication is also balanced by the various posttranslational states of modifications of the S-HDAg, for example methylation (Arg-13) (Li et al. 2004), acetylation (Lys-72) (Mu et al. 2004), phosphorylation (Ser-177) (Mu et al. 2001), and sumoylation (Tseng et al. 2010). The prenylation at Cys-211 of L-HDAg is crucial for viral encapsidation (Glenn et al. 1992).

About 200 HDAg are used to encapsidate the viral RNA into a ribonucleoprotein (RNP) (Wang et al. 1986; Gudima et al. 2002). The RNP is then enveloped with a lipid membrane coated with the surface proteins of HBV (Sureau 2006) explaining why HBV co- or super-infection is always required for a productive HDV infection cycle.

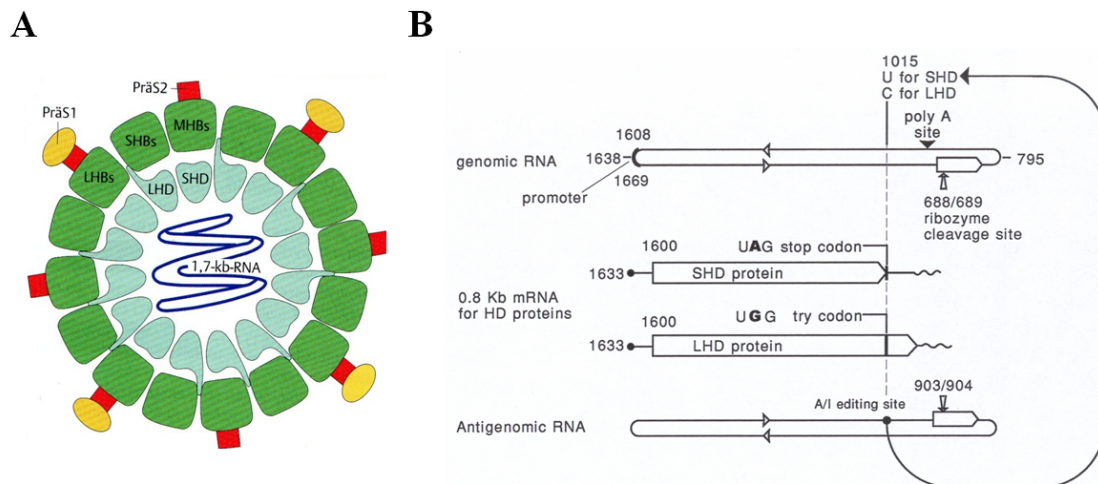


Figure 5: **A)** Schematic model of HDV covered with HBsAg (dark green, red, and yellow). **B)** Structure of RNA genome (upper part), S-HDAg and L-HDAg (middle part), and antigenomic RNA (lower part). Arrows mark the ribozyme cleavage site between nt 688/689 (genomic RNA) and nt 903/904 (antigenomic RNA). Circle presents the nucleotide change from adenine to guanine leading to the change of the stop codon (UAG) to the amino acid tryptophan (UGG). Kindly provided and modified after Doerr and Gerlich 2008.

1.3.3. Viral Life Cycle

Attachment and Entry

As mentioned earlier, HDV requires the surface proteins from its helper virus HBV for attachment and subsequent entry into susceptible hepatocytes. It has been well established, that two sequences in the preS1-domain of the LHBs and the N-terminal myristoylation are needed for specific binding to its high affinity receptor for both viruses, HBV (Neurath et al. 1986a; Leistner et al. 2008) and HDV (Sureau et al. 1993, Sureau et al. 2003, Abou-Jaoudé et al. 2007) . Therefore it is not surprising, that the first contact between virus and hepatocytes is mediated by binding at HSPGs as further described for HBV (Lamas Longarela et al. 2013). HDV also uses the sodium taurocholate cotransporting polypeptide (NTCP) as a receptor for the infection of hepatocytes, similar to HBV (Yan et al. 2012). Nevertheless, many questions remain unclear: Which endocytotic pathway for internalization is used by the viruses? Do HBV and HDV use different post-entry steps? Are there any other receptors involved in the uptake-mechanism?

After successful up-take into hepatocytes, the HDV-RNP is unpacked and transported to the nucleus where viral replication takes place. This process is presumably mediated by a NLS (located at aa 35-88 from the N-terminus) of the HDAg (Xia et al. 1992; Chang et al. 1991; Tavanez et al. 2002).

Replication Cycle

In the nucleus, the initiation of replication is realized via a so called “double-rolling cycle” mechanism (Figure 6) similar to that already proposed for plant viroids and small satellite RNAs (Wang et al. 1986; Chen et al. 1986, Branch et al. 1989). During replication, three major species of RNA occur, the

genomic RNA (negative polarity), the antigenomic RNA (positive polarity), and mRNA (0.8 Kb) encoding for HDV-proteins. Genomic RNA serves as template for the transcription of mRNA, only and therefore as matrix for viral proteins.

Due to the fact that HDV does not possess its own RNA polymerase and both HDAg hold a direct RNA-binding domain (Wang et al. 1994), it is well established that the cellular DNA-dependent RNA polymerase II (pol II) is directly involved in the transcription of viral RNA (Kuo et al. 1989, Filipovska and Konarska 2000, Greco-Stewart et al. 2007) without formation of DNA-intermediates (Fu and Taylor 1993). Some other studies postulate the involvement of RNA pol I and III in viral replication machinery, too (reviewed in Greco-Stewart et al. 2009). With the help of additional transcription factors, the polymerase II and HDAg form a nuclear replication complex to initiate replication of mRNA and genomic-RNA. At first, a multimeric antigenomic intermediate is generated (Chen et al. 1986; Macnaughton et al. 2002), harboring an intrinsic endo- and exonuclease activity of about 85 nt that enclosed the ribozyme restriction site (nt 688 and nt 689). After generating an autocatalytic ribozyme pseudo-knot at the restriction site, the multimeric antigenome is cleaved into linear monomers (Kuo et al. 1988; Wu et al. 1998, Branch et al. 1989, Lazinski and Taylor 1994). The monomeric strands then are ligated to form circular antigenomic molecules which then become the templates for the production of more genomic RNAs by another round of the rolling cycle mechanism (Taylor 1992, Lazinski and Taylor 1994). The involvement of host RNA ligase remains unclear. Newly transcribed and translated S-HDAg is involved in the rolling-cycle mechanism again.

Assembly and Secretion

As long as no L-HDAg is synthesized, replication occurs as described above. Later, during the viral replication cycle, the production of S-HDAg switches to the synthesis of L-HDAg, performed by an RNA editing mechanism (Casey and Gerin 1995; Polson et al. 1996; Wong and Lazinski 2002). The L-HDAg serves as dominant negative inhibitor for viral replication (Chao et al. 1990) and together with S-HDAg, interacts with the genomic RNA to assemble the HDV RNP complex. For covering the RNP complex with the HBV surface proteins, it must travel to the cytoplasm. The L-HDAg harbors a nuclear export signal (NES) at its C-terminus (Lee et al. 2001) and after binding with the protein NESI (nuclear export signal L-HDAg interacting protein), the HDV RNP complex is transported to the cytoplasm (Wang et al. 2005). For the binding of the HDV RNP complex, the L-HDAg exhibits a CXXX motive at its C-terminus that undergoes prenylation (Glenn et al. 1992). In the presence of HBV co-infection, this posttranslational modification anchors the viral RNP in the ER, where it can assemble with the HBV surface proteins. For this purpose, the C-terminus of L-HDAg interacts with the tryptophan-rich motif at the C-terminus of SHBs (Wang et al. 1991; Komla-Soukha and Sureau 2006) creating new infectious virions that trigger secretion of enveloped HDV particles.

In contrast to HBV, assembly and secretion of HDV require SHBs, only (Bruss and Ganem 1991; Wang et al. 1991; Komla-Soukha and Sureau 2006), but for the infection of new hepatocytes, the LHBs of HBV is required for HDV, additionally (Sureau et al. 1993).

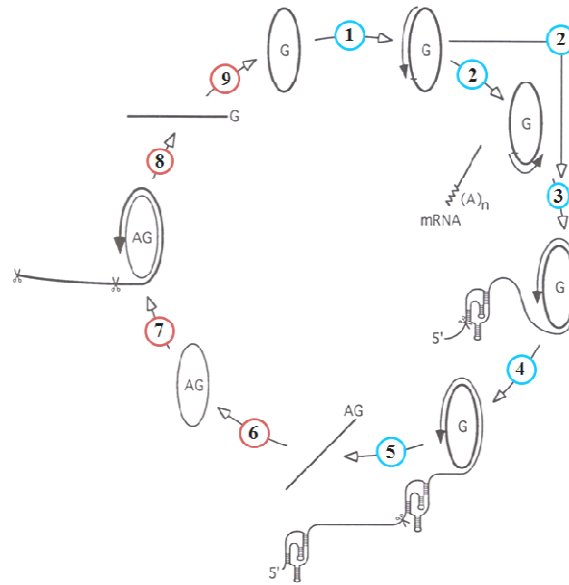


Figure 6: Replication cycle of HDV after the rolling cycle mechanism. (1) transcription of genome (G), (2) transcription of S-HDAg-mRNA ($(A)_n$ mRNA) and (3) multimeric genomic strand, (4) formation of ribozyme pseudo-knot, (5) autocatalytic cleavage of the genomic RNA into monomeric strands, (6) religation of the strand to antigenomic RNA, (7) transcription of the antigenomic RNA with multimeric antigenomic strand, (8) cleavage into monomeric antigenomic strands (9) religation and new replication cycle. Modified and kindly provided after Lai 1995, Doerr and Gerlich 2008.

1.4. Model Systems for HBV and HDV

Several animal models and cell culture systems are used for analyzing replication, infection, and secretion of HBV and HDV. They have several advantages and disadvantages.

For studying viral replication and secretion, human hepatoma cell lines like Huh7 or HepG2 cells are well established *in vitro*, but they are not susceptible for HBV or HDV and therefore have to be transfected with HBV or HDV cDNA (Neurath et al. 1986b; De Falco et al. 2001; Rabe et al. 2006). Apart from them, another human hepatoma cell line (HepaRG) is partly susceptible for HBV and HDV but has to be treated with dimethyl sulfoxide (DMSO) and polyethylene glycol (PEG) for several weeks (Gripon et al. 2002). In contrast to HBV, many different cell types can be transfected with HDV cDNA because the replication of the HDV genome occurs independently from hepatocyte specific transcription factors. In addition, co-transfection of HDV- and HBV-encoding plasmids leads to the reproduction of the complete replication cycle including virion formation and secretion of HDV (Chang et al. 1991; Sureau et al. 1992).

Because HBV shows a narrow host range and infects only humans and higher primates, for example chimpanzees (Barker et al. 1973), the use of suitable animal models to study the infectivity of HBV is difficult. Due to the strong host specificity of HBV and HDV, classical laboratory animals, like mice and rats, are unsuitable because they cannot be infected with HBV and HDV.

In the past, chimpanzees were used for infection and replication assays of HBV and HDV (Rizzetto et al. 1980a) but these *in vivo* experiments were stopped when a debate started regarding ethic and economic reasons. Studies of non-human HBV were done for example with duck hepatitis B virus (DHBV) in ducks and woodchuck hepatitis B virus (WHV) in woodchucks, though infection and replication systems are not completely comparable to that in humans. To name one example only, DHBV differs in its structure (loss of the MHBs) compared to the human HBV. Due to the fact that Eastern woodchucks can be infected with WHV, they are still used as infection models for pathogenesis and antiviral therapy to develop new immunization strategies of a chronic HBV-infection (reviewed in Menne and Cote 2007).

A successful infection with human HBV is not only depending on the species but also on the differentiation status of the hepatocytes.

In some studies, primary human hepatocytes (PHH) were used because they can be infected with HBV and HDV, although handling them is more difficult than immortalized cell lines (Gripon et al. 1988) and the availability is limited. Another mayor problem of PHH are the ethical concerns regarding their origins and their heterogeneity in quality after isolation (reviewed in Glebe and Urban 2007). Freshly isolated primary hepatocytes from the Southeast Asian treeshrew *Tupaia belangeri* are susceptible for human HBV and HDV (Li et al. 1995) and can be infected *in vitro* (Yan et al. 1996) as well as *in vivo* (Su 1987, Walter et al. 1996). They are closely related to primates (Schmitz et al. 2000) and can be infected with Woolley monkey hepatitis B virus (WMHBV), too (Köck et al. 2001).

1.5. Aim of the Work

To date, the chronic HBV infection is treated with either IFN- α or nucleos(t)ide analogs. But during this antiviral therapy, HBV resistance mutants often occur, leading to an antiviral breakthrough. Due to the strong overlapping open reading structure of the HBV genome, mutations in the viral polymerase also affect the genes of the other viral proteins especially the gene for the HBV surface proteins. Mutations in these proteins could lead to an altered virion secretion and infectivity. In the past, an *in vitro* phenotypic resistance assay was established at the Institute of Medical Virology at the University of Gießen (AG Dr. Glebe) in collaboration with the Institute of Virology at the University of Munich (AG Prof. Protzer). In the first part of the present work,

- a) the phenotypic characterization of patient isolates from chronically infected HBV-patients should be continued, focusing patient isolates that possess characteristic HBV surface protein variants.
- b) Furthermore, the consequences of selected mutations in the SHBs on HBV assembly, the expression of viral surface proteins, and virion secretion should be further analyzed.

The second part of this work deals with the satellite virus of HBV: the hepatitis D virus. For assembly and virion secretion, HDV uses the surface proteins of its helper virus HBV. Due to this fact, mutations in the HBV surface proteins that arise during antiviral therapy do not only affect the viral life cycle of HBV, but also have strong consequences for the assembly and secretion of HDV. Therefore,

- c) an *in vitro* transfection system in Huh7 cells should be established generating recombinant HDV pseudo-particles covered with HBV surface protein variants.
- d) In this context, a full length genomic HDV RNA standard should be generated *in vitro* for absolute quantification of HDV RNA.
- e) Using the recombinant HDV variants, an infection system for HDV on PTHs should be established.

To ensure a better comparability with naturally occurring infections,

- f) plasma, derived from a chronically infected patient with HBV and HDV, should be purified and further analyzed for the infectivity of HDV on PTHs.

Using the these methods and collected data,

- g) the influence of typically occurring HBV surface protein mutations arising during antiviral therapy on virion formation and secretion of HDV should be investigated.

2. Materials and Methods

2.1. Materials

2.1.1. Antibiotics

name	stock solution	used concentration	CaNo	company
caspofungine acetate	50 mg/ml	1:10.000	SRP05500c	Sequoia
ampicillin	50 mg/ml	1:500	KO291	Roth
penicilline/streptomycine	100 x	1:100	P11010	PAA

2.1.2. Antibodies and Nuclear Staining

2.1.2.1. Primary Antibodies

specificity	name	epitope	used concentration		source/ company
			ELISA	IF	
anti-SHBs IgG ¹⁾ (1 mg/ml)	C20/02	S-domain, AS 120-160 in a-determinant, conformational	1:1000	1:200	Prof Gerlich, Gießen
anti-SHBs IgG ¹⁾ (1 mg/ml)	HB1	S-domain, binding-motif: CRTCTT/CKTCTT conformational independent	1:1000		Aurelia Zvibliene, Institute of Biotechnology, Vilnius, Lithuania
anti-MHBs IgG ¹⁾ (1 mg/ml)	Q19/10	preS2-domain, N-glycosylation, conformational independent	1:500	1:100	Prof Gerlich, Gießen
anti-LHBs IgG ¹⁾ (1 mg/ml)	MA18/7	preS1-domain, AS 20-23, binding-motif: LDPAF conformational independent	1:1000	1:200	Prof Gerlich, Gießen
anti-HBc AK ²⁾ (10 mg/ml)		HBcAg	1:500	1:200	DAKO (CaNo. B0586)
Anti-HBc AK ²⁾ (concentration unknown)	Gö- Schaf	HBcAg	1:20.000		Prof Gerlich, Gießen
anti-HBs biotin conjugate Enzygnost® HBsAg 6.0		HBsAg	1:40		Dade Behring (CaNo QPW11)

¹⁾ monoclonal; ²⁾ polyclonal

2.1.2.2. Secondary Antibodies

name	concentration	used concentration	company
Alexa-Fluor 549 F(ab') ₂ fragment of goat anti-mouse IgG	2 mg/ml	1:200	Invitrogen (CaNo. A-11020)
Alexa-Fluor 549 F(ab') ₂ fragment of goat anti-rabbit IgG	2 mg/ml	1:200	Invitrogen (CaNo. A-11072)
Streptavidin-POD	1 mg/ml	1:500	Dianova (CaNo.: 016-030-084)
donkey-anti-sheep-POD		1:500	Dianova (CaNo. 713-035-147)

2.1.2.3. Nuclear Staining

name		used concentration	company
DAPI (4',6-diamidino-2-phenylindol-dihydrochlorid)	detached in dH ₂ O [1mg/ml]	1:400	Roth (CaNo. 6335.1)

2.1.3. Peptide

For inhibition of HBV or HDV infection the following peptide was used:

myr HBV preS1-peptide 2-48

It is a synthetic peptide that comprises the aa 2-48 and the myristoylation site of the preS1 region of the hepatitis B virus (genotype D). The peptide was purchased from GenScript.

2.1.4. Antivirals

name	stock concentration	company
adefovir	2 mM	Sigma-Aldrich (CaNo.: SML0240)
entecavir	1 mM	Sequoia (CaNo.: SRP010887e)
lamivudine	10 mM	Sequoia (CaNo.: SRP011251)
tenofovir	2 mM	Sequoia (CaNo.: SRP01194t)

2.1.5. Buffer, Media, and Solutions

2.1.5.1. Buffers

name	components	amount/concentration	company
ELISA coating buffer (NaPP) pH 7.4	NaCl Na ₂ HPO ₄ x H ₂ O KH ₂ PO ₄	83 mM 8.6 mM 2.2 mM	
HBSS (without MgCl ₂ and CaCl ₂)	(+/- 5 mM EGTA)		Invitrogen
PBS (10x) pH 7.4	NaCl, pH 7.4 KCl Na ₂ HPO ₄ x 2 H ₂ O KH ₂ PO ₄	137 mM 3.4 mM 10 mM 1.8 mM	
PBS++	CaCl ₂ MgCl ₂ MgSO ₄ PBS 1x	0.9 mM 0.52 mM 0.16 mM detached in 400 ml	
TNE pH 7.4	NaCl EDTA Tris-HCl	140 mM 1 mM 20 mM	
TFB ₁ (Transforming Buffer 1) pH 5.8 with acetic acid	MES (pH 6,2) RbCl CaCl ₂ x 2 H ₂ O MnCl ₂ x 4 H ₂ O H ₂ O	10 mM 100 mM 10 mM 50 mM ad to 500 ml	
TFB ₂ (Transforming Buffer 2) pH 6.5 with potassium hydroxide	MOPS RbCl CaCl ₂ x 2 H ₂ O Glycerol H ₂ O	10 mM 10 mM 75 mM 15 % (v/v) ad to 100 ml	

1 M MES pH 6.2 with 5 M KOH	MES H ₂ O H ₂ O	19.52 g solve in 80 ml ad to 100 ml	
MOPS (10x) pH 7.0 with NaOH	MOPS EDTA NaOAc	41.9g 10 mM 50 mM	
10x MOPS gel running buffer	MOPS (pH 7.0) Sodium acetate EDTA	0.4 M 0.1 M 10 mM	
SEAP-buffer	Diethanolamin (100 %) MgCl ₂ (1 M stock solution) L-Homoarginine dH ₂ O	10.51 g 50 µl 0.089g ad to 50 ml	Roth
3 M sodium acetate pH 5.2	Sodium acetate dH ₂ O	40.8 g ad to 100 ml	
6x loading dye	Glycerine Bromphenol blue add TAE	60 ml 0.1 g 100 ml	
RNA loading buffer (for formaldehyde gels)	10x MOPS Formamide (deionized) Formaldehyde 37 % H ₂ O	50 µl 250 µl 89 µl 111 µl	Roth
Trypsin/PBS (1:5)	PBS 1x Trypsin/EDTA (5x)	500 ml 100 ml	PAA
TAE (50x) pH 8 with glacial acetic acid	Tris glacial acetic acid EDTA (0.5 M)	242 g 57.1 ml 100 ml	

2.1.5.2. Media

name	components	amount/concentration	company
DMEM with phenolred			Invitrogen
DMEM without phenolred			Invitrogen
HGM (Hepatocytes Growth Medium) (according to Block et al. 1996, modified)	DMEM without phenolred ITS Mix BSA Glutamax I (5 M) Dexamethasone (1:10.000) Gentamycine (50 mg/ml)	1 L 10 ml 2 g 10 ml 100 µl 2 ml	Invitrogen Invitrogen Roth Invitrogen Invitrogen Invitrogen
LB-medium	Bacto TM -Trypton Bacto TM -yeast extract NaCl H ₂ O	10 g 5 g 10 g 1 l	Becton Dickinson Becton Dickinson
Incubation medium (immunostaining)	DMEM without phenolred BSA	1%	Sigma-Aldrich
Cell culture medium 2 % (transfection)	DMEM without phenolred FCS Pyruvat Penicillin/Streptomycin	500 ml 10 ml 5 ml 5 ml	Invitrogen PAA
Cell culture medium 5 %	DMEM FCS Penicillin/Streptomycin	500 ml 25 ml 5 ml	Invitrogen PAA
Cell culture medium 10 %	DMEM FCS Penicillin/Streptomycin	500 ml 50 ml 5 ml	Invitrogen PAA
Freezing medium	DMEM FCS DMSO	6 ml 2 ml 2 ml	Invitrogen PAA

2.1.5.3. Solutions

name	components	amount/concentration	company
0.5 M H ₂ SO ₄			
collagenase solution	Collagenase Type IV DMEM without phenolred	250 mg 100 ml	Invitrogen
matrigel		1:20	Becton Dickinson
substrate for ELISA	OPD-tablets Perhydrol (30) H ₂ O	4 5 µl 12 ml	Merck
substrate for SEAP-assay	pNitrophenolphosphate H ₂ O	0.6 mg 5 ml	Sigma-Aldrich
embedding medium for IF	Mowiol 4-88 H ₂ O Glycerine (87 %) Tris/Cl, pH 8.5; 0 DABCO	2.4 g 6 ml 6 g 12 ml 100 ml	Sigma-Aldrich Merck Sigma
paraform aldehyde, PFA (3 %)	PFA 3M KOH PBS (10x) H ₂ O	6 g 200 µl 20 ml 180 ml	Merck
O-Phtalaldehyde	dH ₂ O H ₂ SO ₄ (conc) O-Phtalaldehyde Brij 35 (10 %) add dH ₂ O	400 ml 37 ml 100 mg 1.5 ml 500 ml	Sigma Pierce
NED-reagent	Boric acid H ₂ O H ₂ SO ₄ conc. NED Brij-30 (10 %) Ad H ₂ O	2.5 g 300 ml 111 ml 300 mg 1.5 ml 500 ml	Sigma-Aldrich Sigma-Aldrich Pierce
PBS/Triton X-100 0.2%	PBS (1x) Triton-X-100	500 ml 1 ml	Sigma
RNA blue marker	Bromphenol blue (1 %) EDTA (250 mM) Glycerine (80 %)	375 µ 25 µl 625 µ	
OPD-ELISA substrate	OPD-tablets H ₂ O Hydrogen peroxide	4 tablets 12 ml 5 µl	DAKO (CaNo S2045)
1 % Casein-Block solution			Thermo Scientific (CaNo 37528)

2.1.6. Commercial Kits, Enzymes, and Competent Bacteria

name	CaNo.	company
Nucleo Spin RNA II	740955	Machery-Nagel
High Pure Viral Nucleic Acid Kit	11858874001	Roche
Sample Preparation System DNA	06K12-24	Abbott
FuGene HD Transfection Reagent Kit	#04709691001	Roche
Plasmid Plus Midi Kit	12943	Qiagen
QIAquick PCR Purification Kit	28104	Qiagen
FuGene HD Transfection Reagent	E2311/2	Promega
Verso 1-Step QRT-PCR Kit + ROX vial	AB-4100c	Thermo Fisher Scientific
ABsolute Blue QPCR SYBR Green Mix + ROX vial	AB-4166b	Thermo Fisher Scientific
ABsolute QPCR SYBR Green Capillary Mix	AB-1285b	Thermo Fisher Scientific
Absolute QPCR Capillary Mix	AB-1283b	Thermo Fisher Scientific

Phusion® High-Fidelity DNA Polymerase	F530s	Thermo Fisher Scientific
Competent bacteria <i>Stellar</i> , In-Fusion HD Cloning System	639643	Clontech
dNTPs mix (10 mM)	R0192	Thermo Fisher Scientific
DNase I, RNase free (1 U/μL)	EN0521	Thermo Fisher Scientific
RNase A, DNase and protease free	EN0531	Thermo Fisher Scientific
Shrimp Alkaline Phosphatase	EF0511	Thermo Fisher Scientific
T7 High Yield RNA Synthesis Kit	#E2040S	NEB Biolabs
DpnI	#ER1705	Thermo Fisher Scientific
wst-1, cell proliferation reagent	11644807001	Roche
TMB Xtra Ready-to-use-substrate	4800L	Biocompare
Proteinase K, recombinant, PCR grade	3L78-60	Abbott

2.1.7. Cell Lines

AML12

The AML12 is a murine hepatoma cell line, that was derived from livers of transgenic mice, overexpressing the transforming growth factor α . These cells show typical hepatocyte features, high expression of mRNA for serum and gap junction proteins for example (Wu et al. 1994).

Huh7

The Huh7 cell line is a human well differentiated hepatoma cell line derived from a hepatocellular carcinoma of a 57-year old Japanese man (Nakabayashi et al. 1982).

Huh7 Munich

The cell line Huh7 Munich is a progeny of the Huh7 cell line. These cells should have no functional reimport of matured core-capsids into the nucleus (personal communication of Prof. Dr. U. Protzer, Institute for Virology, Munich).

HepG2

The HepG2 cell line is an immortal human hepatoma cell line derived from a hepatoma biopsy of a 15-year old American man. This cell line synthesizes several liver specific human plasma proteins and contains no HBV-DNA (Aden et al. 1979).

Primary *Tupaia* Hepatocytes (PTHs)

For infection assays freshly isolated primary hepatocytes from the East-Asian tree shrew *Tupaia belangeri* were used. As well as primary human hepatocytes (PHHs), PTHs belong to the kind of

cells which can be infected with the human Hepatitis B virus (Glebe et al. 2003; Köck et al. 2001). The animals are from the animal breed located formerly at the Institute of Anatomy and Cell Biology, now the animals are hosted at the central animal facility ("zentrales Tierlabor") at the Justus-Liebig-University in Gießen (JLU-No. 410-M, projectID: 767).

2.1.8. Viruses Derived from Serum/Plasma of Chronically Infected Individuals

ID ¹⁾	fraction	GE/ml	used GE
ID 309 pool	4	4x10 ¹¹	1x10 ⁸
ID 395	4	2.4x10 ⁹	1x10 ⁶
ID 423	7	8.65x10 ⁹	1x10 ⁷
¹⁾ internal identification number the Institute of Medical Virology, JLU Gießen			

2.1.9. Plasmids

2.1.9.1. Standard Plasmids

name	template	source/company
pSEAP2-control	pSEAP2-control	Clontech (CaNo. 631717) (Berger et al. 1988)
pCH9-3091 (wild type, wt)	pBR322 derivate with 1.1 HBV overlength genome, genotype D, serotype ayw1 (GenBankID DQ464168.1)	kindly provided by Prof. Dr. U. Protzer
pSVLD3	3x HDV genome	kindly provided by Karin Schultheiß (Institute for Medical Virology, Gießen) (Kuo et al. 1989)

2.1.9.2. HBV-Expression Plasmids for HBV Phenotypic Assay

name	source
pCH9-3091-pol_RK 172-2	kindly provided by Dr. Maria Neumann- Fraune from Uniklinikum Köln
pCH9-3091-pol_RK 172-4	
pCH9-3091-pol_KW 11a-1	
pCH9-3091-pol_KW 6a-6	
pCH9-3091-pol_KW 8-6	
pCH9-3091-pol_KW 14-8	
pCH9-3091-pol_KW 13a-2	
pCH9-3091-pol_KW 4a-7	

For phenotypic characterization of isolates from chronically infected HBV-patients in HBV resistance assay, HBV expression plasmids from different patient isolates were generated. On that score, the HBV polymerase-ORF of isolates from chronically infected HBV-patients was inserted in the HBV wild type plasmid pCH9-3091.

2.1.9.3. Plasmids for Analyzing HBV Variants Harboring Stopmutants within the S-ORF

name of the plasmid	used name in the dissertation	mutation		source
		rt-domain	s-domain	
pCH9-3091-preS1M1T	M1T	silent mutation	M1T	kindly provided by Dr. Maria Neumann-Fraune from Uniklinikum Köln
pCH9-3091-sW172*	172* ¹⁾	A181T	W172*	
pCH9-3091-sW172L	172L	A181V	W172L	
pCH9-3091-sW176*	176*	T184M	W176*	
pCH9-3091-sW182*	182*	V191I	W182*	
pCH9-3091-sW196*	196*	M204I	W196*	
pCH9-3091-sW196S	196S	M204I	W196S	
pCH9-3091-sW196L	196L	M204I	W196L	
pCH9-3091-sW199*	199*	V207I	W199*	
pCH9-3091-sW216TAA	216TAA	V224	W216* (nt-mutation:TAA)	
pCH9-3091-sW216TGA	216TGA	V224	W216* (nt-mutation:TGA)	

¹⁾ * stop mutation

2.1.9.4. Plasmids Encoding HBV Surface Proteins for Generating Recombinant HDV in Cell Culture

plasmid name	name in dissertation	source
pCH9-delCMV-nurLHBs_sM125R_sT125I	LMS	kindly provided by Julia Heger, see masterthesis Heger 2012
pCH9-delCMV-nurLHBs-mM1T_sM125R_sT125I	LXS	
pCH9-delCMV-nurLHBs-mM1T_sM1T_sM125R_sT125I	LXX	
pCH9-delCMV-nurLHBs_lM1T_sM1T_sM125R_sT125I	XXM	
pCH9-delCMV-nurLHBs_lM1T_mM1T_sM125R_sT125I	XXS	
pCH9-delCMV-nurLHBs_lM1T_mM1T_sM1T_sm125R_sT125I	XXX	

The initiation codons (M) of the three surface proteins (l, large; m, middle; s, small) are mutated. The mutations in the subgenomic L-ORF constructs have no influence on the secretion of subviral particles (Heger 2012). All plasmid constructs imply the binding sequence for the HB1-antibody (binding-motif: CRTCTT/CKTCT). The wild type plasmid was marked with the letters LMS implying that all surface proteins are intact. The corresponding mutation was highlighted with X.

2.1.10. PCR, Primer, Probes, and Mastermixes

2.1.10.1. Primer and TaqMan Probes for Quantitative Polymerase Chain Reaction (qPCR)

Primer and probes for qPCR were purchased from Eurofins MWG, metabion, and biomers.net.

X-PCR	<u>Primer</u> X2 sense X2 antisense <u>TaqMan probe</u> HBV-TaqMan	5'- gacgtcctt ¹⁾ gtgtacgtcccgtc 5'- tgcagagttgaagcgaagtgcaca 5'- FAM ²⁾ -ctccccgtctgtgcctctcatctgccg-TAMRA ³⁾
-------	--	--

HOPE-PCR	<u>Primer</u> HOPE-sense HOPE-antisense	5`-actaggaggctgtaggcata 5`-agactctaaggctcccg
HDV-PCR	<u>Primer</u> HDV2-sense HDV2-antisense <u>TaqMan probe</u> HDV-TaqMan	5`-tccagaggaccctca 5`-ccggataagcctcact 5`- FAM ¹⁾ -agaccgaagcaggaggaaagca-TAMRA ²⁾
¹⁾ y: C/T; ²⁾ FAM: 6-Carboxy-Fluorescein; ³⁾ TAMRA: Tetramethylrhodamin		

2.1.10.2. Primer for Generating an HDV-RNA Standard

HDV amplification plasmid pSVLD3	<u>primer</u> HDV3-sense HDV3-antisense	5`- ggtgcaaatcaagaactgc 5`- aggaattctcggaaagaagg
generation of HDV RNA standard <i>in vitro</i>	<u>primer</u> HDV T7-sense HDV T7-antisense	5`- gtacgtcgactaatcagctcactataggagagaattcctttgatgttcccag 5`- gtacgctagcgaattctcggaaagaaggataagg

2.1.10.3. Sequencing Primer for HDV-RNA-Standard

Primer for sequencing HDV template	<u>primer</u> HDV Sequenzierung3 HDV Sequenzierung2	5`- acccccttcgaaagtgc 5`-gaattcctttgatgttcccag
------------------------------------	---	---

2.1.10.4. Mastermixes for Hot Start and Gradient PCR

Amplification of HDV genome out of pSVLD3 plasmid	33 µl 10 µl 1 µl 3 µl (10 pmol/µl) 3 µl (10 pmol/µl) + 5 µl	H ₂ O 5x High Fidelity Buffer dNTPs HDV3-sense HDV3-antisense pSVLD3 plasmid
Polymerase mix	0.5 µl 4 µl 0.5 µl	H ₂ O 5x High Fidelity Buffer Phusion High Fidelity DNA polymerase

2.1.10.5. qPCR Mastermixes

HOPE-qPCR	8 µl 1 µl (10 pmol/µl) 1 µl (10 pmol/µl) + 10 µl	ABsolute Blue QPCR SYBR Green Mix HOPE sense HOPE antisense purified DNA
X-qPCR	7 µl 1 µl (10 pmol/µl) 1 µl (10 pmol/µl) 1 µl (5 pmol/µl) + 10 µl	QPCR Capillary Mix X2 sense X2 antisense HBV-TaqMan probe purified DNA
HDV-RT-qPCR	0.25 µl 12.5 µl 1.25 µl 1 µl (10 pmol/µl) 1 µl (10 pmol/µl) 1 µl (5 pmol/µl) 3 µl + 5 µl	Enzyme Mix QPCR Mix RT Enhancer HDV2 sense HDV2 antisense HDV TaqMan probe H ₂ O purified RNA

All quantitative polymerase chain reactions (qPCR) and reverse transcription qPCRs were performed in a 96-well Light Cycler 480 II (Roche). Before running the PCR, mastermixes and purified RNA or DNA were pipetted into a 96-well microtiter plate and centrifuged at 700 g for 2 minutes to spin down included mastermixes and purified RNA or DNA.

2.1.11. Equipment, Consumable Supplies, and Software

Centrifuges and rotors

Rotina 420R	Hettich
Centrifuge 5810R	Eppendorf
Tablecentrifuge 5417R	Eppendorf
Tablecentrifuge 5417	Eppendorf
Tablecentrifuge 5430	Eppendorf
Beckmann LE 80, water cooled	Beckmann
SW28.38 rotor	Beckmann
SW60 TiD rotor	Beckmann

Tubes and plates

CryoTubes	Nunc/Thermo Scientific
reaction tube (0.5 ml, 1.5 ml, 2 ml)	Eppendorf
reaction tube low bind (0.5 ml, 1 ml)	Eppendorf
reaction tube (1.5 ml)	Sarstedt
Maxisorp 96-wellplate	Nunc, Thermo Scientific
Polysorp, 96-wellplate	Nunc, Thermo Scientific
96-well PCR plate	KISKER, Biotec
96-deepwell plate	Thermo Fisher Scientific
96 well cell culture plate	Becton Dickinson
96 well microtiter plate	Thermo Fisher Scientific
Cellstar Tissue Culture dishes 145x20 mm	Greiner Bio-one GmbH
Cellstar Tissue Culture dishes 100x20 mm	Greiner Bio-one GmbH
Multiwell 24 well	Becton Dickinson
Multiwell 6-well	Becton Dickinson
Falcon 15 ml 17x120 ml	Becton Dickinson
Falcon 50 ml 30x115 ml	Becton Dickinson
Reaction tube 12 ml	Greiner Bio-one GmbH
Reaction tube 8 ml	Sarstedt
Open top Polyclear centrifuge tubes (26428)	Seton Scientific
Open top Polyclear centrifuge tubes (25116)	Seton Scientific

Pipettings

pipette tip plugged (10 µl, 200 µl 1000µl)	Axym
pipette tip unplugged (10 µl, 200 µl 1000µl)	Sarstedt
low-bind pipette tip (10 µl, 200 µl, 1000µl)	Sorenson
Single-serving pipette (1 ml, 5 ml, 10 ml, 25 ml, 50 ml)	BD Bioscience

Incubator

Incubator (213)	Thermo Fisher Scientific
Stericult 200 incubator	Forma Scientific
HERATherm	Thermo Fisher Scientific
Innova 44 Incubator Shaker Series	New Brunswick Scientific

Immunofluorescence

Microscope cover glasses 12 mm Ø	MAGV, Germany
Microscope slide 76x26 mm	Menzel-Gläser

Other equipment

Picodrop Microliter UV/Vis spectrophotometer	Biozym
Refractometer	Carl Zeiss
Flexible-tube pump masterflex easyload model 7521-35	COLE-Parmer instrument CO
Flexible-tube pump masterflex 45 easy load II, model 77201-60	COLE-Parmer instrument CO

Freedom Evo 100/4D
LightCycler 480 II
Mastercycler gradient
ELISA-washer Hydroflex
ELISA-shaker ZLI 164
EL808 microplate reader
TCS SP5 confocal microscope

Software

LAS AF
Microsoft Office 2010 Excel
Microsoft Office 2010 Word
Microsoft Office 2010 PowerPoint
SigmaPlot 8.0
SPSS
Picodrop software

Tecan
Roche
Eppendorf
Tecan
Amersham Bioscience
BioTec
Leica

Leica
Microsoft
Microsoft
Microsoft
Systat Software GmbH
IBM
Biozym

2.2. Methods

2.2.1. Preparation of an RNA-Standard *in vitro* for HDV qPCR

2.2.1.1. Amplification of one HDV Genome out of the Plasmid pSVLD3

To absolutely quantify the viral RNA of HDV in a specific reverse transcription quantitative polymerase chain reaction (RT-qPCR) an RNA-standard had to be synthesized. Due to the fact that the HDV-genome was present three times in the plasmid pSVLD3, specific primers were synthesized (see 2.1.10.2) in order to amplify only one of the trimers of the plasmid. Therefore, a manual hot start PCR was performed in combination with a gradient PCR (58 °C–70 °C). Because of the fact that this DNA is then used in the T7 High Yield RNA Synthesis Kit (NEB) to generate *in vitro* RNA for the HDV RT-qPCR, specific primers were used attaching the T7-promotor at the amplified HDV DNA.

The plasmid pSVLD3 (560 ng/μl) was diluted 1:100 and 1:1000. 5 μl of each dilution were mixed with 40 μl PCR mastermix (see 2.1.10.4). Twelve different gradient steps of both dilutions were used. The samples were incubated in the gradient cycler at 98 °C for 1 minute and then cooled down to 80 °C. Now 5 μl of the polymerase mix were added (see 2.1.10.4) and PCR was continued with following steps:

temperature	time	cycles
98 °C	1 min	1
98 °C	10 sec	35
62 °C	30 sec	
72 °C	36 sec	
72 °C	10 min	1
4 °C	∞	1

Thereafter a 0.9 % ethidium bromide (EtBr) gel was performed to examine if there were additional bands beneath the specific bands. Three fractions without additional bands of each dilution were pooled and *DpnI* digested. Therefore, 50 μl of the pooled PCR template were incubated with 1 μl *DpnI* and 10 μl Tango-Buffer at 37 °C for 1 h. Inactivation of the enzyme was done at 80 °C for 20 minutes. To isolate the PCR template, a methylene blue gel was done.

2.2.1.2. Isolation and Purification of the PCR Templates

To isolate and purify the PCR template, a methylene blue gel was performed. For this purpose, PCR templates were mixed with 6x loading dye, pipetted on a 0.9 % agarose gel without EtBr and unpicked at 75 V. After running of the gel, it was stained with 0.02 % methylene blue solution (in H₂O) for 15 minutes under constant shaking. Following, the gel was washed with H₂O under constant shaking until the gel was discoloured. Then, bands were cut out, transferred into two reaction tubes including 450 μl QG buffer and dissolved at 50 °C for 10 minutes under constant shaking.

DNA was purified out of the gel with the PCR purification Kit (Qiagen), eluted in 30 μ l elution buffer and measured with the picodrop microlitre UV/V spectrophotometer (Biozym).

2.2.1.3. Synthesis of RNA *in vitro* and Phenol/Chloroform Extraction

The synthesis of RNA *in vitro* was done with the T7 High Yield RNA Synthesis Kit (NEB) as described in the manufacturer's instructions. This kit was designed for *in vitro* transcription of RNA using the T7 RNA polymerase. This polymerase is derived from the phage T7 and is extremely promoter-specific. The linearized and amplified DNA encoding the HDV genome and containing the T7 specific promoter was used as a template for *in vitro* transcription. Therefore, the T7 DNA-dependent RNA polymerase binds to its specific promoter and catalyzes the synthesis of RNA in 5'-3' direction. Then, the newly synthesized RNA can be purified and used as a standard for RT-qPCR.

After linearization and amplification of HDV DNA encoding for the HDV genome containing the T7-promotor 1 μ g and 2 μ g of purified PCR product was used to synthesize HDV-RNA.

Amplified DNA was mixed as followed

1 μ g or 2 μ g	PCR product
2 μ l	10x Reaction Buffer
2 μ l	ATP
2 μ l	GTP
2 μ l	UTP
2 μ l	CTP
2 μ l	T7 RNA Polymerase Mix
add to 20 μ l	H ₂ O

RNA-synthesis mixture was incubated for 2 h at 37 °C.

Subsequently a phenol/chloroform extraction was performed to purify the newly synthesized RNA. 20 μ l reaction volume were filled up with 160 μ l RNase free water to an end volume of 180 μ l. Then 20 μ l of 3 M sodium acetate (pH 5.2) and 20 μ l 5 M ammonium acetate were added and gently mixed by pipetting up and down. The following reaction steps were done under an extractor hood. After mixing, 200 μ l phenol/chloroform (1:1) were added and mixed by gently pipetting up and down. After that, the reaction mixture was centrifuged at 14000 rpm for 5 minutes. The aqueous phase was taken off and transferred into a new reaction tube. 200 μ l chloroform were added and mixed by gently pipetting up and down. Then the reaction mixture was centrifuged at 14000 rpm for 15 minutes. Aqueous phase was taken off again and transferred into a new reaction tube. This step was repeated once again. Afterwards 1000 μ l 100 % Ethanol (EtOH) were added and the approach was incubated for 30 minutes at -20 °C. After another centrifugation step (14000 rpm, 15 minutes, 4 °C) the supernatant was gently removed and abolished. The pellet was eluted in 30 μ l RNase and DNase free water. The RNA concentration was measured with the

picodrop microliter UV/Vis spectrophotometer (Biozym) and quality was checked with a formaldehyde gel.

2.2.1.4. Formaldehyde Gel

5 μ l RNA probe were mixed with 5 μ l RNA loading dye and loaded onto a 1 % formaldehyde gel. To produce a denaturing formaldehyde gel (endvolume 100 ml) 1 g agarose powder was added to 72 ml nuclease-free water and melted. Then 10 ml 10x MOPS buffer were added. Following steps were performed under an extractor hood. 18 ml formaldehyde (37 %) solution were added and mixed well. RNA was separated for 6 h at 30 V under an extraction hood. Finally, the formaldehyde gel was stained with EtBr and bands were visualized with UV-light.

2.2.1.5 Calculation of Genome Equivalent

Two different amounts (1 μ g and 2 μ g) of HDV-plasmid DNA were used to generate an RNA-standard for quantitative HDV PCR. After RNA synthesis the concentration of total RNA was measured. The RNA-concentration of both approaches was above 2 μ g/ μ l. For further calculation of genome equivalents in the quantitative PCR, the amount of each single nucleotide in the HDV-RNA sequence was determined and the exact weight of the ss HDV-RNA was calculated. The total amount of RNA was then determined for each approach. Thereafter, the calculated amount was multiplied with the Avogadro constant and the amount of substance was calculated to the total amount of genome equivalent per microliter (GE/ μ l).

2.2.2. Preparation of Competent Bacteria for Transformation ("chemical method")

For the transformation of plasmid-DNA into the *E.coli* strain *Stellar* (component of the In-Fusion HD Cloning System, Clontech), competent bacteria were prepared. Therefore 4 ml LB-medium were inoculated with 20 μ l of an existing bacteria suspension and incubated for 12-16 h at 37 °C. Then 2 ml of the overnight bacteria culture were transferred into 40 ml of fresh LB-medium and incubated at 37 °C until an optical density (OD)₅₅₀ of 0.45 was measured. After that, bacteria suspension was aliquoted into 50 ml flasks and incubated on ice for 15 min. The following steps were performed on ice at 4 °C. The bacteria suspension was centrifuged at 2500 revolutions per minute (rpm) for 15 minutes at 4 °C. The pellets were gently resuspended in 2 ml ice cold TBF1. 14 ml of ice cold TBF1 were added and bacteria were incubated on ice for 15 minutes again. The centrifugation (2500 rpm, 15 minutes, 4 °C) was repeated, pellets were gently taken up in 1.6 ml precooled TBF2 and incubated on ice for another 15 minutes. The bacteria suspension was aliquoted and stored at -70 °C. To test the competence of the bacteria, a control transformation with a control plasmid was performed.

2.2.3. Transformation

2.2.3.1. Transformation of Plasmid-DNA into *E.coli*

The transformation of plasmid-DNA into *E.coli* was performed on ice. Competent bacteria were incubated for 5 minutes in a precooled reaction tube, then 50 µl bacteria were added to 2 µl (approx. 20 ng) plasmid-DNA and incubated for 20 minutes. Afterwards, the bacteria were exposed to a heat-shock (42 °C) for 45-50 sec and subsequently incubated on ice for 2 minutes. Then 950 µl of LB-medium were added to each tube. Bacteria were transferred to an Erlenmeyer flask and incubated at 37 °C on a shaker for 1 hour. 20 µl of each transformation culture were exposed on LB-agar-plates containing an adequate amount of antibiotics and incubated over night at 37 °C. A single colony was picked with a sterile pipette tip and cultivated over night at 37 °C in an Erlenmeyer flask with 40 ml LB-medium and ampicillin (final concentration: 50 µg/ml) on a shaker at 180-200 rpm.

2.2.3.2. Plasmid-Preparation with the Plasmid-Plus-Midi-Kit (Qiagen)

The plasmid preparation was performed with the Plasmid-Plus-Midi-Kit (Qiagen) according to the manufacturer's recommendations.

The isolated plasmid DNA was eluted from the column using DNase and Rnase free H₂O. To define the plasmid-DNA concentration, the Picodrop Microliter spectrophotometer was used. The results were converted into µg/µl according to a standard DNA-curve.

2.2.4. Cultivation of Immortalized Cell Lines

2.2.4.1. Freezing and Thawing of Eukaryotic Cell Lines

For freezing, cells were trypsinized from 10 cm cell culture plates, resuspended in DMEM 5 % FCS, and then centrifuged by 1500 rpm for 10 minutes in a cooled table top centrifuge. After centrifugation, the cell pellet was carefully resuspended in 1.5 ml freezing medium. The cells were incubated on ice for 10 minutes. Afterwards, another 1.5 ml freezing medium were added. Then the cell-suspension was aliquoted in 1 ml freezing tubes, frozen at -70 °C overnight and stored in the gas phase (-178 °C) of a liquid nitrogen tank the other day.

To thaw immortal cell lines, the freezing tubes were warmed in a water bath at 37 °C. Then, the cell-suspension was mixed with 10 ml DMEM 10 % FCS and then carefully transferred to a 15 ml falcon tube. The cell-suspension was centrifuged at 200 g for 3 minutes. Then the cell pellet was resuspended with 10 ml DMEM 10 % FCS. The cells were sown on 10 cm cell-culture plates and incubated at 37 °C, 5 % CO₂.

2.2.4.2. Passaging of Immortalized Cell Lines

Huh7, AML12 and HepG2 cells were cultivated in 5 % FCS/DMEM and regularly splitted before reaching a confluent stage. Cells were incubated into an incubator at 37 °C, 96 % humidity, 7 % CO₂.

Before passaging HepG2 cells, cell culture plates were coated with collagen type I. For this purpose 5 ml of a collagen Type I solution (0.2 mg/ml) were layered on the cell culture plate. Collagen solution was distributed by gently swinging and then removed from the plate.

2.2.5. Phenotypic Resistance Assay for Characterization of Patient Isolates

The phenotypic resistance assay was established in the working group of D. Glebe at the Institute of Medical Virology by A. Geipel (2011), and further modified by H. Niekamp (2013) and performed in this thesis after following protocols.

2.2.5.1. Transfection

Huh7 Munich cells were sown in a ratio 1:3 on 10 cm cell culture dishes in DMEM 5 % FCS. After reaching a confluency of 80 %, cells were transfected with plasmid-DNA using the transfection reagent FuGene HD (Promega) in a ratio of 4:1 (FuGene (µl):plasmid-DNA (µg)). A total amount of 8 µg plasmid-DNA (7 µg plasmid-DNA, 1 µg pSEAP2control-plasmid) and 32 µl FuGene HD transfection reagent were transfected. The transfection mixture was pipetted in DMEM without FCS, vortexed well and incubated at RT for 15 minutes. In the meantime, the medium was removed and the cells were washed 1x with 5 ml PBS++. 10 ml of fresh and preheated DMEM 2 % FCS were added to the cells. After the incubation time, the transfection mixture was added and cells were incubated over night at 37 °C. The replication efficiency of the transfected HBV in the presence of nucleos(t)ide analogs was tested by a phenotypic assay (see 2.2.5.2).

For transfection of HBV variants with stop mutations in the S-ORF, cells were sown 1:2 on 10 cm plates and transfection was performed as described before. Then, the supernatant was analyzed for secreted HBV virions and subviral particles **by an** ELISA (enzyme linked immunosorbent assay), qPCR or caesium chloride (CsCl)-gradient.

For transfection of HDV-genome in combination with differently mutated surface proteins of HBV, 3 µg pSVLD3, 4 µg plasmids encoding LHBs-expressing HBV-constructs, and 1 µg pSEAP2control were incubated on Huh7 cells over night. After washing as described in 2.2.5, cells were cultivated on 24 cm cell culture dishes for the following 12 days with DMEM without FCS. The supernatant of day 2, 4, 6, 9 and 12 after transfection were analyzed for HDV-genomes. A SEAP-assay was performed at day 3 after

transfection to calculate the transfection efficiency (see 2.2.5.3). Cell viability was tested by WST-1 test (see 2.2.6).

2.2.5.2. Phenotypic Assay

Four nucleos(t)ide analogs were diluted in 2 % FCS/DMEM without phenolred. 100 μ l of each dilution were provided on a 96 cell cell culture plate depicted in Table 1. Each nucleos(t)ide analog was prepared with six different dilutions and six not inhibited wells (without any nucleos(t)ide analogs). These samples were prepared three times (Table 1). For every analyzed plasmid, 96 data points could be produced. The HBV wild type plasmid pCH9-3091 was additionally transfected and served as control for the replication capacity of the tested patient isolates.

Table 1 Schematic overview of pipetted nucleos(t)ide analogs with different concentrations.

	Adefovir			Entecavir			Lamivudine			Tenofovir		
	1	2	3	4	5	6	7	8	9	10	11	12
A	200 μ M			2000 nM			200 μ M			200 μ M		
B	40 μ M			400 nM			40 μ M			40 μ M		
C	8 μ M			80 nM			8 μ M			8 μ M		
D	1.6 μ M			16 nM			1.6 μ M			1.6 μ M		
E	0.32 μ M			3.2 nM			0.32 μ M			0.32 μ M		
F	0.064 μ M			0.64 nM			0.064 μ M			0.064 μ M		
G	no inhibitor			no inhibitor			no inhibitor			no inhibitor		
H												

Therefore, transfected cells were washed 1x with 10 ml PBS and 5 ml of trypsin/PBS (1:5) were added and trypsinized at 37 °C. The cells were gently resuspended and carefully transferred into 50 ml falcon tubes including 20 ml preheated DMEM 2 % FCS. The cells were centrifuged at 60 g for 6 minutes (first washing step). Afterwards the supernatant was decanted and resuspension and centrifugation steps were repeated two more times. After the second washing step the resuspended cells were transferred into a new 50 ml falcon tube. Finally, the cell pellet was gently resuspended in 20 ml preheated 2 % FCS/DMEM (without phenolred). 100 μ l of each transfection sample were added to a single well of a 96-well cell culture plate prepared with six different dilutions of four nucleos(t)ide analogs. Cell culture plates were incubated for three days at 37 °C. Then, the supernatant was removed and transferred into a new 96-well plate to isolate the viral DNA using the automated pipette robot Freedom Evo (Tecan) (see 2.2.8).

2.2.5.3. Calculation of Transfection-Efficiency by Secreted Alkaline Phosphatase- (SEAP-) Detection Assay

Detection of secreted alkaline phosphatase assay was used to calculate the transfection efficiency. Therefore, 50 μ l supernatant (eight-fold samples) of cells that were not inhibited with any nucleos(t)ide analog were transferred to a 96-well plate and the endogenous phosphatase was inactivated at 65 °C for 30 minutes. Due to the fact that the secreted alkaline phosphatase is heat-resistant, this enzyme is not inactivated during this inactivation-process. Afterwards, 100 μ l 2x SEAP-buffer and 50 μ l SEAP-substrate were added to each well. The optical density (OD) was measured at a wavelength of 450 nm in an ELISA-reader when the first standard reached an OD of 1.0. To calculate the transfection efficiency in %, an internal SEAP-standard was used. For this purpose, the supernatant of pSEAP2-control transfected cells served as a positive control and was diluted in a 1:2 dilution series. The supernatant of untransfected cells served as a negative control. The mean value of eight-fold samples was calculated and compared to the signal of the internal SEAP-standard. The values that were obtained were calculated to the transfection efficiency in %.

2.2.5.4. Statistical Analysis of the Data from Phenotypic Resistance Assay *in vitro*

Newly synthesized viral genome equivalents, measured in the supernatant of Huh7 cells transiently transfected with HBV-expressing plasmids, were converted to relative numbers. Therefore, the mean value of all non-inhibited numbers was calculated and determined as 100 %. The data were analyzed using a non-linear regression model with three parameters to calculate the IC_{50} and IC_{90} values and based on that, the resistance factors 50 (RF_{50}) and RF_{90} were calculated (Figure 7 A). The IC_{50} indicates the half of maximum of viral replication at a given concentration of the inhibitor. The IC_{90} indicates the inhibition by 90 % of a tested inhibitor on viral replication. The resistance factors indicate the differences of the IC from wild type to the tested mutant (Figure 7 B). For calculation of resistance factor, consensus curves of the tested wild types were generated and used.

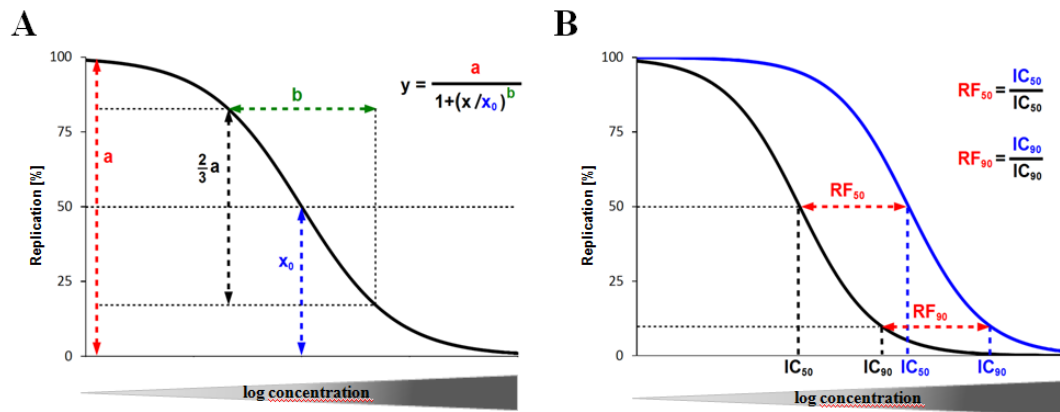


Figure 7: A) Regression model for calculation of IC_{50} and IC_{90} . Figure shows replication (% , Y-axis) depending on used concentration of inhibitor (logarithmic scaling, X-axis). Inhibition curves are indicated with sigmoid functions in the upper right area. The amplitude is presented as **a** and indicates the difference between no and maximum inhibition. The parameter **b** defines the gradient of the curve (difference of the X-axis between the x-values with corresponding y-values of $1/6 a$ and $5/6 a$). The parameter x_0 defines the inflection point ($y=1/2$). **B) Calculation of IC_{50} and IC_{90} as well as resistance factor 50 and 90 (RF_{50} , RF_{90}).** Figure shows replication (% , Y-axis) depending on used concentration of inhibitor (logarithmic scaling, X-axis). The IC_{50} indicates the inhibition by half of a particular substance on the viral replication. The IC_{90} indicates the inhibition by 90 % of a tested inhibitor on viral replication. The RF_{50} and RF_{90} indicate the differences of the **IC** from wild type to the tested mutant. Figures were kindly provided and modified by H. Niekamp (Niekamp 2013 in press) and Dr. A. Geipel (poster presented at International Meeting on Molecular Biology of Hepatitis B Virus, Oxford, UK, 2012).

The significance of the IC differences of the tested mutants compared to the wild type was statistically analyzed with an univariate ANOVA (analysis of variants). For ANOVA, concentrations of tested inhibitors with no inhibitory effects on the wild type were not considered. If many data records were compared to the consensus wild type curves, the α -niveau after Bonferroni (Köhler et al. 2007) was adjusted. The resistance limits were indicated in the results.

2.2.6. Cell Viability Test with WST-1 (Roche)

The viability test was done after manufacturer's recommendations. 5 ml of a 1:50 dilution of WST-1 reagent (water soluble tetrazolium salt) diluted in 2 % FCS/DMEM without phenolred was pipetted onto the cells and incubated for 30 minutes at 37 °C. 100 μ l of each supernatant were transferred into a 96 well microtiter plate. Extinction of the colored substrate was measured by a photometer at a wave length of 450 nm (reference wavelength: 620 nm).

The WST-1 reagent is a colorimetric assay that allows the measurement of the relative amount of cell proliferation in cell culture. It includes soluble tetrazolium salt which is cleaved into formazan by cellular enzymes. For a long time, the reduction of the tetrazolium salt into formazan was attributed to the mitochondrial succinate-dehydrogenase and was therefore an indicator of an active cell redox activity. Recent studies show that this reduction process is largely more dependent on other enzymes in different cellular compartments, for example in the cytoplasm and in the regions of plasma membranes (Bernas and Dobrucki 2002). Nevertheless, the amount of reduced tetrazolium salt correlates to the number of metabolically active cells and is manifested in a color change from light red into yellow.

2.2.7. Isolation of Viral Genomes from Supernatant, Plasma, or Cell Lysates

For quantification of viral nucleic acid by qRT-PCR the viral RNA or DNA has to be purified from serum or out of infected cells. Therefore different commercial kits were used.

2.2.7.1. Isolation of Intracellular Viral RNA and DNA

12 to 15 days after infection of PTHs with HBV or HDV, the intracellular RNA was purified with the Nucleo Spin RNAII Kit (Macherey-Nagel) after manufacturer's instructions. Isolated RNA was dissolved in 60 µl elution buffer and frozen at -70 °C.

2.2.7.2. Manual Isolation of Viral RNA and DNA in the Supernatant or in Serum

Viral RNA or DNA from serum, plasma or supernatant was purified by using the High Pure Viral Nucleic Acid Kit (Roche). Purification procedure was performed after manufacturer's recommendations with following modifications: the lysis was stopped by adding 100 µl of isopropanol after incubation at 72 °C for 10 minutes. Purified DNA or RNA was eluted in 50 µl elution buffer.

2.2.7.3. Automated Isolation of viral DNA in the Supernatant with Freedom EVO

To isolate the viral DNA from the supernatant of transiently transfected cells for the phenotypic characterization, the automatic pipette robot Freedom EVO 100/4D (Tecan) was used in combination with the Sample Preparation System DNA Kit (Abbott). Used buffers were adjusted to the volume of the probe and a pipetting protocol was established for the automatic pipette robot.

Lysing the supernatant was done by mixing 100 µl supernatant from transiently transfected cells with 120 µl lysis buffer (70 µl H₂O, 40 µl lysis buffer, 10 µl external proteinase K (Abbott)). After incubation (58 °C, 15 minutes), additional 300 µl lysis buffer and 20 µl magnetic beads were added and incubated once again. Purified DNA binds to the magnetic beads. By the use of a magnet, the beads were pulled to the wall of the reaction tube and the supernatant could be removed. 300 µl of washing buffer (*Wash1*) were added and the DNA was incubated at 58 °C for 2 minutes. Supernatant was removed and the beads with bound DNA were washed twice with washing buffer (300 µl, *Wash2*). To eliminate remaining ethanol, magnetic beads were incubated at 80 °C for 15 minutes. Separation and elution of the DNA from magnetic beads was done by adding 100 µl H₂O and incubation at 80 °C for 8 minutes.

2.2.8. qPCR

2.2.8.1. SYBR-Green Based qPCR

For the detection of HBV-DNA in the supernatant of cell culture the HOPE-PCR was performed with SYBR Green as the detection dye. Concerning the HOPE-project, the quantitative HOPE-PCR was established (Geipel 2011) that is able to discriminate between plasmid-DNA and the relaxed circular HBV DNA. The specific HOPE-primers are deliberately chosen to bind preferentially to regions of the newly synthesized viral genomes amplifying a 300 bp fragment. The binding of the specific HOPE-primers on the plasmid-DNA would lead to the amplification of a longer PCR fragment. Due to the fact that the elongation time is optimized for the shorter fragments (300 bp), the amplification of the plasmid-DNA is about 1000-fold less efficient than the amplification of the newly synthesized, relaxed circular HBV DNA (Geipel 2011). Purified HBV DNA from Huh7 cells transiently transfected with the HBV wt plasmid served as a standard for absolute quantification. Therefore, Huh7 cells were transfected with the HBV wt plasmid pCH9-3091 (see 2.2.5.1) and incubated for three days without any inhibitor. Then, the supernatant was purified (see 2.2.7.2) and HBV genome equivalents were calculated with the help of the WHO-standard.

Before running the PCR, 10 µl of the mastermix were pipetted into the well of a 96-well plate. 10 µl template DNA were also added and the HOPE-PCR was performed (Table 2) in a 96- well LightCycler 480 II (Roche).

Table 2: Light Cycler program for HOPE-PCR

	activation	amplification			melting curve			cooling
cycles	1	40			1			1
target temperature (°C)	95	95	60	72	95	60	95	40
measurement				single			continuously	
time	15 min	15 sec	10 sec	20 sec	10 sec	15 sec		30 sec
step size (°C/min)							6	
acquisition mode		quantification						

2.2.8.2. TaqMan Probe Based qPCRs

For X-PCR and HDV-PCR, specific TaqMan-probes were used as the detection dye (Heid et al. 1996).

2.2.8.2.1. X-PCR

The detection of HDV DNA using the X-PCR was performed after Jursch et al. (2002). This PCR is very sensitive and highly specific because the used primers and probes recognize a highly conserved region in the X-ORF of the viral genome.

To perform the X-PCR, 10 µl of mastermix (see 2.1.10.5) were mixed with 10 µl purified DNA. PCR was performed as described in Table 3 in a 96- well Light Cycler 480 II (Roche). For absolute quantification,

HBV DNA, purified from human serum of a chronically infected HBV patient with a certain concentration of HBV DNA, was used.

Table 3: Light Cycler Program for X-PCR

	activation	amplification			cooling
cycles	1	45			1
target temperature (°C)	95	95	62	72	40
measurement	none	none	single	none	none
time	15 min	10 sec	15sec	13 sec	30 sec
temperature (-1°C per cycle)			50 sec		
step size (°C/min)			1		
acquisition mode		quantification			

2.2.8.2.2. HDV RT-qPCR

For the detection of HDV RNA, primers were used that recognize highly conserved regions at the C-terminus of the small hepatitis delta antigen. For HDV RT-qPCR 5 µl purified RNA in solution were pipetted into each well of a 96-well PCR plate. The probes were incubated for 1 minute at 95 °C in the Light Cycler to denature secondary structures of the RNA. Afterwards, 20 µl of mastermix (see 2.1.10.5) were added and the PCR was performed as described in Table 4. Plasmid contaminations were removed by DNase-digestion before HDV RT-qPCR. Therefore 1 µl DNase I (RNase free, protease free), 0.2 µl H₂O and 0.8 µl 10x Reaction Buffer with MgCl₂ were mixed. 2 µl of the DNase mastermix were mixed with 5 µl purified RNA and incubated for 1 h at 37 °C. To inactivate the DNase I the probes were incubated for 5 minutes at 95 °C. After cooling down, the RT-qPCR mastermix was added. For absolute quantification, an *in vitro* generated full length genomic HDV RNA standard was used (see 2.2.1).

Table 4: Light Cycler Program for HDV-PCR

	reverse transcription	activation	amplification			cooling
cycles	1	1	40			1
target temperature [°C]	50	95	95	60	72	40
measurement	none	none	none	none	single	none
time	15 min	15 min	15 sec	30 sec	15 sec	30 sec
ramp rate (°C/s)	4.4	4.4	4.4	2.2	4.4	4.4
temperature (-1°C per cycle)				50		
step size (°C/min)				1		
step delay (cycles)				1		
acquisition mode			quantification			

2.2.9. Preparation of a Sucrose Gradient for Isolation and Purification of HBV and HDV

The isolation and purification of HBV and HDV from serum or plasma of chronically infected patients was done with a continuous sucrose gradient as described previously (Glebe et al. 2003, Glebe and Gerlich 2004). Plasma or serum of chronically infected patients was centrifuged at 3000 rpm for 15 min to purify the plasma or serum from larger aggregated particles. 30 ml of the purified plasma or serum were layered on a sucrose cushion consisting of 6 ml 15 % sucrose/TNE (w/w) and 2 ml of 10 %

sucrose/TNE (w/w) and centrifuged at 25.000 rpm, 16 hours at 10 °C in a SW28.38 rotor in the LE 80 ultracentrifuge (Beckmann, water cooled). After centrifugation the supernatant was decanted and the pellet, containing virus and subviral particles was dissolved in 1 ml cold TNE and layered on a discontinuous sucrose density gradient (3 ml 60 %, 4 ml 45 %, 4 ml 35 %, 5 ml 25 %, 5 ml 15 % sucrose dissolved in TNE (w/w)). The sucrose gradient was centrifuged at 25.000 rpm, 15 hours at 10 °C and then fractionated from the bottom to the top. Protein concentration was measured with the picodrop microlitre spectrophotometer (Biozym) and density was measured via refractrometry. 20 µl of each fraction were purified for the qPCR. HBV DNA was detected with the HBV X-PCR and HDV RNA was detected with the HDV RT-qPCR. The concentration of virions was calculated as genome equivalent per ml (GE/ml).

2.2.10. Preparation of a Linear Caesium-Chloride (CsCl)-Gradient

To analyze viral particles, a linear caesium chloride (CsCl)-gradient was performed (Gerlich et al. 2010; Bremer et al. 2009b). In a total volume of 1 ml, plasma or cell culture supernatant was treated with or without Nonident P-40 (NP40) (1 % final concentration (f.c.)) and TCEP (50 mM f.c.) for 1 h at room temperature. In the meantime 1.7 ml of 24 % CsCl (density: 1.21 g/ml) and 1.42 ml of a 42 % CsCl (density: 1.45 g/ml) dissolved in TNE (w/w) were mixed using a gradient-mixer to make a linear gradient. After the incubation, the treated or untreated samples were gently layered on the CsCl-gradient and centrifuged at 37.000 rpm, 18 hours at 10 °C a SW60 TiD rotor in the LE 80 ultracentrifuge (Beckmann, water-cooled). Afterwards the gradient was fractionated from the bottom to the top in 300 µl aliquots with a peristaltic pump. In each fraction the density of CsCl was measured by refractrometry. For the detection of viral DNA or RNA, 200 µl of each fraction were purified with the High Pure Viral Nucleic Acid Kit (Roche) (see 2.2.7.2). Then a qPCR for HBV or a RT-qPCR for HDV was performed.

2.2.11. Isolation and Cultivation of Primary *Tupaia* Hepatocytes (PTHs)

Primary hepatocytes from the Asian tree shrew *Tupaia belangeri* were freshly isolated and cultivated to perform infection assays with HBV and HDV purified from serum, plasma or cell culture supernatant. The isolation was carried out according to a modified two-step-collagenase method first described by Seglen et al, (1976). After isolation, cells were cultivated in modified hepatocytes growth medium as described by Glebe et al (2003).

In brief, the liver of a 2-4 year old tupaia was prepared and perfused via the portal vein with first 5 mM EGTA/HBSS (20 minutes) following 5 mM EGTA free HBSS (10 minutes). After that, the liver was incubated in a recirculation system with preheated (37 °C) sterile filtrated collagenase solution (20 minutes) until the liver capsules became porous. After washing and pelleting the cells (3 times, 4 °C, 40x g, 6 minutes), they were gently resuspended in 40 ml ice-cold hepatocytes growth medium including

10 % FCS and collagen-coated 24-well cell culture plate with or without cover slips. After an incubation time of 4 h (37 °C, 5 % CO₂), plating medium was removed and switched to FCS free HGM (500 µl).

2.2.12. Infection of PTHs with HBV and HDV

If not described differently, three days after isolation, PTHs were infected with purified HBV or HDV. Virus fractions were thawed and kept on ice. For infection, PTHs were washed once with 500 µl preheated hepatocytes growth medium containing caspofungine (5 µg/µl f.c.). Hepatocyte growth medium for infection contains a final concentration of 5 µg/µl caspofungine, 4 % PEG 8000, and 1×10^8 GE (0.2 µl) purified HBV or 1×10^7 GE (0.6 µl) purified HDV. To inhibit the infection with HBV or HDV, cells were preincubated with myr preS1 peptide (1 µM f.c.) for 30 minutes. PTHs were infected with a total volume of 300 µl infection medium for 16 h at 37 °C. Then, the inoculum was removed and cells were washed two times with 500 µl preheated hepatocytes growth medium/caspofungine. Cells were incubated and cultivated with 500 µl fresh hepatocytes growth medium/caspofungine for the following 12 (for HDV) to 15 (for HBV) days. Supernatants of day 4, 7, 11, and 15 of HBV infected cells were analyzed by ELISA. HDV infected cells were lysed on day 12 after infection with Nucleo Spin RNAII Kit from Macherey-Nagel (see 2.2.7.1).

2.2.13. ELISA against Secreted HBV Surface Proteins

Secreted subviral particles and uncoated capsids were detected with a sandwich-ELISA against the LHBs (1 µg/ml MA18/7), MHBs (2 µg/ml Q19/10), and SHBs (1 µg/ml C20/02), or HBc (20 µg/ml DAKO, 1:20.000 Gö-Schaf). A 96-well microtiter plate was coated with 100 µl of the respective capture antibodies listed above and diluted in coating buffer for 24 h at 4 °C. For washing of the microtiter plates, an automated ELISA-washer (TECAN) was used. The washing program included four washing steps (2 x 0.1 % Tween20/PBS and 2 x PBS, 300 µl per well). Afterwards, the wells were blocked with 200 µl of 10 % FCS/TNE for 2 h at room temperature. After washing, 100 µl of cell culture supernatant or supernatant from infected PTHs were incubated over night at 4 °C. For quantification, an HBsAg-standard (ID1) was used; diluted 1:2 in 1 % Casein/PBS (10-0.3 ng/ml HBsAg). On the next day the washing steps were repeated and 100 µl of the detection antibody (anti-HBs biotin conjugate Enzygnost HBsAg 6.0, 1:40 diluted in 0.1 % Casein/PBS) were incubated on a shaker for 1 h at room temperature. After washing, streptavidin-POD (diluted 1:500 in 0.1 % Casein/PBS) was added and incubated on a shaker for another 30 minutes. Wells were incubated on a shaker with 100 µl of OPD-ELISA-substrate (for MA18/7-, C20/02- and core-ELISA) or TMB Xtra Ready-to-use-substrate (for Q19/10-ELISA) in the dark for 5-15 minutes. The reaction was stopped with 50 µl 0.5 M sulphuric acid. If the OPD-ELISA-substrate was used, extinction of the colored substrate was measured photometrically at 492 nm

(reference-wavelength: 620 nm). If the TMB Xtra Ready-to-use-substrate was used, extinction of the colored substrate was measured photometrically at a wave length of 450 nm.

2.2.14. UREA-Assay

Urea production and secretion of primary hepatocytes can be used to determine their cell viability. Therefore 100 µl of the supernatant of infected PTHs were pipetted into a 96 microtiter plate. 75 µl o-phthalaldehyde and 75 µl naphthylethylendiamine-reagent were added. After an incubation of 5-15 minutes in the dark at room temperature, reaction was measured photometrically at 492 nm (reference-wavelength: 620 nm). To calculate the secreted amount of urea, an urea-standard was pipetted (25 mM–0.3 mM urea, 1:2 diluted). The measured amount of secreted urea was allocated with the detected amount of HBsAg or HDV-RNA.

2.2.15. Staining for Immunofluorescence

After fixation, cells on cover slips were permeabilized with 0.2 % TritonX 100/PBS at RT for 30 minutes. Afterwards, the cover slips were washed with PBS and blocked with 10 % FCS/DMEM without phenolred for 30 minutes. The cells were incubated with a monoclonal primary antibody against the HBV surface antigens (5 µg/ml C20/02, 5 µg/ml MA18/7, 10 µg/ml Q19/10) and the HBV capsid (50 µg/ml anti HBc, DAKO) for 1.5 hour at 37 °C. After incubation, the cover slips were washed five times with 1x PBS and stained with a secondary antibody either anti-mouse-Alexa-594 (10 µg/ml) or anti-rabbit-Alexa-488 (10 µg/ml) respectively, at 37 °C for 30 minutes. Then the washing steps were repeated and finally nuclei were stained with DAPI (2.5 µg/ml) at RT for 10 minutes. Afterwards, the cover slips were washed again and embedded on microscope slides using moviol.

All samples were analyzed with the TCS SP5 confocal microscope (Leica).

3. Results

3.1. Phenotypic Characterization of Isolates from Chronically Infected HBV-Patients

The long-term treatment of chronically HBV-infected patients with nucleoside- and nucleotide analogs often leads to the selection of resistance mutants in the gene of the viral polymerase (Zoulim and Locarnini 2009). For phenotypic characterization of isolates from chronically infected HBV-patients, an *in vitro* phenotypic resistance assay was established at the Institute of Medical Virology at the University of Gießen (AG Glebe) in collaboration with the Institute of Virology at the University of Munich (AG Protzer), to test the sensitivity of resistance mutations against the four commonly used nucleoside and nucleotide analogs in clinical practice (Geipel 2011). To continue this work, phenotypic characterization of five patient isolates from chronically infected HBV-patients possessing characteristic HBV surface protein variants was done. The results are shown in Table 5. The corresponding resistance profiles can be found in the appendix, Figure 31-35.

Table 5: Results of the phenotypic resistance test of five patient isolates against four clinical used nucleos(t)ide analogs adefovir (ADV), tenofovir (TDV), entecavir (ETV) and lamivudine (LMV). Five isolates from chronically infected HBV-patients were analyzed with the phenotypic resistance assay to characterize their resistance profiles against four clinically used nucleos(t)ide analogs. Relevant mutations for resistance are indicated within the rt-domain. Mutations in the rt-domain and the s-domain of the viral polymerase as well as genotype (gt) of each isolate are noted. No resistance is marked in **green**, intermediate resistance is marked in **orange** and full resistance is marked in **red**. The viral fitness describes the replication capacity of the patient isolate and was calculated relative to the replication capacity to the wild type and is presented in %. The resistance factors RF₅₀ and RF₉₀, the correlation of tested mutant to wild type (R²), as well as the significance (sign) are indicated. The α -niveau was adjusted after Bonferroni (Köhler et al. 2007) with following limits of significance: non-significant (ns) \triangleq p > 0.01, significant (*) \triangleq p < 0.01

isolate	mutation		gt		ADV	TDV	ETV	LMV	viral fitness [%]
	rt-domain	s-domain							
wt			D	RF ₅₀	1	1	1	1	100
				RF ₉₀	1	1	1	1	
				sign	---	----	----	----	
				R ²	0.97	0.99	0.99	0.99	
KW 6a-6	V191I	W182*	D	RF ₅₀	---	1.3	10.3	1.3	247
				RF ₉₀	---	0.9	10.3	0.9	
				sign	*	*	*	ns	
				R ²	0.99	0.89	0.95	0.96	
KW 11a-1	L164M I266R	S143L, L175S, L216*	D	RF ₅₀	---	1.1	7.2	652.5	25
				RF ₉₀	0.3	1.2	24.4	134.8	
				sign	*	ns	*	*	
				R ²	0.86	0.99	0.89	0.35	
KW 14-8	M204I	W196S	A	RF ₅₀	1.0	2.1	134.9	>1000	37
				RF ₉₀	0.7	2	>1000	>1000	
				sign	Ns	*	*	*	
				R ²	0.98	0.91	0.87	0.03	
RK-172-2	L180M M204V	I195M L209V	A	RF ₅₀	2.0	2.3	52.09	>1000	19
				RF ₉₀	1.9	2.5	660.53	>1000	
				sign	*	*	*	*	
				R ²	0.99	0.99	0.91	0.75	
RK 172-4	A181T M204V	W172*	A	RF ₅₀	2.0	3.1	2.7	653	2
				RF ₉₀	1.54	7.3	12.5	>1000	
				sign	*	*	*	*	
				R ²	0.99	0.97	0.99	0.94	

In the phenotypic resistance assay, an intermediate resistance to the drug ETV could be detected for this isolate (Table 5, KW 6a-6, appendix Figure 31). Due to the strong overlap of the open reading frame of the relaxed circular HBV genome, mutations in the ORF of the viral polymerase directly affect the ORF of the viral surface proteins (Figure 8 A, page 45). Patient isolate KW 6a-6 showed the mutation rtV191I, which leads to a stop mutation at position 182 in the SHBs (sW182*).

The stop mutation at position 216 in the SHBs (sL216*) was observed in patient isolate KW 11a-1. Phenotypic analysis of this clone showed a resistance to LMV and a weak resistance to ETV, a resistance to ADV or TDV could not be detected (Table 5, KW 11a-1, appendix Figure 32).

A long-term treatment with the nucleoside analogue LMV is known to induce the primary mutation rtM204I, as shown in the patient isolate KW 14-8. The mutation rtM204I leads to the amino acid change from tryptophan to serine in the SHBs (sW196S) (Figure 8 B). The isolate KW 14-8 demonstrated a strong resistance to LMV and ETV. It also showed a weak resistance to TDV. A resistance to ADV was not observed (Table 5, KW 14-8, appendix Figure 33).

The isolate RK 172-2 had the mutations L180M and M204V in the rt-domain, which also leads to the changes I195M and L209V in the viral S-ORF. The consequences of these mutations for the SHBs are unknown. A strong resistance to LMV and ETV could be observed in the phenotypic assay. These mutation patterns also showed a weak resistance to TDV and ADV (Table 5, RK 172-2, appendix Figure 34).

The amino acid change from alanine (A) to threonine (T) or valine (V) at position 181 of the rt-domain induces a stop mutation at position 172 of the SHBs (Figure 8 A, page 45). Sequence analysis of the isolate RK 172-4 showed the mutation rtV181T with the additional mutation rtM204V. The data from phenotypic resistance assay demonstrated a strong resistance to LMV but only an intermediate resistance to ADV. Surprisingly, a weak resistance to ETV and TDV could also be observed (Table 5, RK 172-4, appendix Figure 35).

The phenotypic characterization of five tested isolates, derived from chronically infected HBV patients, showed typical resistance patterns for all four common nucleos(t)ide analogs. In most of the cases, the viral fitness of the tested patient isolates was strongly decreased compared to the viral fitness of the wildtype.

3.2. Characterization of Known HBsAg-Mutations During Antiviral Therapy of Chronic Hepatitis B

During long-term antiviral therapy with nucleos(t)ide analogs, mutations in the catalytic subdomain of the viral polymerase arise. Due to the strong overlapping open reading structure of the HBV genome, mutations in this domain lead to mutations in the internal loop in the SHBs between transmembrane II and IV (Zoulim and Locarnini 2009) (Figure 8). Some mutations in the viral surface proteins are known to induce altered infectivity or virion secretion (Warner and Locarnini 2008). In this work, the consequences of mutations in the viral surface proteins especially in the SHBs on the viral life cycle should be analyzed in more detail, because it is known from the literature that the SHBs is crucial for viral assembly and secretion (Bruss 1997).

3.2.1. Secretion of Enveloped Virions and Subviral Particles

To analyze if mutations in the internal loop of the SHBs influence the secretion of virions and subviral particles, single mutations (stop mutations or amino acid changes, see Figure 8) were inserted into the HBV full genome wild type plasmid pCH9-3091 via site directed mutagenesis by Dr. Maria Neumann-Fraune (Uniklinikum Köln), and kindly provided by her for this thesis. With the help of these plasmids, these HBV surface protein mutants should be analyzed in terms of their ability to secrete virions and subviral particles. To do so, Huh7 cells were transiently transfected with HBV expression plasmids encoding HBV full genomes with mutations in the SHBs depicted in Figure 8.

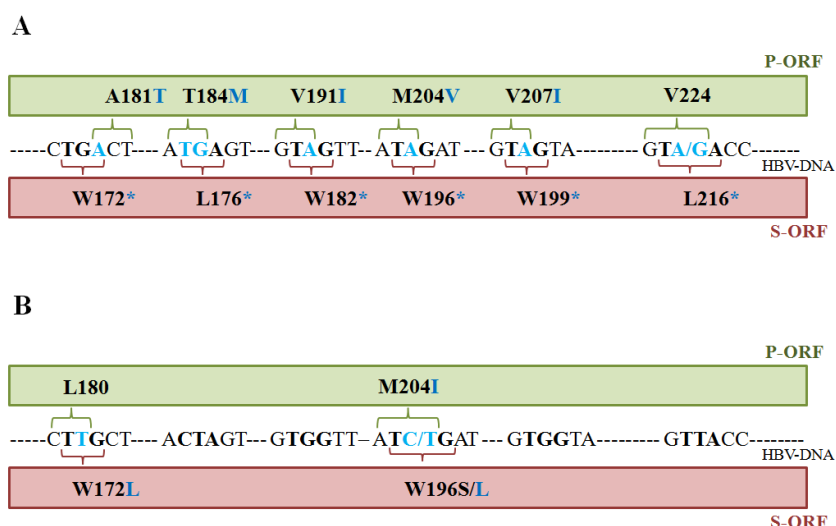


Figure 8: Overview of the generated HBV surface protein variants. Generated HBV surface protein variants in the HBV S-ORF with the corresponding mutations in the P-ORF and nucleic acid changes in the viral DNA. Nucleotide changes were introduced via site-directed mutagenesis. Viral DNA is depicted as a **black** dotted line. Nucleotide changes in the viral DNA are highlighted in **light-blue**. Typical amino acid changes that resulted from the nucleotide change in the P-ORF (**green** bar) and stop mutations and/or amino acid changes in the S-ORF (**red** bar) are highlighted in **dark-blue**. **A)** Generated nucleotide changes in the viral DNA causing stop mutations in the S-ORF at position W172, L176, W182*, W196*, W199, and L216. **B)** Generated nucleotide changes in the viral DNA causing amino acid changes in the S-ORF at position W172 and W196.

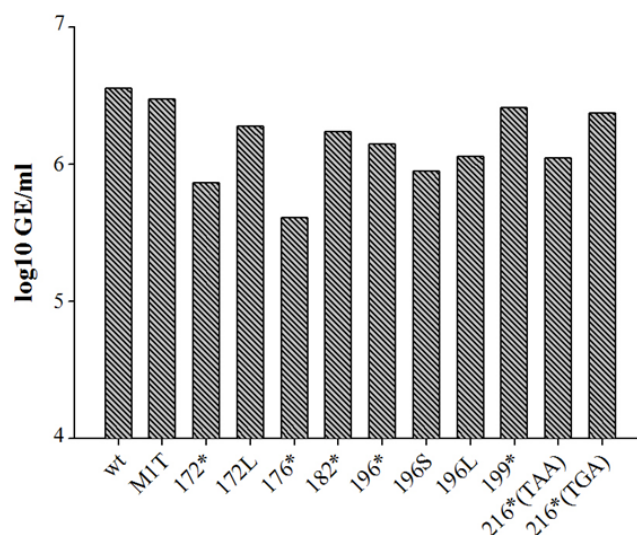


Figure 9: Detected genome equivalents in the supernatant of Huh7 cells transiently transfected with HBV expression plasmids encoding stop mutants within their S-ORF. Newly secreted viral particles were detected with qPCR in the supernatant of cells transiently transfected with stop mutants three days after transfection. Figure presents data of one approach (duplicates). The results are representative data of three independent experiments.

Three days after transfection, viral DNA could be detected in the supernatant of all stop mutants (Figure 9). The secretion of viral DNA was decreased by a factor of 5 to 10 in supernatant of mutants with a stop mutation at position 172 or 176 of the SHBs (Figure 9). Mutations at other positions of the SHBs had no influence on the secretion of viral DNA (Figure 9).

According to the literature, some mutations, for example the 172* mutation in the HBV surface protein, are believed to be defective in secretion of subviral particles and virions (Warner and Locarnini 2008). The analysis of viral DNA in the supernatant of transiently transfected cells cannot distinguish between viral DNA encapsidated in virions or uncoated core-particles. Therefore, the secretion of HBsAg was screened by a sandwich-ELISA against LHBs, MHBs, and SHBs.

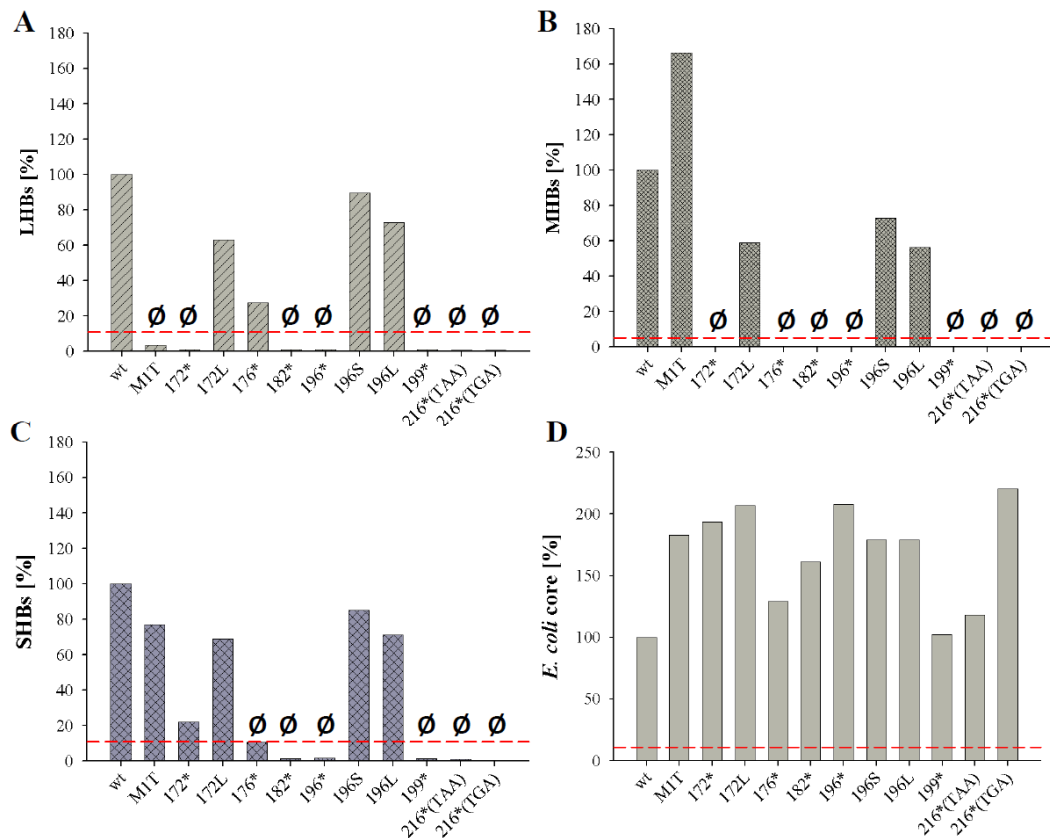


Figure 10: Results of the ELISA against all three HBV surface proteins and HBV core. Supernatant of Huh7 cells transiently transfected with HBV surface protein variants was tested for newly secreted HBsAg and HBV core-particles, three days after transfection. **A)** Results of the ELISA against LHBs using MA18/7. **B)** Results of the ELISA against MHBs using Q19/10. **C)** Results of the ELISA against SHBs using C20/02. **D)** Results of the ELISA against HBV core, using a polyclonal antibody against the core antigen derived from rabbit (DAKO). Cut-off for each ELISA is presented with red dotted line.

In the supernatant of Huh7 cells transfected with the HBV wt, all three HBV surface proteins could be detected (Figure 10 A, LHBs-ELISA, B MHBs-ELISA, C SHBs-ELISA). When initiation codon of LHBs was mutated (mutant M1T), only SHBs and MHBs but no LHBs could be found (Figure 10, M1T B and D). In most of the tested HBV variants with mutations in the S-ORF, a stop mutation in the SHBs prevented secretion of HBsAg (Figure 10, A, B, C, all mutants including a stop mutation) with the exception of the mutant 172* and 176*. A stop mutation at position 176 in the SHBs leads to the secretion of 30 % LHBs (Figure 10 A). 20 % of SHBs secretion compared to the wt could be observed for mutant 172* (Figure 10 C). An amino acid change from tryptophan to serine or leucine did not affect the secretion of HBsAg (Figure 10, A, B, C, 172L, 196S, 196L). MHBs-secretion was reduced after amino acid changes at position 172 and 196 (Figure 10 B).

During the synthesis of HBV in cell culture, a considerable amount of uncoated capsids is secreted (Nassal 1992; Bremer et al. 2009a; Bardens et al. 2011). Therefore, a sandwich-ELISA against HBV core was used to detect HBcAg in the supernatant of transfected cells. Uncoated capsids could be detected for all tested mutants and wild type HBV. Stop mutations or amino acid changes at positions 172, 196 as well as at position 216 in the SHBs seemed to increase the secretion of uncoated core-capsids (Figure 10 D).

To show that the effects found in ELISA and qPCR were not cell type- or species-specific, stop mutants were also transiently transfected in two other hepatoma cell lines; the murine AML12 and the human HepG2 cell lines. Analysis of the supernatant for newly synthesized and secreted virions and subviral particles showed the same results as already described for Huh7 transfected cells (see appendix Figure 36, Figure 37).

The present data show, that a stop mutation at the position 182, 196, 199, and 216 blocks the secretion of HBsAg. A stop mutation at position 172 results in the decreased secretion of SHBs, whereas secreted LHBs is detectable if a stop mutation at position 176 in the SHBs takes place. An amino acid change at position 172 and 196 in the SHBs rescued the secretion of HBsAg.

3.2.2. Immunohistochemical Analysis of HBV Surface Protein Variants

To analyze the synthesis of HBsAg of HBV variants in cell culture, immunohistochemical staining for selected mutants was performed.

After immunohistochemical staining against LHBs, MHBs, and SHBs, newly synthesized HBV surface proteins could be detected in Huh7 cells transfected with the HBV wild type plasmid (Figure 11, left section, red panel). These Huh7 cells also expressed the HBV core antigen (Figure 11, left section, green panel). MHBs and SHBs could be observed in cells transfected with the HBV plasmid encoding for a LHBs deficient mutant, with the preS1-start codon (methionine, M) of LHBs mutated into a codon for threonine (T) (M1T) (Figure 11, M1T, right section, red panel). No LHBs could be visualized after immunohistochemical staining (Figure 11, M1T, right section, red panel LHBs). For both, wt and M1T mutant, most of the transfected cells express HBV core simultaneously with HBV surface proteins (Figure 11, white arrow).

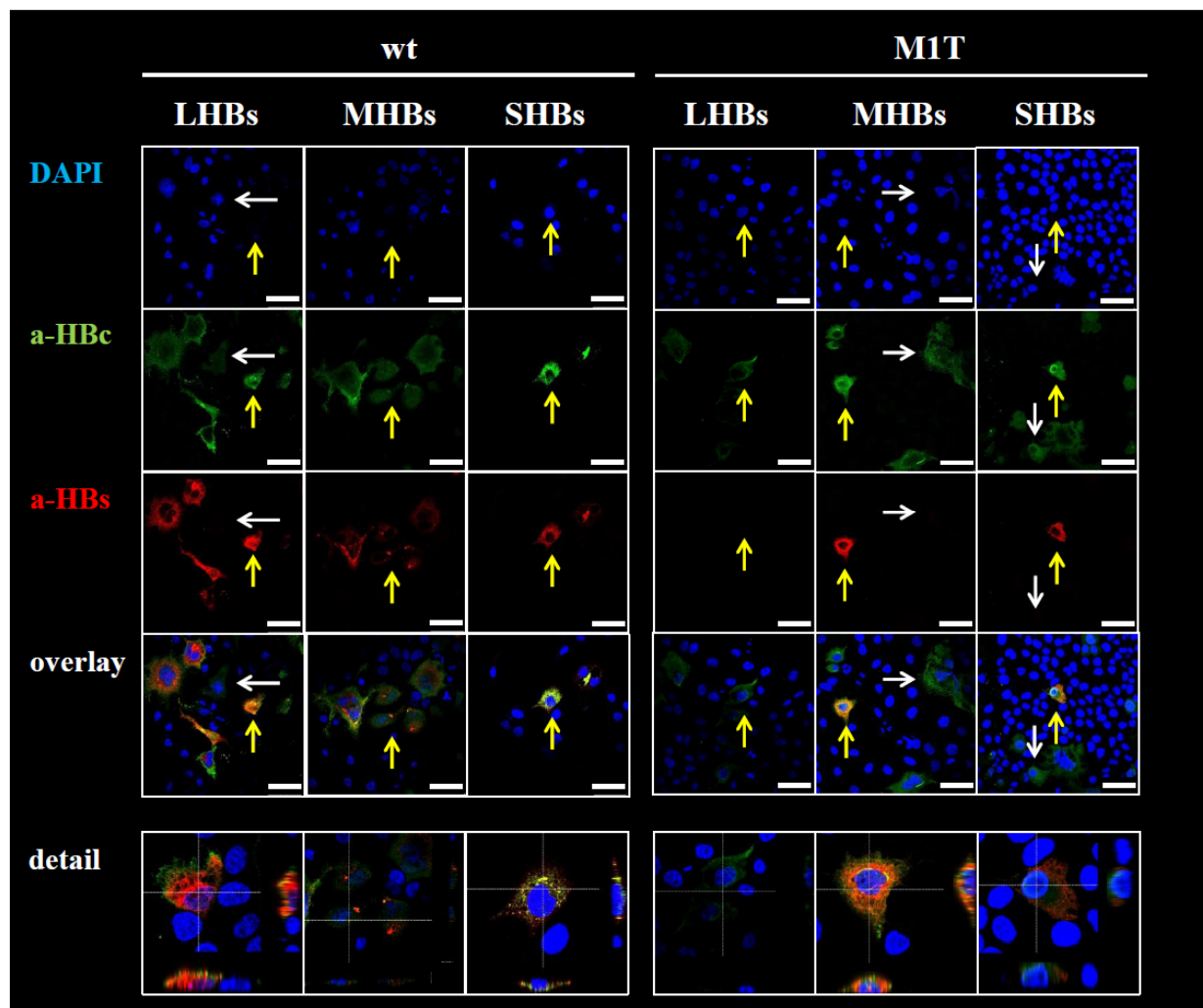


Figure 11: Immunohistochemical analysis of HBV proteins of wt or M1T transfected Huh7 cells. Three days after transient transfection, cells were stained for HBsAg (red, Alexa-594) and HBV core (green, Alexa-488). Newly synthesized HBsAg was detected using monoclonal antibodies against LHBs (MA18/7), MHBs (Q19/10), and SHBs (C20/02). As a marker for newly synthesized hepatitis B virions, core capsids were stained with a polyclonal antibody (DAKO). Nuclei were stained with DAPI (blue). White arrows mark cells expressing only HBV core. Yellow arrows mark cells that are shown in more detail in the lowest panel with a cut view through z-stack-images of single cells. Scale bars: 50 μm .

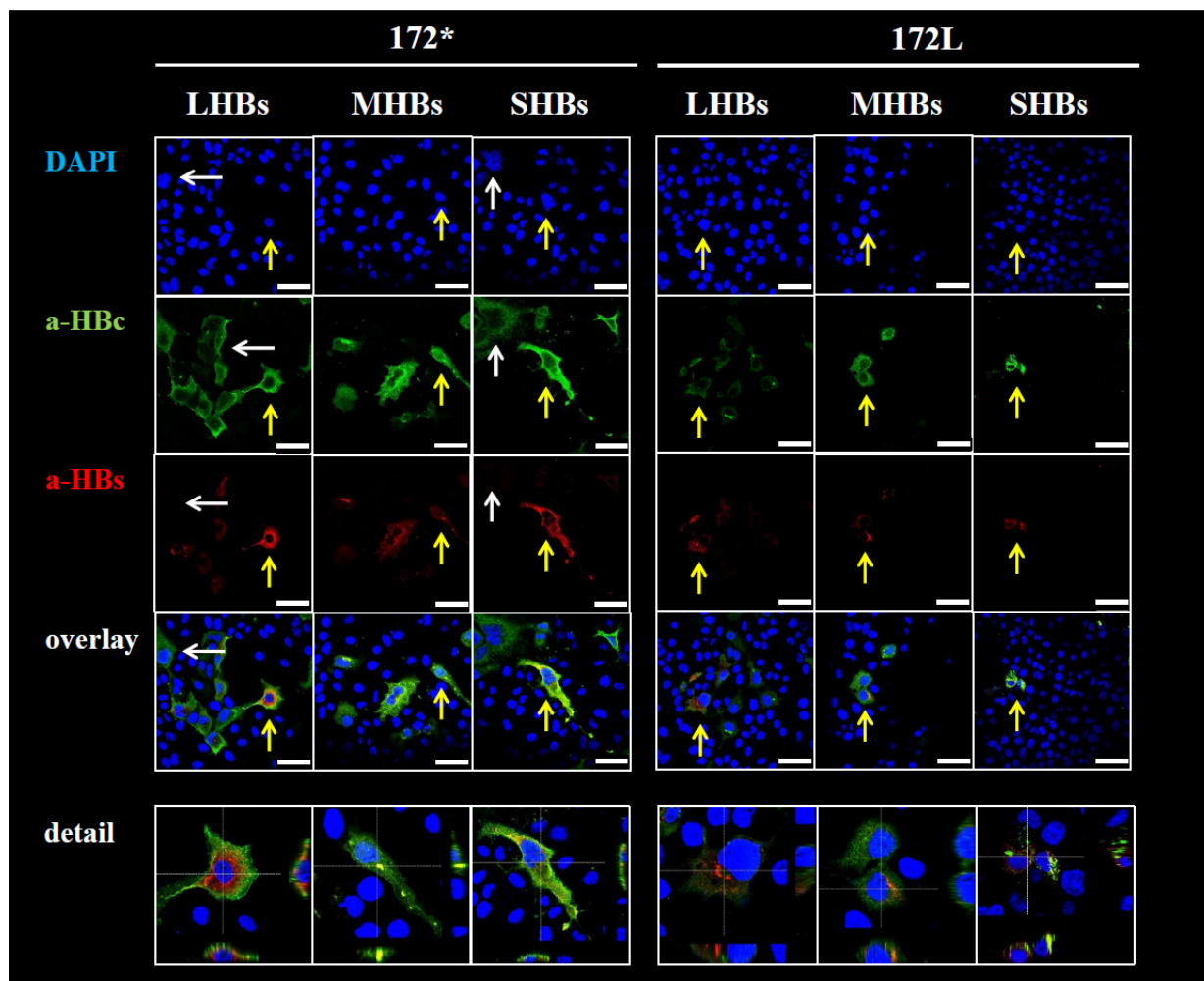


Figure 12: Immunohistochemical analysis of HBV proteins of HBV-variants with mutations at position 172 of the SHBs. Huh7 cells were transfected with plasmids encoding either a stop mutation at position 172 (172*) or an amino acid change from tryptophan to leucine (172L) in the SHBs. Newly synthesized HBsAg was detected using monoclonal antibodies against LHBs (MA18/7), MHBs (Q19/10), and SHBs (C20/02) (**red** panel, Alexa-594). As a marker for newly synthesized hepatitis B virions, capsids were stained with a polyclonal antibody (DAKO) (**green** panel, Alexa-488). Nuclear staining was performed with DAPI (**blue**). White arrows mark cells expressing only HBV core. Yellow arrows label cells that are shown in more detail in the lowest panel with a cut view through z-stack- images of single cells. Scale bars: 50 μ m.

In case of a stop-mutation or an amino acid change at position 172 in the SHBs, expression of all HBV surface proteins can still be detected (Figure 12, red panel). As seen in wt or M1T transfected cells, some cells show expression of HBV core antigen, only (Figure 12, green panel, white arrows).

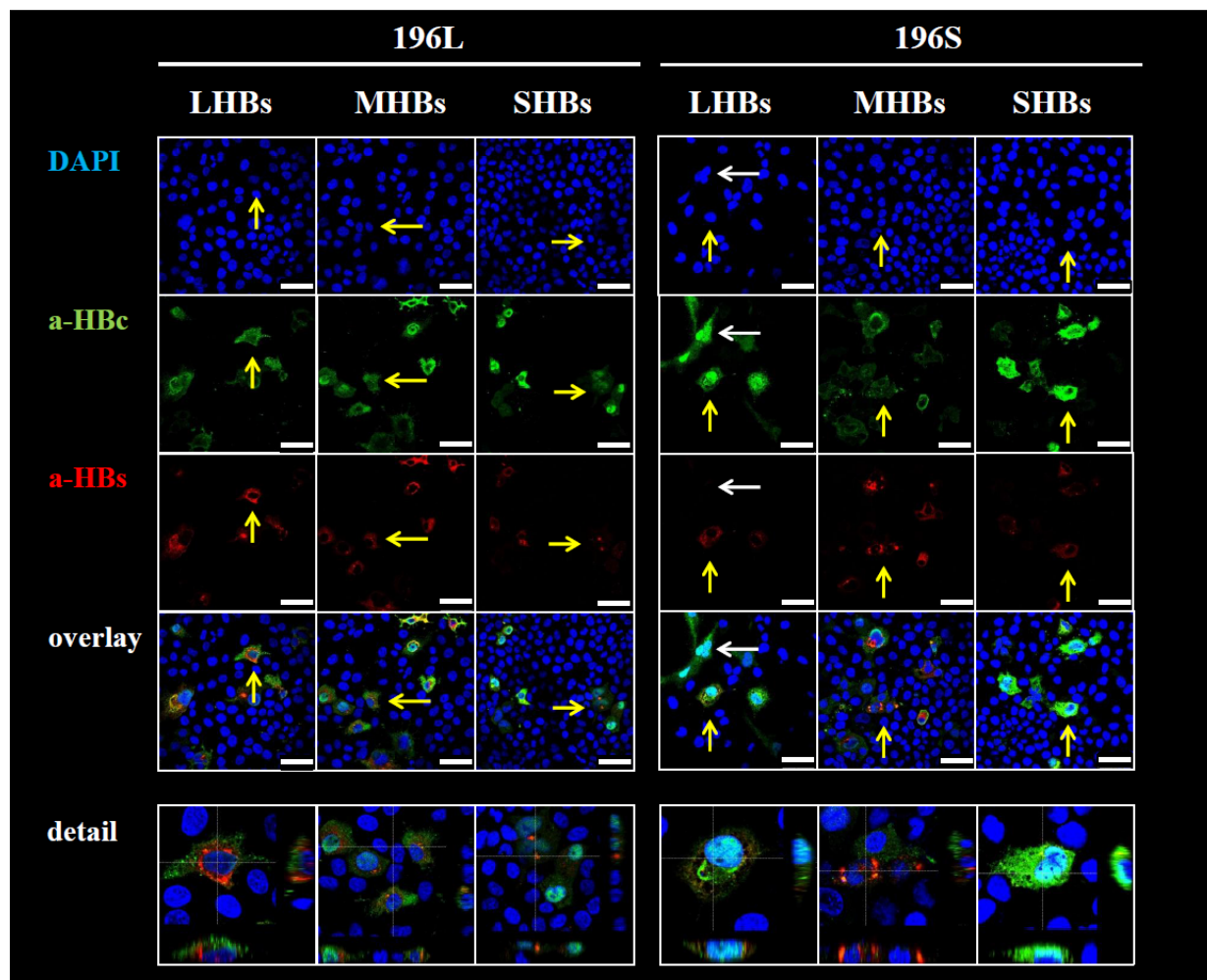


Figure 13: Immunohistochemical analysis of HBV proteins of HBV-variants with mutations at position 196 of the SHBs. Huh7 cells were transfected with plasmids encoding for amino acid changes in SHBs at position 196 (196S or 196L). Newly synthesized HBsAg was detected using monoclonal antibodies against LHBs (MA18/7), MHBs (Q19/10), and SHBs (C20/02) (red panel, Alexa-594). As a marker for newly synthesized hepatitis B virions, capsids were stained with a polyclonal antibody (DAKO) (green panel, Alexa-488). Nuclear staining was performed with DAPI (blue). White arrows mark cells expressing only HBV core. Yellow arrows label cells that are shown in more detail in the lowest panel with a cut view through z-stack- images of single cells. Scale bars: 50 μ m.

Expression of HBV surface proteins still could be visualized even though mutants had an altered amino acid sequence from tryptophan (W) to serine (S) (W196S) or leucine (L) (W196L) at position 196 (Figure 13, red panel, yellow arrow). But if there is a mutation to a stop-codon at position W196 (196*) instead of a tryptophan, expression of HBsAg could not be detected by IF (compare Figure 14, 196* left section, red panel with Figure 13 and Figure 14, right section, red panel, yellow arrow). Synthesis of HBV core antigen could also be observed in transfected Huh7 cells with plasmids encoding for mutants at position 196 in the SHBs (Figure 13 and Figure 14, with white arrow).

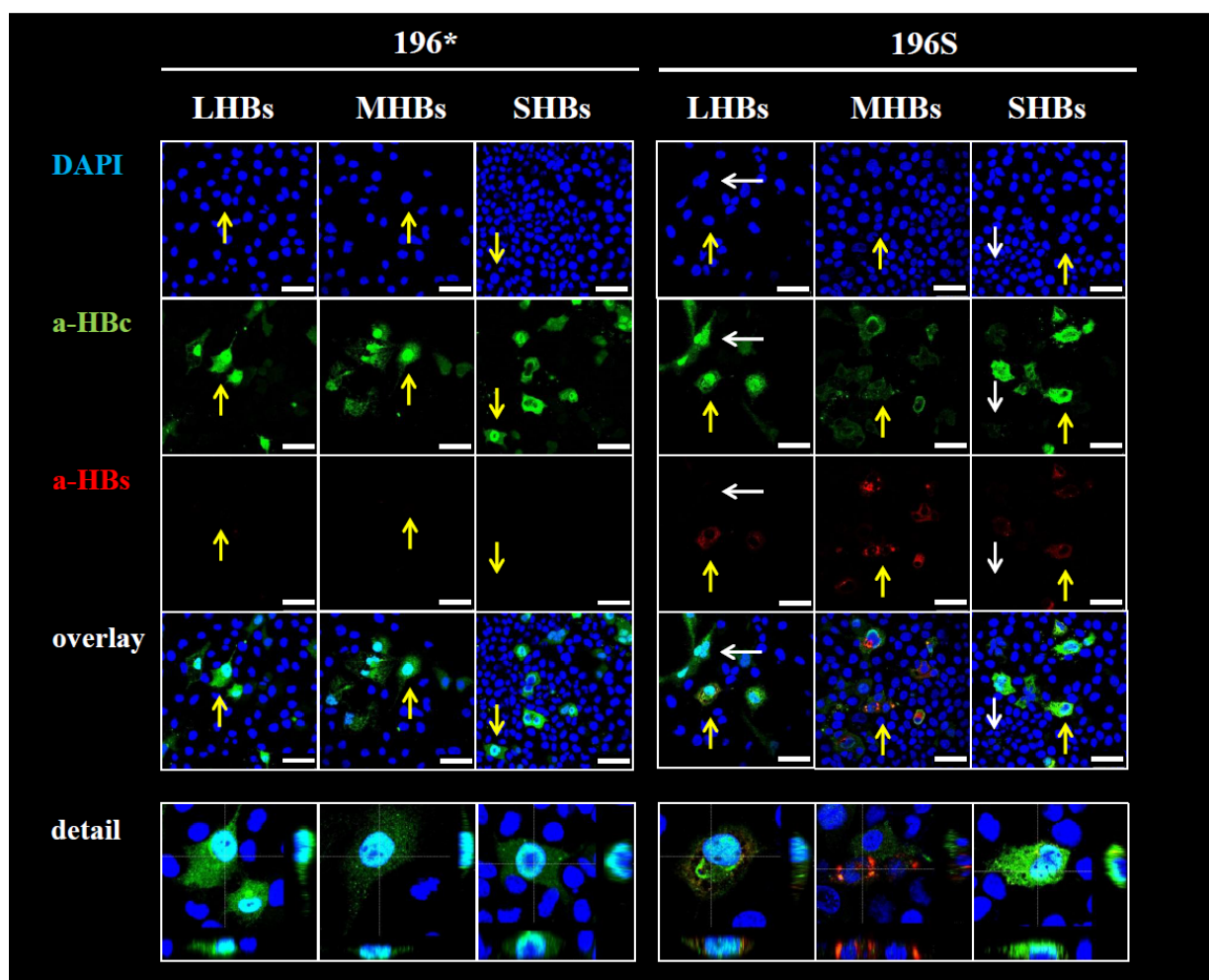


Figure 14: Immunohistochemical analysis of HBV proteins of HBV-variants with mutations at position 196 in the SHBs. Huh7 cells were transfected with plasmids encoding for either a stop mutation at position 196 (196*) or an amino acid change from tryptophan to serine (196S) of the SHBs. Newly synthesized HBsAg was detected using monoclonal antibodies against LHBs (MA18/7), MHBs (Q19/10), and SHBs (C20/02) (red panel, Alexa-594). As a marker for newly synthesized hepatitis B virions, capsids were stained with a polyclonal antibody (DAKO) (green panel, Alexa-488). Nuclear staining was performed with DAPI (blue). White arrows mark cells expressing only HBV core. Yellow arrows show cells co-expressing HBsAg and HBV core. These cells are shown in more detail with a cut view through z-stack-images of single cells. Scale bars: 50 μ m.

Untransfected cells stained with monoclonal antibodies against HBsAg as well as wt transfected cells stained with the secondary antibodies only, showed no positive fluorescence signal (see appendix Figure 38).

Cells transfected with surface protein mutants do not differ in their morphology from the HBV wild type. All surface proteins could be detected in Huh7 cells transfected with the wt plasmid or plasmids encoding for HBV with amino acid changes in the SHBs (172L, 196S, 196L). The amino acid change from methionine to threonine at position 1 of the LHBs, resulting in a stop mutation of the HBs start codon, leads to inhibited synthesis and thus not to a secretion of LHBs in subviral particles. Instead, synthesis of MHBs and SHBs and secretion of subviral particles was not influenced when LHBs was mutated. A stop mutation at position 172 in the SHBs did not change the expression of SHBs. In contrast, a stop mutation at position 196 in the SHBs led to the loss of HBsAg expression. The results are summarized in Table 6, page 77.

3.2.3. Comparison of Sedimentation Behavior for Purified HBV with Cell Culture Derived HBV in the CsCl-Gradient

To distinguish between the secretion of enveloped virions and uncoated core capsids and to verify which effect stop mutations have on the packaging of virions, a caesium chloride-gradient was performed.

Normally, virions peak at 1.24–1.25 g/ml CsCl after centrifugation, whereas naked core-particles have their maximum at a CsCl-density of 1.30 to 1.36 g/ml (Sureau et al. 1986). Supernatant of stop mutants or purified HBV from human serum were treated with detergent (NP40) and reducing agent (TCEP) to remove the coat of the virions. Then uncoated cores and enveloped virions were separated by CsCl-gradient.

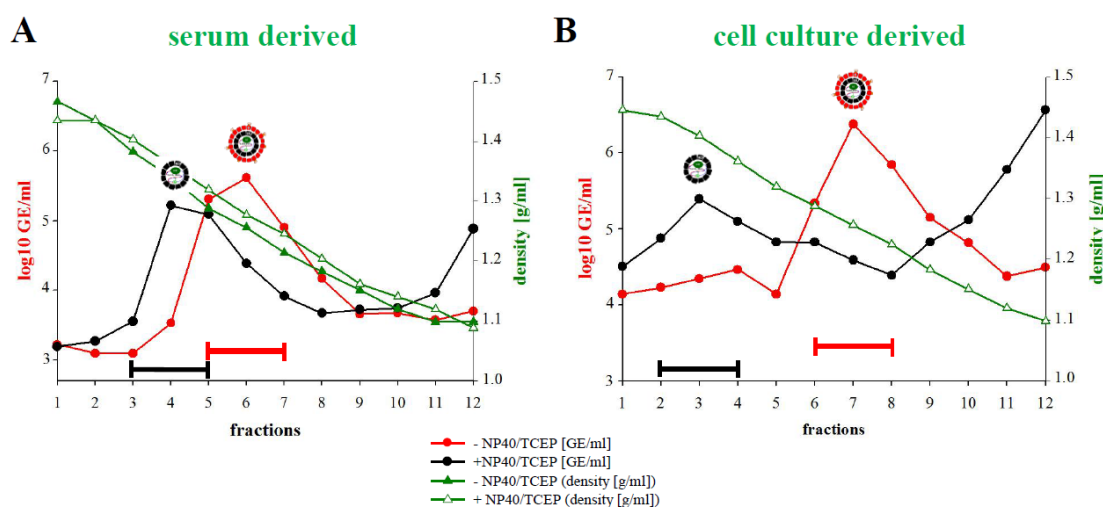


Figure 15: CsCl-gradient of serum derived HBV compared to cell culture derived HBV. To distinguish between enveloped virions and uncoated core-capsids, supernatant of HBV wt transfected cells or HBV purified from human serum was treated with detergent (NP40) and reducing agent (TCEP) (1 h, RT). For serum derived HBV and cell culture derived HBV 1×10^6 GE/ml were used. Afterwards, samples were layered on a linear CsCl-gradient and centrifuged. Gradient was fractionated from the bottom to the top, purified and analyzed with qPCR for viral DNA. **A)** CsCl-gradient of purified HBV derived from serum of a chronically infected patient. **B)** CsCl-gradient of cell culture derived HBV (wt). **Red line** exhibits genome equivalents of untreated virus-sample. **Black line** shows genome equivalents after treatment with detergent and reducing agent. **Green lines** indicate the density of CsCl. **Red bars** indicate the fractions where enveloped virions are expected. **Black bars** indicate the fractions where uncoated capsids are expected. Representative data of three independent experiments are depicted.

Detected density of CsCl decreased from lower to higher fractions (Figure 15, green lines). Without NP40/TCEP-treatment, a peak of viral DNA could be observed at a density of 1.26 g/ml CsCl (fraction 6, see also appendix Table 7) using purified HBV from human serum (Figure 15 A, red line). This peak is in consistence with the density where enveloped HBV virions normally peak (Sureau et al. 1986) (Figure 15, red virion). After treatment with detergent (NP40) and reducing agent (TCEP) the peak of viral DNA shifted to higher densities of CsCl (1.36 g/ml, fraction 4) (Figure 15 A, black line and appendix Table 7), corresponding to uncoated capsids (Sureau et al. 1986) (Figure 15, black capsid). The cell culture derived HBV behaved the same in the CsCl-gradient. Without treatment, enveloped virions could be detected at a density of 1.26 g/ml CsCl (fraction 7) (Figure 15 B, red line, and appendix Table 7), too. A second peak

of viral DNA was observed (fraction 4) (Figure 15 B, red line) in the same densities (1.4 g/ml) and fractions (fractions 3-4) as uncoated core-capsids (Figure 15 B, black line and appendix Table 7). A second characteristic peak of viral DNA accumulating in low densities in the last fractions can be measured in all treated CsCl-gradients (Figure 15 A and B, black lines and appendix Table 7 and following Figures 17, 18, 19, 37, 38).

HBV purified from human serum and cell culture derived HBV behaved similarly in CsCl-gradient and on that score they are comparable with each other.

3.2.4. Analysis of a LHBs Deficient HBV Mutant Using the CsCl-Gradient

An HBV variant with a mutated start codon (M1T) was designed to analyze virus secretion without LHBs (Figure 16 A). The amino acid change from methionine (M) to threonine (T) at position 1 in the LHBs leads to the skipping of the LHBs start codon, resulting in the inhibition of LHBs secretion. The supernatant from cells transiently transfected with the HBV mutant M1T was either untreated or reduced with NP40 and TCEP, ultracentrifuged in the CsCl gradient, and examined.

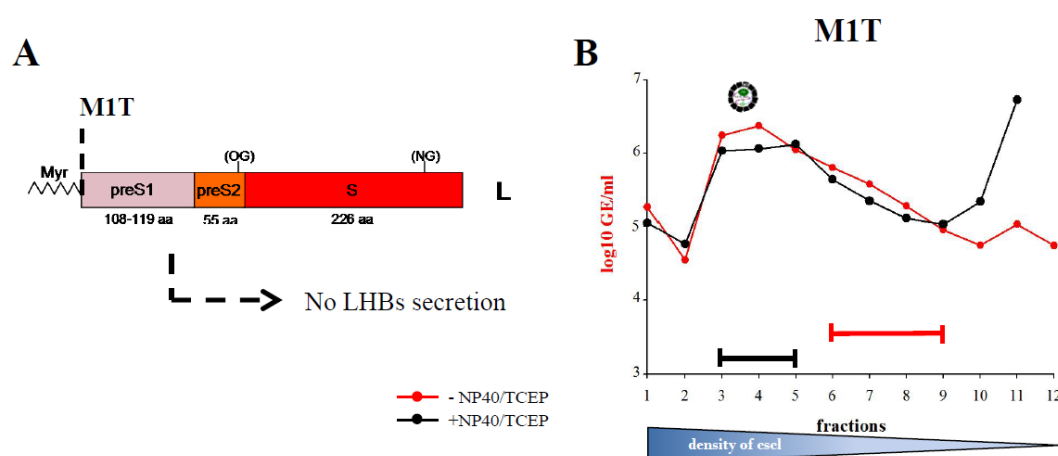


Figure 16: CsCl-gradient of mutant with amino acid change in the start codon of LHBs. Supernatant of transiently transfected cells with HBV surface protein variant M1T was treated with NP40 and TCEP (1h, RT), layered on a linear CsCl-gradient and ultracentrifuged. 1×10^6 GE/ml were used. The gradient was fractionated from the bottom to the top, purified, and analyzed for viral DNA with qRT-PCR. **A)** Schematic presentation of the mutation M1T in the LHBs start codon, inhibiting LHBs production. **B)** CsCl-gradient of mutant M1T. **Red bars** indicate the fractions where enveloped virions are expected. **Black bars** indicate the fractions where uncoated capsids are expected. Representative data of three independent experiments are depicted.

After centrifugation, the CsCl-gradient shows that a peak of viral DNA could be detected in lower fractions (fractions 3-5) with higher densities of cesium chloride (1.37 g/ml–1.29 g/ml) independent of the treatment (Figure 16, red and black line and appendix Table 8). The peak of viral DNA presumably corresponds to uncoated core capsids. A second characteristic increase of viral DNA was also detected in the last fractions after treatment with NP40 and TCEP (Figure 16 B, black line and appendix Table 8).

This CsCl-gradient shows that the loss of the initiation codon of LHBs does not only lead to an inhibited secretion of subviral particles, but also to a complete block of the secretion of enveloped virions.

3.2.5. Analysis of HBV Variants with Mutations at Position 172 into the SHBs Using the CsCl-Gradient

During antiviral therapy with adefovir, the mutation V181T in the rt-domain of the viral polymerase occurred, leading to the S-ORF mutation at position sW172 to sW172* or sW172L. A stop mutation at this position results in a truncated SHBs variant missing the C-terminus (Figure 17 A). This truncated SHBs variant loses the transmembrane domain III and IV and the internal loop between both domains. An amino acid change at this position probably maintains the C-terminus of the SHBs (Figure 17 A). To examine the influence of these mutations on virion secretion, reduced and non-reduced supernatant of transfected cells was analyzed using a linear CsCl-gradient.

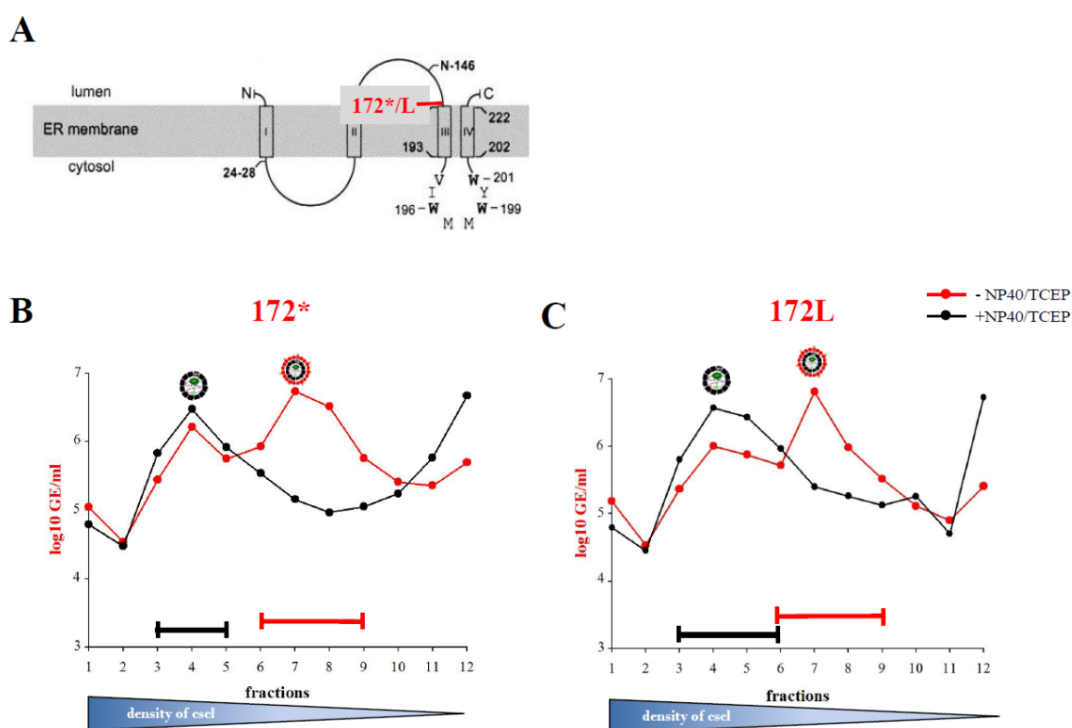


Figure 17: CsCl-gradient of mutants with changes at position 172 of the SHBs. Supernatant of transiently transfected cells with HBV surface protein variant 172* or 172L was treated with NP40 and TCEP (1h, RT), layered on a linear CsCl-gradient and ultracentrifuged. 1×10^6 GE/ml for both HBV surface protein variants were used. The gradient was fractionated from the bottom to the top, purified, and analyzed with qPCR for viral DNA. **A)** Schematic depiction of localization of mutations in the SHBs at position 172 highlighted in red (modified after Komla-Soukha and Sureau 2006). To analyze the influence on viral assembly and secretion, the tryptophan at position 172 was mutated into a stop codon (172*) or an amino acid change from tryptophan to leucine (172L) was performed **B)** CsCl-gradient of mutant 172*. **C)** CsCl-gradient of mutant 172L. **Red bars** indicate the fractions where enveloped virions are expected. **Black bars** indicate the fractions where uncoated capsids are expected. Representative data of three independent experiments are depicted.

A stop mutation at position 172 or an amino acid change at the same position led to the secretion of enveloped virions in densities of 1.24 g/ml as well as uncoated core-capsids in densities between 1.35 g/ml and 1.36 g/ml (Figure 17 B and C, red lines and appendix Table 9) for both mutants without treatment. After reducing procedure, all enveloped virions were uncoated and the viral DNA shifted to higher densities (1.35 g/ml-1.36 g/ml for both mutants).

3.2.6. Analysis of HBV Variants with Mutations at Position 196 into the SHBs Using the CsCl-Gradient

The antiviral treatment with lamivudine leads to the mutation M204I in the viral polymerase. Due to the overlap of the ORFs, this mutation leads also to a mutation at position 196 into the S-domain. For further analysis of the influence of mutations at position 196 on virion secretion, supernatant of transfected cells was examined in a CsCl-gradient in its reduced and non-reduced form.

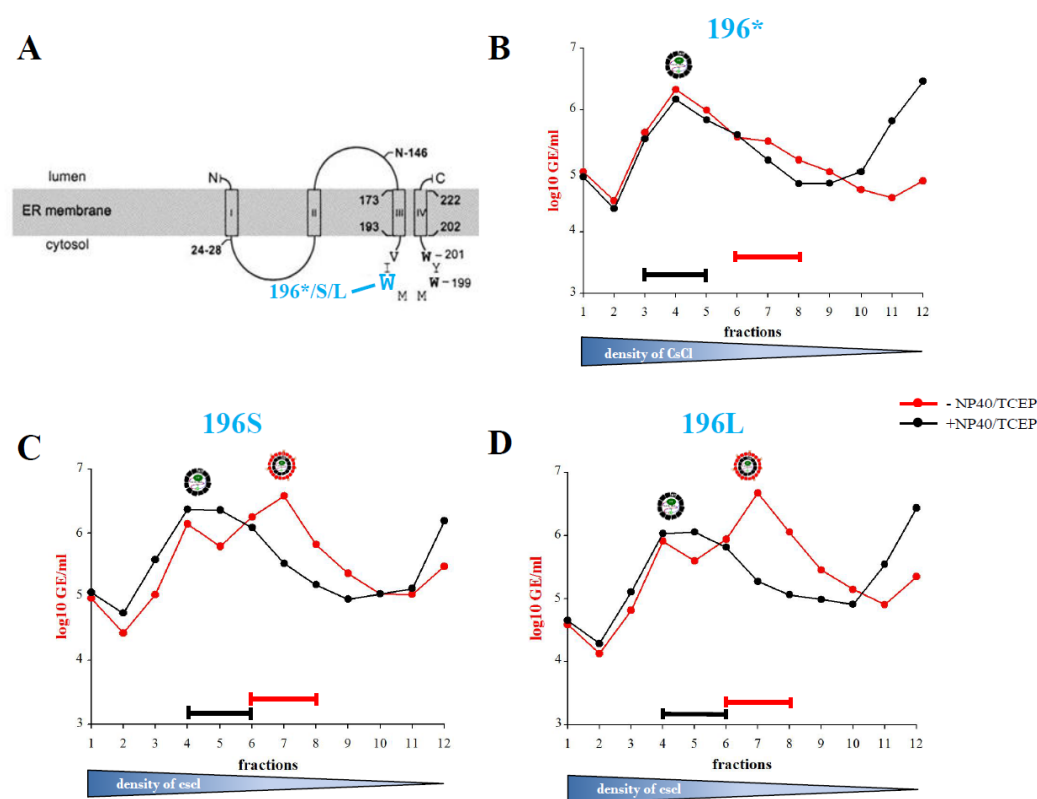


Figure 18: CsCl-gradient of mutants with mutations at position 196 into the SHBs. Supernatant of transiently transfected cells with HBV surface protein variants 196*, 196S, 196L were treated with NP40 and TCEP (1h, RT), layered on a linear CsCl-gradient, and ultracentrifuged. 1×10^6 GE/ml for all three HBV surface protein variants were used. The gradient was fractionated from the bottom to the top, purified and analyzed with qPCR for viral DNA. **A)** Schematic depiction of mutations into the SHBs at position 196 highlighted in bright blue (modified after Komla-Soukha and Sureau 2006). To analyze the influence on viral assembly and secretion, the tryptophan (W) at position 196 was mutated into a stop codon (196*) or an amino acid change from tryptophan to leucine (196L) or serine (196S) was performed. **B)** CsCl-gradient of tested mutant W196*. **C)** CsCl-gradient of tested mutant 196S. **D)** CsCl-gradient of tested mutant 196L. **Red bars** indicate the fractions where enveloped virions are expected. **Black bars** indicate the fractions where uncoated capsids are expected. Representative data of three independent experiments are depicted.

CsCl-analysis of SHBs mutants 196S (Figure 18 C and appendix) and 196L (Figure 18 D and appendix Table 10) showed enveloped hepatitis B virions in densities of 1.25 g/ml (196S) and 1.26 g/ml (196L). Uncoated capsids could be detected in densities of CsCl of about 1.36 g/ml (196S) and 1.37 g/ml (196L) (Figure 18 C and D, red lines and appendix Table 10). The treatment with reducing agent and detergent lead to the uncoating of the virus and to a shift of the viral DNA to higher densities of CsCl (Figure 18 C and D, black lines and appendix Table 10). In contrast to the altered amino acid sequence, the stop mutation at position 196 results in the secretion of uncoated capsids, only, because with or without treatment, the sole peak of viral DNA was localized in densities of CsCl between 1.35 g/ml and 1.37 g/ml, typical for the sedimentation density for core particles (Figure 18 B, black and red line and appendix Table 10).

Stop mutations in the SHBs at positions 176, 182, 199, and 216 lead to the secretion of uncoated capsids, but enveloped virions are only observed in mutants possessing a stop mutation at position 176 and 216 in the SHBs. A stop mutation at these positions does not inhibit the packaging of virions. The HBV surface variants 182* and 199* only secrete uncoated core capsids. (see Figure 39 and Table 11, Figure 40 and Table 12).

Table 6 (page 77) summarizes the previously gained results from the HBV surface protein variants.

3.3. Establishment of a Transfection and Infection System for HDV Pseudo-Particles

To test the infectivity of HBV mutants, a new recombinant infection system had to be established. The hepatitis delta virus is a satellite virus of HBV and uses the HBV surface proteins for viral assembly, secretion, and infection (Bruss and Ganem 1991; Sureau et al. 1993). In this context, it is an excellent opportunity to analyze the ability of HBV surface protein mutants to infect PTHs. Due to the fact that there is no adequate RNA-standard for absolute quantification of HDV-RNA, an RNA-standard had to be established *in vitro*. Therewith, it would be possible to absolutely quantify HDV-RNA in cell culture or human plasma.

3.3.1. Production and Establishment of an HDV RNA-standard for RT-qPCR

HDV-plasmid DNA was used to generate a full length RNA-standard for quantitative HDV PCR. After the synthesis of RNA the concentration of total RNA was measured with the picodrop Microlitre UV/Vis spectrophotometer (Biozym) and the amount of genome equivalents per microliter was calculated. A total particle number of 3.31×10^{12} GE/ μ l for sample one and 2.25×10^{12} GE/ μ l for sample two was calculated. The purity of *in vitro* generated RNA-standard was analyzed performing a formaldehyde gel.

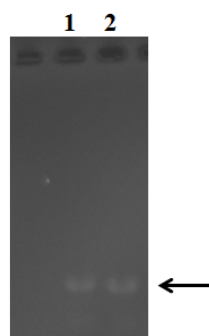


Figure 19: Formaldehyde gel of *in vitro* generated HDV RNA-standard. HDV genome was amplified out of the HDV encoding plasmid pSVLD3, which served as a template for the synthesis of HDV RNA. After *in vitro* transcription of the HDV RNA, a formaldehyde gel was performed to examine the purity. 5 μ l of each sample (**1**: 1.66×10^{13} GE, **2**: 1.13×10^{13} GE) were loaded onto the gel.

As shown in Figure 19, there was a single band detected for each sample indicating that an *in vitro* RNA-standard was generated by the T7 High Yield RNA Synthesis Kit (NEB) with high purity.

Both approaches were diluted to a final concentration of 1×10^9 GE/ μ l. To test the sensitivity of the newly generated RNA-standard by RT-qPCR, one sample was used in a tenfold serial dilution, starting with 2×10^8 GE. The original plasmid DNA (pSVLD3, *EcoRI* digested) served as a control and was used in the same concentrations.

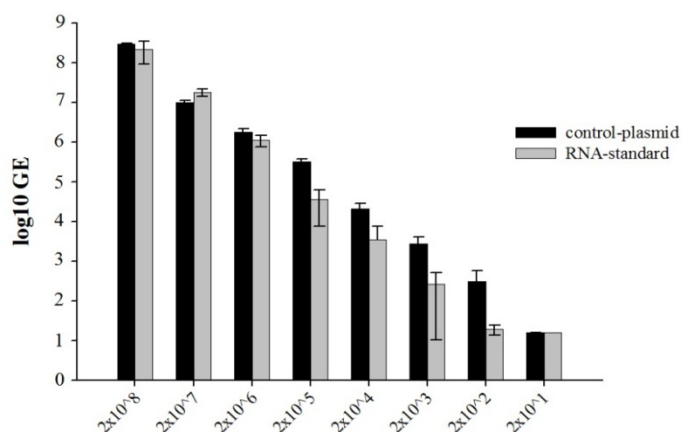


Figure 20: Titration of control plasmid (pSVLD3, *EcoRI* digested) and *in vitro* generated RNA-standard. The HDV encoding plasmid pSVLD3 (*EcoRI* digested) and the newly synthesized RNA standard were titrated from 2×10^8 GE to 2×10^1 GE and analyzed in the HDV RT-qPCR. Data presented the average \pm SD of three independent experiments including three repetitions.

Titration of RNA-standard and control plasmid showed a continuous decrease in RNA and plasmid concentration to a total concentration of 2×10^3 GE. From that point the qPCR gets inaccurate. In a range of 2×10^8 to 2×10^4 GE RNA standard was as sensitive as the control-plasmid (Figure 20).

Because of a high plasmid background from the transfection procedure in cell culture derived HDV pseudo-particles, a DNase I digestion was done before starting the RT-qPCR. To test if RNA-standard was influenced by the DNase digestion, a DNase I and RNase A digestion was realized (see 2.2.8.2.2) and plasmid-DNA was used as a control.

To further investigate if the DNase treatment influences the amount of used RNA, freshly thawed RNA-standard was pipetted after the DNase digestion and before the qPCR was running (Figure 21, lane 9).

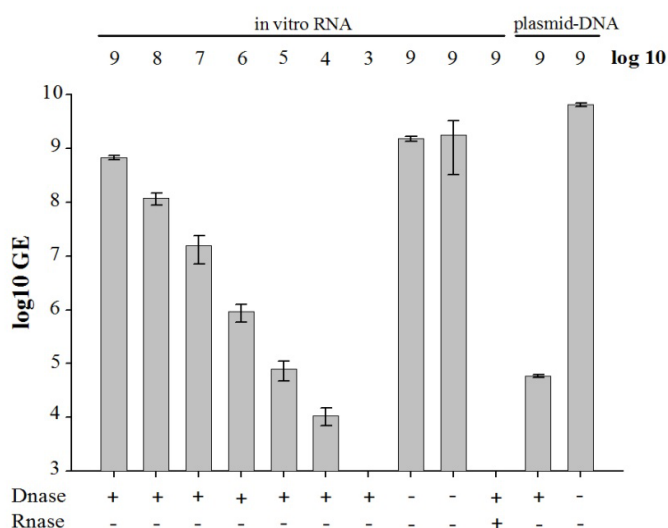


Figure 21: RNA-standard with and without RNase A and DNase I digestion. Data present the average \pm SD from titrated RNA-standard (from 1×10^9 GE to 1×10^3 GE) compared to control-plasmid-DNA (pSVLD3, *EcoRI* digested). Experiment includes three repetitions. RNA-standard was titrated and treated with DNase I and/or RNase A. Lanes 1 to 7 show titrated RNA-standard with 10^9 up to 10^3 GE. In lane 8 highest RNA-standard is shown without DNase-treatment. Lane 9 shows highest RNA-standard freshly thawed before running the qPCR. Lane 10 shows highest RNA-standard with DNase and RNase treatment. Lanes 11 and 12 show DNase treated and untreated control-plasmid-DNA.

The quality and amount of RNA-standard is not influenced by DNase treatment (Figure 21, compare lane 1-7 with lane 8). After RNase A digestion, no RNA could be observed (Figure 21, lane 10). The amount of DNase I treated control-plasmid was reduced (Figure 21, compare lane 11 and 12).

Thus, it was possible to generate an RNA standard in a clearly defined manner, which was suitable as a standard for the absolute quantification of newly synthesized RNA of the subsequent experiments.

3.4. Characterization of HDV from Human Plasma

3.4.1. Characterization of HDV Derived from Human Plasma in a Linear CsCl-Gradient

Human plasma of a chronically infected patient, co-infected with HBV and HDV, was analyzed with a linear CsCl-gradient. Therefore, 5×10^6 GE/ml HDV derived from this human plasma were treated with NP40 and TCEP, and a CsCl-gradient was performed.

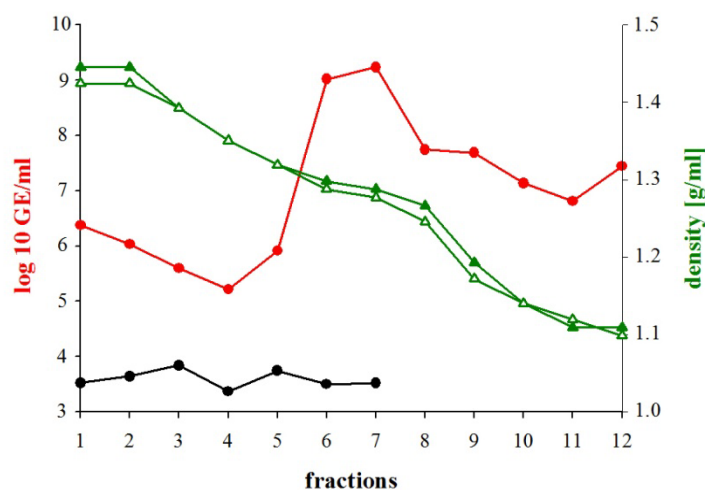


Figure 22: CsCl-gradient of a human plasma chronically infected with HDV and HBV. Human plasma (5×10^6 GE/ml HDV) was treated with or without NP40/TCEP (1 h, RT). Afterwards, samples were layered on a linear CsCl-gradient and centrifuged. Then, the gradient was fractionated from the bottom to the top, purified and analyzed for viral RNA with specific RT-qPCR. **Green triangles** show density of CsCl for each fraction. **Red dots** show GE of untreated human plasma. **Black dots** show GE of treated human plasma.

After centrifugation, taken fractions were purified and the HDV specific RT-qPCR was performed to detect viral RNA. A peak of hepatitis delta RNA was observed in densities between 1.29 g/ml-1.30 g/ml CsCl (fractions 6 and 7) (Figure 22, red line). After treatment with detergent and reducing agent, HDV RNA could not be traced anymore (Figure 22, black line). HBV DNA could not be observed.

3.4.2. Purification of Plasma-Derived HDV with a Continuous Sucrose Gradient

For infection assay with PTHs, HDV, derived from human plasma, was purified with a continuous sucrose gradient (7.7×10^6 GE/ml) (see 2.2.9). After centrifugation, the fractions were photometrically and refractometrically determined. HDV-RNA was detected and quantified with RT-qPCR.

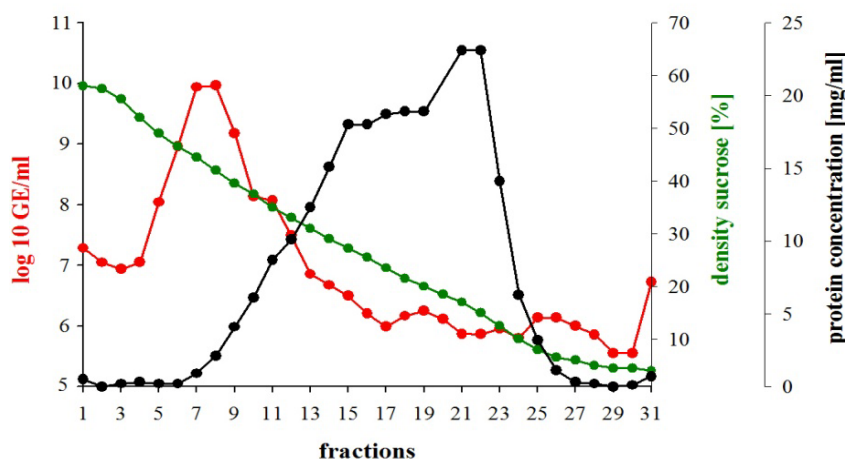


Figure 23: Sucrose gradient of a human plasma from a patient chronically infected with HDV/HBV. Human plasma from a chronically infected patient was purified with a continuous sucrose gradient. After ultracentrifugation, the gradient was fractionated from the bottom to the top. Then, the fractions were photometrically (protein concentration) and refractometrically (density of sucrose) determined. After purification, HDV-RNA was detected and quantified with RT-qPCR. **Red line** shows measured GE/ml in a logarithmic order. **Green line** shows measured density of sucrose in %. **Black line** shows measured protein concentration in mg/ml.

The protein concentration increased up to 27 % sucrose (fraction 15) and demonstrated a small plateau between 30 – 20 % sucrose (fractions 15-20), resulting in a peak in 17 – 15 % sucrose (fraction 21 and 22) (Figure 23, black line). The protein accumulation in these fractions was also detectable, which is visualized in an orange protein-cloud (also see appendix Figure 41, orange arrow). Viral RNA peaked in fractions with a density of 39-45 % sucrose (fractions 7 and 8) (Figure 23, red line). HBV-DNA could not be detected again.

3.4.3. Infection of PTHs with Purified HDV Derived from Human Plasma

To find out if purified HDV is also able to infect primary *Tupaia* hepatocytes, the fractions seven to nine of the sucrose gradient in Figure 23 were tested. To inhibit the infection with HBV or HDV, cells were preincubated with myr preS1 peptide. Twelve days after infection, the cells were lysed and analyzed for newly synthesized HDV-RNA. As a control for susceptibility of PTHs for HDV, some cells were mono-infected with HBV and newly synthesized and secreted HBsAg was measured in a SHBs specific ELISA (C20/2) as a marker of infection.

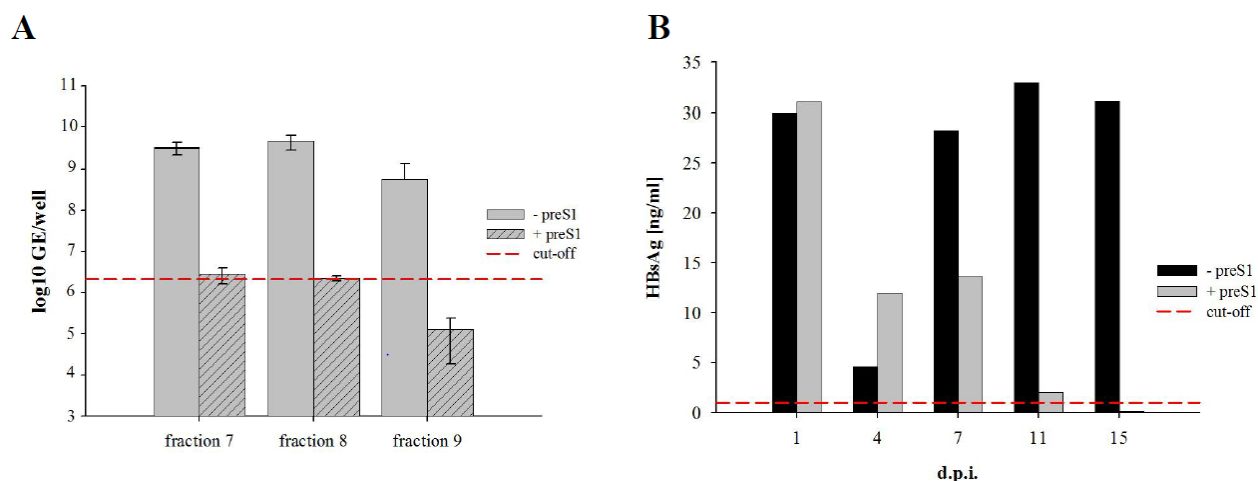


Figure 24: Infection of PTHs with patient derived HDV purified by sucrose gradient centrifugation. Freshly isolated PTHs were infected with purified HBV (1×10^8 GE) or HDV (1×10^7 GE) on day three after isolation. To inhibit the HBV or HDV infection, cells were preincubated with myr preS1-peptide ($1 \mu\text{M}$ f.c.) for 30 minutes at 37°C . **A)** Infection of PTHs with purified HDV from fraction seven, eight, and nine with (dotted grey bars) and without (monocolored grey bars) myr preS1-peptide inhibition. **B)** Control-infection with HBV with (grey bars) and without (black bars) myr preS1-peptide inhibition. Data present the average \pm SD from three repetitions. **Red** line shows cut-off. d.p.i = days post infection.

Successful infection with purified HDV on PTHs could be detected in all tested fractions. The HDV-infection could be inhibited with myr preS1-peptide (Figure 24 A). Figure 24 B presents a typical infection curve of PTHs with purified HBV. From the seventh day after the infection, a higher amount of HBsAg could be measured. Detected SHBs decreased over time when the infection was inhibited with preS1 (Figure 24 B, grey bars), resulting in a successful inhibition of infection (Figure 24 A, black bars).

3.4.4. Analysis of the Kinetic of Infectivity for HBV and HDV on PTHs

It was reported that PTHs are susceptible for HBV on day one to day four after isolation, but infection was more effective on day two and three after isolation (Çağ 2004). To show if this effect is the same with HDV, PTHs were infected with HBV and HDV, purified from human serum or plasma, at several points of time after isolation. Infection was inhibited by pre-incubation of PTHs with myr preS1-peptide (30 minutes, 37°C) on every infection day. The supernatant of infected cells was changed at day 1, 4, 7, and 12 after infection. On day 12 after infection, PTHs were lysed. The supernatant was analyzed for newly synthesized and secreted HBsAg as a marker for a successful HBV infection. Cell lysates were analyzed for newly synthesized HDV RNA as a marker for an effective HDV infection.

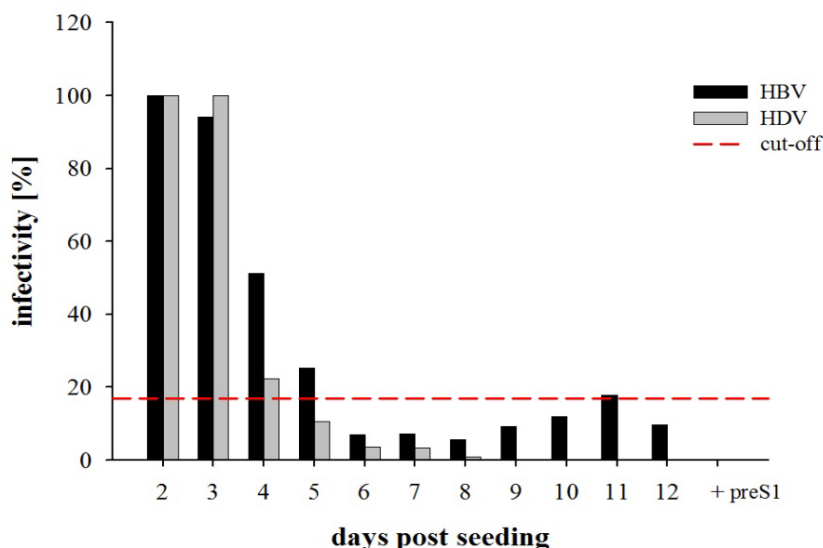


Figure 25: Kinetic of HBV and HDV susceptibility of PTHs. PTHs were infected with purified HBV (1×10^8 GE) or HDV (1×10^7 GE) from day two to day 12 after isolation. On each infection day, cells were pre-incubated with myr preS1-peptide ($1 \mu\text{M}$ f.c., 30 min, 37°C) to inhibit HBV or HDV infection. Detection of newly secreted SHBs in the supernatant was done by SHBs-ELISA (C20/02). Lysed cells were analyzed for newly synthesized HDV-RNA. Data from all preS1-inhibited days were pooled, the mean value was determined, and the percentage of infectivity compared to infection day two was calculated and depicted as + preS1. Infectivity of HBV and HDV was expressed as percentage of infectivity. Cut-off is marked with red dotted line. Duplicates for each point of time of infection were performed. (published in A. König, B. Döring, C. Mohr, J. Geyer, D. Glebe. "Hepatitis B virus and bile acids compete for binding to the Na⁺/taurocholate cotransporting polypeptide (NTCP) to enter hepatocytes". (in revision). modified).

Freshly isolated primary hepatocytes from the Asian treeshrew *Tupaia belangeri* were susceptible for HBV as well as HDV two to three days after isolation (Figure 25, black and grey bars). Four days after isolation, susceptibility decreased to an amount of 50 % for HBV (Figure 25, black bars) and about 80 % for HDV (Figure 25, grey bars). After the fifth day of isolation, PTHs were no longer susceptible for HBV or HDV. An effective inhibition of HBV and HDV infection by incubation with myristoylated preS1 peptide was achieved on every infection day (Figure 25 + preS1).

PTHs are susceptible for HBV and HDV two to four days after isolation. The infection efficiency decreased on day four, after isolation.

3.4.5. HBV/HDV Co- and Super-Infection of PTHs

Two types of HBV/HDV infection are known: co-infection and super-infection. Due to the fact that HBV/HDV co- or super-infection have not been systematically investigated in cell culture experiments *in vitro* on primary hepatocytes, the following experiments were done. To analyze HBV/HDV super-infection, PTHs were infected with purified HDV or HBV two days after isolation, and two days later they were infected with the other virus. For imitation of an HBV/HDV co-infection, PTHs were infected with both viruses two days after isolation. As a negative control, infections were inhibited by adding an

HBV myr preS1-peptide at all times. After 15 days, supernatant and cell lysates were analyzed for newly synthesized and secreted HBV or HDV as further described.

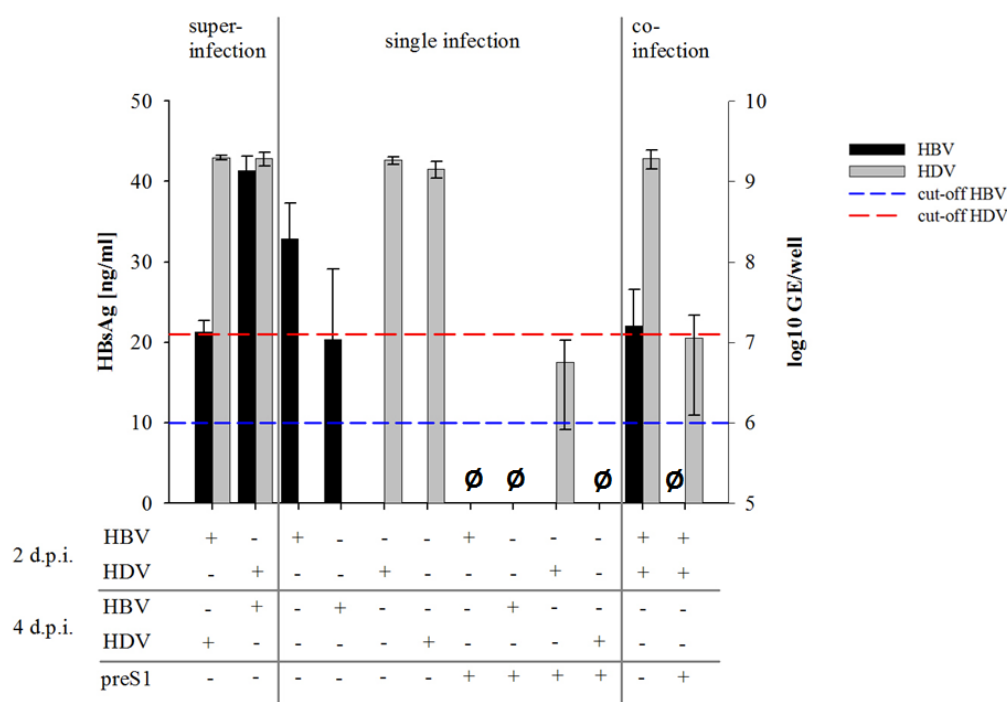


Figure 26: HBV/HDV co- and super-infection of PTHs. PTHs were infected with purified HBV (1×10^8 GE) and HDV (1×10^7 GE) simultaneously to imitate a HBV/HDV co-infection. To analyze HBV/HDV super-infection, PTHs were infected with purified HBV or HDV on day two after isolation and then infected vice versa four days after isolation. HBV and HDV single-infections were performed on day two and four after isolation. Inhibition of infection was performed by pre-incubation of PTH with myr preS1-peptide ($1 \mu\text{M}$ f.c.) for 30 min. 15 days after infection, the supernatant was analyzed for newly secreted HBsAg. Furthermore, cells were lysed and analyzed for newly synthesized HDV RNA. HBsAg in the supernatant of infected cells was measured with C20/02-ELISA as a marker for newly secreted HBV and is depicted as HBsAg [ng/ml]. Cut-off of HBsAg is presented with blue dotted line. Newly synthesized HDV was detected with RT-qPCR and depicted as log₁₀ GE/well. Cut-off of HDV RT-qPCR is presented with red dotted line. Data present the average \pm SD from three repetitions. 2 d.p.i. = 2 days post isolation, 4 d.p.i. = 4 days post isolation

Infection of PTHs with HBV and HDV was possible on day two and four after isolation (Figure 26, black and grey bars part in the middle). Susceptibility for HBV infection decreased over time (Figure 26, single black bars, part in the middle) while PTH are equally susceptible for HDV on both days (Figure 26, single grey bars, part in the middle). The imitation of HBV/HDV super- and co-infection seemed to be possible in PTHs (Figure 26). HBV/HDV co-infection was as effective (Figure 26 co-infection) as super-infection with HBV and HDV (Figure 26, super-infection). The infection of HBV seemed to be more effective when PTHs were firstly infected with HDV (Figure 26, super infection right bars).

Infection of PTHs with HBV and HDV was possible on day two and four after isolation. HBV/HDV super- and co-infection seemed to be possible in PTHs.

3.5. Characterization of Recombinant HDV Pseudo-Particles from Cell Culture

3.5.1. Production of HDV Pseudo-Particles in Cell Culture with Different Variants of HBV Surface Proteins

It is well known that the hepatitis delta virus needs the surface proteins of its helper virus HBV for secretion and infection (Sureau et al. 1993; Komla-Soukha and Sureau 2006). For following infection assays with recombinant HDV, HDV pseudo-particles with mutated HBV surface proteins were produced to analyze the influence of surface proteins on secretion. Co-transfected Huh7 cells were cultivated for 12 days and supernatant was investigated for newly secreted viral RNA

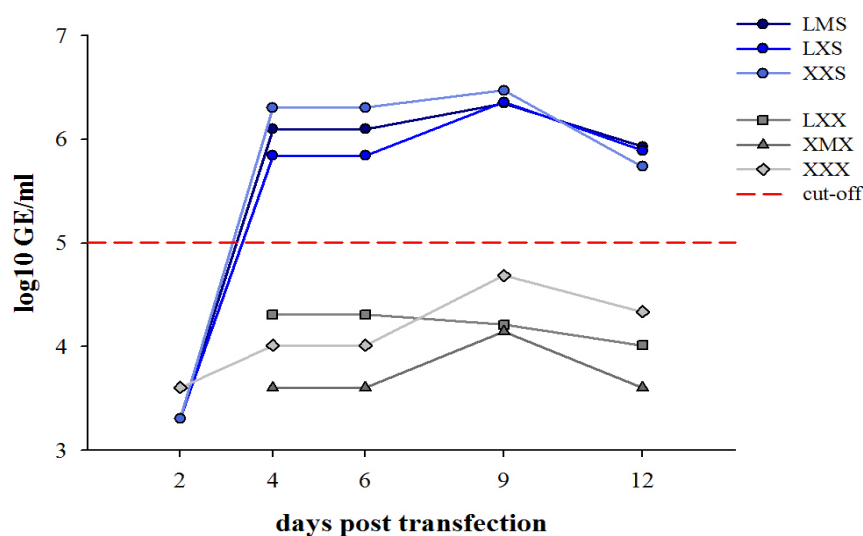


Figure 27: Kinetic of generated recombinant HDV pseudo-particles with several combinations of HBV surface proteins. After transient transfection of Huh7 cells with plasmids encoding for HDV and HBV surface proteins, supernatant was collected on day two, four, six, nine, and twelve after transfection and analyzed for newly secreted HDV pseudo-particles, HDV like-particles were generated with all three surface proteins (LMS), with LHBs, and SHBs (LXS) or with only LHBs (LXX), MHBs (XMX), or SHBs (XXS) respectively. As a negative control HDV pseudo-particles were generated without any surface proteins (XXX). The X marks mutated HBsAg. **Red** dotted line marks the cut-off for HDV RT-qPCR. Pictured kinetic is an example for three independent experiments.

Secreted HDV RNA was observed if Huh7 cells were co-transfected with the plasmid encoding for HDV in combination with HBV plasmids encoding for either all three HBV surface proteins (LMS), as well as the LHBs and SHBs (LXS), or the SHBs (XXS), solely (Figure 27). These data show that SHBs alone is sufficient for HDV-secretion. HDV pseudo-particles exclusively enveloped with LHBs or MHBs could not be observed (Figure 27, LXX, XMX). In addition, HDV-pseudo-particles could not be secreted if an HBsAg-deficient plasmid was co-transfected (Figure 27, XXX).

The SHBs alone was sufficient for HDV-secretion. The secretion of HDV pseudo-particles could be observed if LHBs and SHBs or all three HBV surface proteins surrounded the HDV pseudo-particles.

3.5.2. Infection of PTHs with Recombinant HDV Pseudo-Particles

Synthesized HDV pseudo-particles, derived from cell-culture, were tested in the infection assay to verify their ability to infect PTHs. Therefore, supernatant containing HDV pseudo-particles after transfection of day six to twelve was concentrated with Vivaspin20. Then, concentrates were analyzed in HDV specific RT-qPCR again for absolute quantification of HDV like-particles. Equal amounts of HDV RNA were used to infect PTHs. As a control for infection, HDV purified from human plasma, was used. To inhibit the HDV infection, cells were pre-incubated with myr preS1-peptide ($1 \mu\text{M}$ f.c., 30 min, 37°C). Twelve days after infection, cells were lysed and newly synthesized HDV-RNA was detected with specific RT-qPCR.

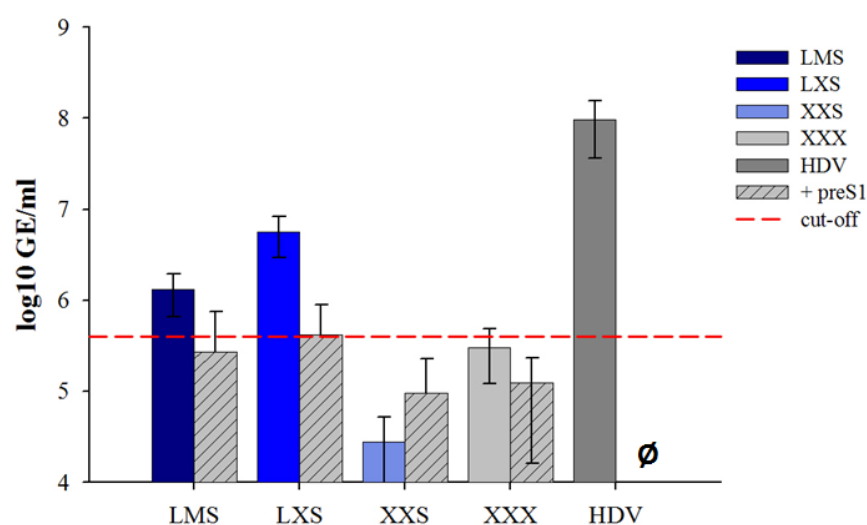


Figure 28: Infection of PTHs with recombinant HDV from cell culture. Infection assay was done with concentrated supernatant of generated HDV pseudo-particles (1×10^6 GE). 12 days after infection, PTHs were lysed, viral RNA was purified and analyzed for newly synthesized RNA by HDV specific RT-qPCR. Infection was inhibited by pre-incubation of the cells with myr preS1-peptide ($1 \mu\text{M}$) (30min, 37°C) (dotted grey bars) and served as a negative control. The X marks mutated HBsAg in the surface proteins. As a positive control, PTHs were also infected with purified HDV (1×10^6 GE) derived from human plasma. Cut-off is shown with red dotted line. Data present the average \pm SD from three repetitions.

The infection was effective in PTHs if purified HDV (Figure 28, HDV) or HDV pseudo-particles including the LHBs (Figure 28, LMS, LXS,) were used. PTHs were not infected with HDV pseudo-particles enveloped with SHBs, only. Supernatant from transiently transfected cells with HDV and an HBsAg deficient plasmid was used as a negative control. The infection of purified HDV and HDV pseudo-particles derived from cell culture could be inhibited by applying HBV myr preS1-peptide (Figure 28, dotted grey bars).

A successful HDV infection of PTHs was observed if HDV like-particles possessed the LHBs.

3.5.3. Neutralization of Infection of Cell Culture-Derived and Plasma-Derived HDV Using Monoclonal Antibodies

Monoclonal antibodies against the HBV surface proteins were reported to inhibit HBV-infection (Sureau et al. 1992, Glebe et al. 2003). The following study should show, if monoclonal antibodies against the HBsAg can neutralize the HDV infection, too. Therefore purified and recombinant HDV possessing all three HBV surface proteins was preincubated with monoclonal antibodies against HBsAg before infection of PTHs was done. Twelve days after infection newly synthesized HDV-RNA was detected with RT-qPCR.

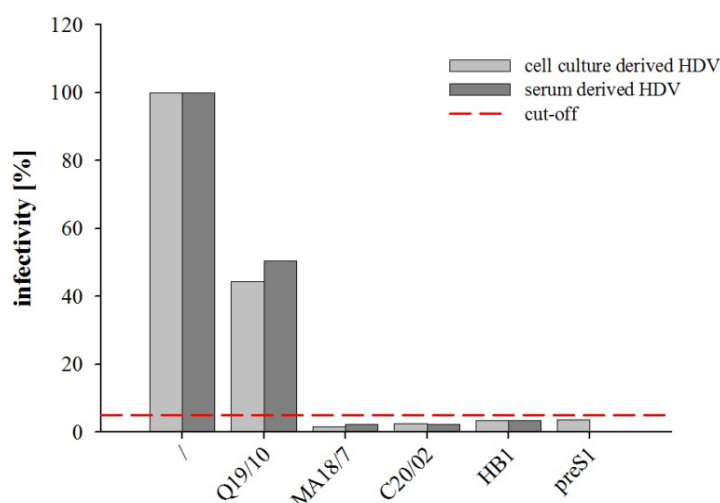


Figure 29: Infection of PTHs with recombinant HDV pseudo-particles and purified HDV derived from human plasma neutralized with mAbs against HBV surface proteins. Recombinant HDV and HDV purified from human plasma were preincubated (1 h, 20 °C) under continuously shaking with monoclonal antibodies (5 µg f.c.) against HBV surface proteins. Then, PTHs were infected with cell culture derived HDV pseudo-particles including all three surface proteins (LMS) and purified HDV derived from human plasma (1×10^6 GE), three days after isolation. Duplicates for each approach were performed. Data present infectivity in %.

Recombinant HDV as well as purified HDV were neutralized with mAbs against LHBs (MA18/7) and SHBs (C20/02, HB1) (Figure 29) and hence did not infect PTHs. The infection rate was reduced about 40 %-50 % when HDV was neutralized by an antibody that recognizes MHBs (Q19/10) (Figure 29). These results indicate the significance of LHBs and SHBs for an effective infection. The MHBs seems to be of minor importance for viral infectivity.

Infection of PTHs with purified HDV from human serum and recombinant HDV pseudo-particles could be neutralized with monoclonal antibodies against LHBs and SHBs.

3.6. Production of Recombinant HDV with Mutations in the HBV Surface Proteins

To analyze the influence of HBV surface protein variants (with stop mutants or amino acid changes in their S-ORF) on HDV assembly and secretion, HDV pseudo-particles were generated including selective HBV stop mutations. Therefore, Huh7 cells were co-transfected with plasmids encoding for HDV and selected HBV surface protein variants (M1T, 172*, 172L, 196*, 196S, 196L), and cultivated over nine days. The supernatant was then examined for newly secreted HDV pseudo-particles using the HDV specific RT-qPCR.

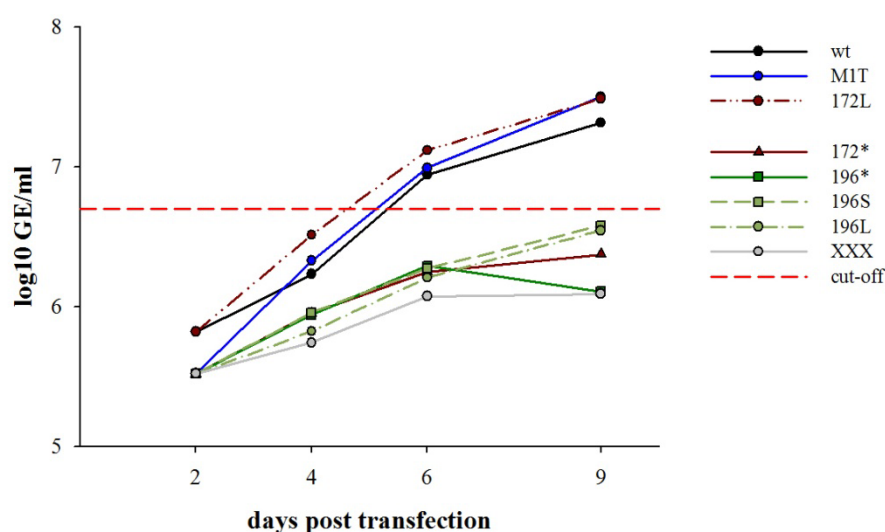


Figure 30: Kinetic of HDV-production with stop mutants. Huh7 cells were co-transfected with plasmids encoding HDV and selected HBV surface protein variants (M1T, 172*, 172L, 196*, 196S, 196L). As a negative control an HBsAg lacking plasmid was used (XXX). A plasmid encoding HBsAg from wt (wt) was used as a positive control. The supernatant was harvested on day two, four, six, and nine after transient transfection, purified and viral RNA was detected with HDV specific RT-qPCR. Cut-off is presented with red dotted line.

Mutations at position W172* or W196*/S/L in the SHBs seemed to have crucial functions for virion assembly and secretion. The assembly and secretion of HDV pseudo-particles is inhibited when HDV is co-transfected with HBV stop mutants W172* and W196* as well as an HBsAg deficient plasmid (XXX) (Figure 30). An altered amino acid sequence at position W196 leads to decreased virion assembly and secretion, too (Figure 30, W196S, W196L). In contrast, HDV pseudo-particles enveloped with wild type HBsAg (wt), a mutant with the amino acid change from tryptophan to leucine at position 172 in the SHBS (172L), exhibited normal virion assembly and secretion (Figure 30). The missing LHBS had no effects on virion assembly and secretion (Figure 30, M1T).

The position 172 in the SHBs and the position 196 in the internal loop of the SHBs have crucial functions in secretion of HDVpseudo-particles.

4. Discussion

During the long-term treatment of a chronic hepatitis B infection with antiviral inhibitors, HBV resistance mutants often occur, leading to an antiviral breakthrough. The genome of HBV is highly compact and, due to this, mutations that arise in the viral polymerase, during the antiviral therapy, also affect the genes of the other viral proteins, especially the gene for the HBV surface proteins. These mutations do not only affect the secretion and infectivity of HBV, but also have strong consequences for its satellite virus: the hepatitis delta virus. HDV is dependent on the HBV surface proteins for assembly and virion secretion. Due to this, mutations in the HBV surface proteins also influence the viral life cycle of HDV.

In the first part of this study, the phenotypic characterization of patient isolates from chronically infected patients should be continued, focusing patient isolates that possess characteristic HBV surface protein variants. Then, HBV surface protein mutants were generated, possessing single mutations in the SHBs, to analyze the influence of these selected single-mutations in the SHBs on the assembly and secretion of virions. In the second part, an *in vitro* transfection system in Huh7 cells should be established to generate recombinant HDV pseudo-particles. Using these HDV pseudo-particles, an infection system for HDV on PTHs should be established. To ensure a better comparability, plasma, derived from a chronically co-infected HBV/HDV patient, was further characterized. In this context, a full length genomic HDV RNA standard should be generated for absolute quantification of HDV RNA. Using these methods, the influence of the selected HBV surface protein variants on the ability of recombinant HDV to assemble and secrete HDV like-particles should be investigated.

4.1. Phenotypic Resistance Profile of Special Patient Isolates During Antiviral Therapy

In the last years, many projects on the analysis of resistance mechanism induced by different nucleos(t)ide analogs and its consequences on virion formation, secretion, and viral fitness were performed. Therefore, a large number of *in vitro* assays were established to characterize resistance mutants. Furthermore, with the help of such resistance assays, several characteristic primary mutations could already be defined, that obviously are the results of the treatment with one of the four common nucleos(t)ide analogs; (lamivudine (LMV), entecavir (ETV), adefovir (ADV), and tenofovir (TDV)) (reviewed in Zoulim and Locarnini 2009, 2013). In this work, typical resistance patterns for all four common nucleos(t)ide analogs were also observed with the phenotypic resistance assay.

The sequence analysis of patient isolate KW 11a-1 revealed a stop mutation at position 216 in the SHBs (sL216*), which is not correlated with any known resistance mutation in the rt-domain of the viral polymerase. Phenotypic analysis of this clone showed resistance to lamivudine (LMV) and a weak resistance to entecavir (ETV), only. This mutation pattern is not yet described in the literature. Therefore,

more tests have to be done to characterize the stop mutation at position 216 in the SHBs in more detail, which probably indicates a new resistance pattern for LMV and ETV.

A long-term treatment with the nucleoside analog LMV is known to induce mutations, especially in the YMDD motif, the catalytic domain of the HBV polymerase (Stuyver et al. 2001) mediated primarily by the mutations at position V191I, M204I, or M204V in the rt-domain. These mutations were also found in the tested patient isolates including characteristic mutations in the SHBs. The patient isolate KW 6a-6 exhibits the mutation pattern rtV191I sW182* (Wakil et al. 2002, Kazim et al. 2006). In contrast to what was published, a lamivudine resistance could not be observed, but a weak resistance to ETV was detected. It can be speculated that a second, compensatory mutation leads to this special phenotype. Compensatory mutations have known influence on the viral fitness, and can also affect the known resistance pattern.

In the literature, the primary mutation rtM204I is often associated with the secondary mutation rtL80I/V, but can also occur in combination with rtL180M to a lesser extent (Warner and Locarnini 2008). In the case of the patient isolate KW 14-8, no typical secondary mutation was observed. The primary mutation rtM204I leads to the amino acid change from tryptophan (W) to serine (S) in the SHBs (sW196S). As expected, the patient isolate KW 14-8 demonstrated a strong resistance to LMV and ETV, and also showed a weak resistance to tenofovir (TDV), but a resistance to adefovir (ADV) was not observed. These findings are conform to the observations of other groups (reviewed in Zoulim and Locarnini 2009, 2013). Another important primary mutation, correlated with LMV resistance, is the mutation rtM204V, that is often associated with the mutation rtL180M (Warner and Locarnini 2008). This mutation pattern is known to result in a strong LMV resistance and it was shown that patients who exhibit this mutation are also less responsive against EDV (Bartholomeusz and Locarnini 2006). In addition, this mutation pattern is described to not influence ADV or TDV (Ghany and Liang 2007). As expected, these observations are consistent to the tested patient isolate RK 172-2 that has the mutation pattern rtI195M rtM204V. This isolate shows a strong LMV resistance, but also presents a weak resistance to TDV and ADV. The resistance to ADV cannot be explained with the mutation pattern rtI195M rtM204V of this patient isolate. This effect has already been described by A. Geipel and H. Niekamp (Geipel 2011; Niekamp 2013). The additional ADV and TDV resistance in this isolate needs to be observed and analyzed in more detail. It can be assumed that more unknown secondary mutations influence these two primary mutations significantly.

A resistance to ADV is associated with the mutations rtA181T/V and rtN236T (Warner and Locarnini 2008; Villet et al. 2008; Angus et al. 2003), and is also known to induce a LMV resistance (Yatsuji et al. 2006). The mutation rtV181T induces a stop mutation in the SHBs at position 172 (Warner and Locarnini 2008). The tested patient isolate RK 172-4 showed the mutation rtV181T with the additional mutation rtM204V. The results from the phenotypic resistance assay demonstrated a strong resistance to LMV, but only a weak resistance to ADV. Surprisingly, an intermediate resistance to EDV and tenofovir could also

be observed that could not be linked to a known resistance mutation. Similar to the patient isolate RK 172-2 deeper analyses are needed, but they are beyond the scope of this thesis.

4.2. Influence of Mutations within the HBV S-ORF that Arise During Antiviral Therapy on the Viral Life Cycle of HBV

Many phenotypic resistance assays were established to characterize special mutations in the rt-domain that were selected during the treatment with the commonly used nucleos(t)ide analogs. Due to the strong overlapping open reading structure of the HBV genome, mutations in the rt-domain also induce mutations in the other viral proteins. The s-gene (surface-gene) is completely overlapped by the polymerase-ORF and, therefore, mutations in this region lead to amino acid changes in the s-gene, too, resulting in mutations in the viral envelope proteins (Figure 8, page 45). These mutations may lead to modified secretion, infectivity, and immunogenicity. For some of these envelope protein mutations, altered virion secretion (sW172* (Warner and Locarnini 2008)) or the loss of binding capacity for neutralizing antibodies (sG145R, vaccine escape mutant (Torresi et al. 2002a)) are already described (Billioud et al. 2012).

In this study, most of the tested HBV-isolates of patients treated with antiviral inhibitors showed typical resistance profiles, some of them resulting in characteristic surface protein mutations. To analyze them in more detail, autonomously replicative-competent HBV variants, possessing typically occurring envelope protein mutations, were generated and kindly provided by Dr. M. Neumann-Fraune (Uniklinikum Köln) for this work (Figure 8, page 45 and Table 6 page 77). After the transient transfection in Huh7 cells, the supernatant was harvested and analyzed by qPCR, ELISA, immunohistochemical staining, and CsCl-gradients. The data are summarized in Table 6. After analyzing the supernatant of the transfected cells for viral DNA, it seemed to be the case that all HBV mutants secreted virions (Table 6 page 77). Cells that are transfected with wild type HBV replicative plasmids are known to secrete uncoated capsids in addition to enveloped virions in the cell culture. On that score, a sandwich-ELISA against the HBcAg was performed to verify if the detected DNA is derived from enveloped virions or uncoated capsids. Using the results of the ELISA as a basis, uncoated HBV capsids were secreted into the supernatant of transfected cells in addition to enveloped virions. This effect was already described in the literature (Nassal 1992; Sun and Nassal 2006; Bremer et al. 2009a). It is speculated by some authors that these capsids are secreted at the plasma membrane via an alternative mechanism requiring the adaptor protein ALIX (apoptosis-linked gene 2-interacting protein X) that is involved in the concentration and sorting process of cargo proteins of the MVB (Bardens et al. 2011). But the reasons for this phenomenon are still unknown.

It is described in the literature that some HBsAg mutants show a modified replication capacity that leads to a reduced secretion (reviewed in Sheldon et al. 2006). These observations are conform to the findings

of the ELISA and the phenotypic resistance assay, because the viral fitness as well as the secretion of HBsAg is reduced if a stop mutation takes place in the SHBs. In this context, one exception has to be mentioned: the 172* mutant, because a weak signal for SHBs is observed in the ELISA (summarized in Table 6, page 77). It also has to be mentioned that the missing HBsAg signal in the ELISA does not contribute to the presumption that the stop mutants are secretion deficient. It can be supposed that amino acid changes in the SHBs lead to conformational changes of this protein which then can affect the antigenic loop. The antigenic loop bears important epitopes for the recognition of neutralizing antibodies (Peterson et al. 1984; Emini et al. 1986), and it is an important region for the detection of several antibodies of diagnostic kits. The need of the correct folding of the antigenic loop for the recognition of antibodies was already shown by Glebe *et al* (2003). A "misfolded" SHBs and, therefore, antigenic loop, induced by different stop mutations, may lead to an altered conformational structure and modified antigenicity that can result in a diagnostic escape. The ELISA-kit that was used is able to detect the 172* mutant, but nothing is known concerning the detection capacity for the other stop mutants (Avellón et al. 2011). Due to the fact that these observations were also made in two other hepatoma cell lines (human: HegG2; murine: AM12) it could be shown that the results are not cell type- or species-specific. The suggestion of an altered conformational structure of the SHBs resulting in detection-escape of diagnostic kits is supported by the fact that enveloped virions are detected in the CsCl-gradient. This method takes advantage of the fact that molecular particles can be separated because of their different densities. The comparison of cell-culture derived wild type HBV to serum derived HBV illustrates that both types of viruses behave the same in CsCl-gradient and, therefore, the results of this study can prove if virions and/or uncoated capsids are secreted. The treatment of the virions with detergent and reducing agent leads to the removal of the viral envelop resulting in a shift of the uncoated capsids to higher densities. The fact that after the reducing procedure, the HBV DNA is detected in the same densities in which uncoated capsids are supposed to be, leads to the suggestion that the envelopes of all virions are removed. The results of the present work show that a stop mutation in the C-terminus of the SHBs (176*, 216*) leads to a reduced secretion of enveloped virions. This is true for most of the tested mutants (summarized in Table 6 page 77). In this context, two stop mutants attract attention: the SHBs mutants 182* and 199*. For both mutants, no HBsAg could be detected in the HBsAg-specific ELISA but analyses of both mutants in the CsCl-gradient detected a very small amount of secreted HBV virions. It can be assumed that the secretion of these HBV surface protein variants is too low and, therefore, detection of HBsAg in the ELISA is located under the detection limit. During CsCl-gradient centrifugation, these secreted virions were concentrated in fractions where enveloped virions float and, therefore, they could be measured with the HBV specific qPCR. Nevertheless, the HBV surface protein mutants 176*, 182*, 199*, and 216* should be further analyzed with immunofluorescent staining, verifying the expression of HBV envelope proteins. Because of what has been found so far, the question arises, if these stop mutants secrete virions that are also competent to infect hepatocytes.


























In this experimental procedure, three stop mutations are of special interest: the mutant M1T, the 172* mutant, and the 196 stop mutant. A stop mutation at position 172 in the SHBs can occur during long-term treatment with the nucleotide analog adefovir. In 2008, Warner and Locarnini postulated that this mutant is defective in the secretion of virions and HBsAg, leading to the retention and accumulation of virions within the cells (Warner and Locarnini 2008). This is contrary to the fact that the SHBs-specific ELISA has proven the secretion of 20 % of SHBs for the mutant 172*. Immunohistochemical staining against the LHBs, MHBs, and SHBs confirmed this result. All envelope proteins can be visualized in the immunofluorescence indicating that the surface proteins are synthesized and expressed in mutants bearing a stop mutation at position 172. The western-blot analysis of Warner and Locarnini (2008) also demonstrated that the expression of LHBs and MHBs is inhibited, although a stop mutation at position 172 in the SHBs takes place. Specific ELISA against secreted LHBs and MHBs that were done in the present work confirmed these results, although both proteins were synthesized and expressed (immunohistochemical staining). According to these findings, it can be speculated that a stop mutation at position 172 does not inhibit the expression of LHBs and MHBs but blocks the secretion of both HBV surface proteins leading to the rebound and accumulation of virions within the cells. Proceeding from these data, the question arises if HBV surface protein variants, having a stop mutation at position 172 in the SHBs that leads to the inhibition of LHBs and MHBs secretion, but shows a reduced SHBs secretion, are able to infect hepatocytes? To prove its ability to infect new hepatocytes, this mutant should be tested in infection assays. Due to the missing LHBs on the secreted HBV surface protein variant sW172*, it can be assumed that an effective infection will not be possible.

In contrast to the work of Warner and Locarnini (2008), the CsCl-gradient of the HBV variants with a stop mutation at position 172 in the SHBs shows that enveloped virions are secreted. Based on this finding, this study showed that mutants bearing a stop mutation at position 172 in the SHBs are secretion competent, but this competence is strongly reduced compared to the wild type. Due to this reduced secretion capacity, one might assume that the detection methods which were used in the mentioned paper (Warner and Locarnini 2008) are less sensitive than the ones used in this study and, therefore, the residual secretion of the HBV mutant 172* could not be detected. This detection escape could be a crucial problem for the HBV diagnostics, too. Warner and Locarnini (2008) could additionally show that the mutant 172* can have a dominant negative effect on the HBV wt. A minor sensitivity of commercial diagnostic kits in combination with a strongly decreased secretion capacity of mutants plus a strongly decreased viral load that probably is located under the detection limit of several diagnostic methods could mask a viral break-through during antiviral therapy and would lead to a wrong diagnosis. This diagnostic escape plays a crucial role for the infection and treatment of naïve patients because it could mean that also these infections remain undetected and antiviral therapy failed. To analyze this possible scenario, future studies should take a closer look at the dominant negative effect of the 172* mutant.

Two other interesting stop mutants attracted attention because it was shown that both mutations, the mutation 196* and the mutation M1T, significantly affect the virion packaging and secretion as only uncoated capsids were detected in the supernatant of transfected cells. For the HBV variant M1T, the results confirmed the expectations. The start codon of LHBs is changed, leading to the loss of its start signal during transcription and to no expression of the LHBs. In this experimental setting, the secretion deficient mutant M1T was generated as a control for the wild type virus. Due to the fact that the LHBs is necessary for the interaction of the viral envelope with the mature core-capsids for the secretion of mature HBV virions (Bruss 1997), LHBs plays an essential role for the viral life cycle.

Surprisingly, a stop mutation at position 196 in the SHBs seemed to block the secretion of enveloped virions and subviral particles as well as the synthesis and expression of all three surface proteins, completely. The secretion of virions was rescued if a serine or leucine was present at position 196 instead of the amino acid tryptophan. The analyzed HBsAg mutations sW196L/S/stop are typical mutations associated with a resistance to LMV at position M204I/V.

Table 6: Summary of expressed and secreted HBV surface proteins variants, subviral particles, uncoated HBV capsids, and secreted HDV pseudo-particles enveloped with different HBV surface protein variants.

name of the wt/mutant	position and aa sequence of the mutation in		HBV									HDV	
			expression of HBV surface proteins			secretion of HBV virions, subviral particles and uncoated capsids						secretion of HDV pseudo-particles	
			P-ORF	S-ORF	LHBs	MHBs	SHBs	GE	LHBs	MHBs	SHBs	Core	CsCl-gradient
serum /plasma derived	-	-	n.d.			+	+	+	+	+			
wt	-	-	+	+	+	+	+	+	+	+	 < 		
M1T	H181 ^Δ	M1T	-	+	+	+	-	+	+	+			
172*	A181T	W172*	+	+	+	+	-	-	+	+	 = 	-	
172L	L180 ^Δ	W172L	+	+	+	+	+	+	+	+	 = 		
176*	T184M	L176*	n.d.			+	-	-	+	+	 > 	n.d.	
182*	V181I	W182*	n.d.			+	-	-	-	+		n.d.	
196*	M204V	W196*	-	-	-	+	-	-	-	+		-	
196S	M204I	W196S	+	+	+	+	+	+	+	+	 < 	-	
196L		W196L	+	+	+	+	+	+	+	+	 < 	-	
199*	V207I	W199*	n.d.			+	-	-	-	+		n.d.	
216*(TAA)	V224 ^Δ	L216*	n.d.			+	-	-	-	+	 = 	n.d.	
216*(TGA)			n.d.			+	-	-	-	+	 = 	n.d.	

+ = detectable; - = not detectable
 * = stop mutation; n.d. = not determined; ^Δ = no change in amino acid sequence

4.3. Establishment of an RNA Standard for HDV RT-qPCR

HDV infections are diagnosed by three common procedures: 1) an ELISA to detect anti-HDV antibodies (anti-HDAg IgM and IgG) in human serum or plasma, 2) the radioimmunoassay, 3) the visualization by immunofluorescence or immunohistochemical staining in liver biopsies. The detection of HDV RNA in plasma or serum of infected individuals is done in each laboratory by individual in-house PCRs using internal laboratory standards if any is available. These PCR systems and individual standards strongly differ in their quality. Due to the fact that, compared to HBV, an infection with HDV is rare, neither a standardized detection method nor an international reference standard for quantification presently exists (Olivero and Smedile 2012). Some laboratories use serum of a chronically infected HDV patient for quantification, but the availability of this material is limited. In order to optimize this situation, a full length genomic HDV RNA standard (clade 1) was generated *in vitro* for the in-house PCR of the laboratory in Gießen, to be able to set up a reliable quantification of HDV RNA in cell lysates, human serum, plasma, or supernatant from transfected cells. It could be shown that the *in vitro* generated full length genomic HDV RNA standard can be used in a range from 2×10^8 GE down to 2×10^3 GE. RNA standards generated by others (Ferns et al. 2012; Scholtes et al. 2012; Katsoulidou et al. 2013) demonstrated an equal sensitivity for their standards and qPCR systems. But it has to be taken into consideration that the PCR systems strongly differ in their use of individual PCR kits, probes, primers, and standards (HDV plasmid-DNA, HDV purified from plasma, RNA of a short subgenomic fragment). These differences can affect the efficiency of the qPCR. To name some examples, short subgenomic fragments of HDV RNA probably possess extremely strong rod-like structures (Schaper et al. 2010) that complicate the effective binding of the primers, whereas the use of HDV plasmid-DNA as a standard does not provide any information about the efficiency of the reverse transcription step. Therefore, it still remains difficult to compare and interpret the efficiency of the different PCR protocols and standards of different research groups.

The sequence analysis of all eight known HDV clades (after Le Gal et al. 2006) was used to analyze if the primers were able to detect all HDV clades. The analysis showed that the primers bind in regions at the C-terminus of the S-HDAg that are highly conserved (Casey et al. 1993), predicting the recognition of all eight HDV clades. Therefore, the in-house PCR of Gießen in combination with the *in vitro* generated full length genomic HDV RNA standard makes this system appropriate for the detection and quantification of HDV RNA in plasma samples, supernatant of cell culture, as well as cell lysates. However, no other serum samples or cloned HDV genomes of other HDV clades were available during this work.

In future studies, the competence to detect all eight HDV clades should be tested. In addition, it would be desirable to generate an international reference standard as well as a uniform qPCR protocol for the quantitative detection of HDV RNA that can be used by different laboratories.

4.4. Characterization of HDV Derived from Human Plasma of a Chronically Infected Patient

For characterization, HDV-positive plasma was analyzed with a linear CsCl-gradient to separate virions and uncoated capsids. In the present work, it could be shown that the virions floated at a density of 1.29-1.3 g/ml CsCl. These findings are in line with the data of Roggendorf *et al.* and Bordier *et al.* (Roggendorf *et al.* 1987, Bordier *et al.* 2003). In contrast to these findings, Rizzetto *et al.* and Bonino *et al.* specified the buoyant density of HDV in CsCl-gradient to 1.25 g/ml (Rizzetto *et al.* 1980b, Bonino *et al.* 1986). The reason why HDV could be detected in different densities of CsCl is not the use of different HDV clades because HDV-3 (Bordier *et al.* 2003) and HDV-1 (Roggendorf *et al.* 1987) float in similar densities. Different origins of the HDV particles (purified virions from liver tissue of humans, chimpanzees, woodchucks, mice, or from plasma of chimpanzees) as a reason for differences in buoyant density of HDV can also be neglected because Rizzetto *et al.* analyzed the serum of infected chimpanzees, and Roggendorf *et al.* analyzed HDV derived from liver tissue samples of an infected chimpanzee (Rizzetto *et al.* 1980b; Roggendorf *et al.* 1987a). Both HDV-samples float at a density of 1.25 g/ml. The discrepancy in the detected buoyant density of HDV in CsCl-gradient cannot be explained and, therefore, further investigation is needed to analyze this mismatch. Nevertheless, the findings of the present work confirm the results of Roggendorf *et al.* (1987) and Bordier *et al.* (2003) who showed that HDV floats at a density of 1.29-1.3 g/ml CsCl.

The treatment with detergent and reducing agent lead to the complete degradation of the HDV particle. This means that the RNP dissociates if the integrity of the viral envelope is affected, and the viral RNA is not protected against RNase-based destruction, anymore. The HDV RNP does not seem to provide comparably efficient protection of the viral genome as the HBV capsids do. Abou-Jaoudé and Sureau (2007) demonstrated this effect for HDV, too.

4.5. Infection of PTHs with Purified HDV

In the past, infection assays of primary human hepatocytes (PHH), primary woodchuck hepatocytes (PWH), as well as primary hepatocytes from chimpanzees (PCH) were always done with HDV derived from cell culture or serum of HDV-infected chimpanzees treated with HDV cDNA (Sureau *et al.* 1991; Gudima *et al.* 2007, 2008). For the first time, it could be shown in this thesis that HDV, purified from chronically infected patients, can infect PTHs.

Before performing the infection assay, the virus was purified from the plasma, as described for HBV (Glebe *et al.* 2003; Glebe and Gerlich 2004). The peak of viral RNA was observed at densities of 39-45 % sucrose. In contrast to the data obtained by the CsCl-gradient, results from the sucrose gradient are in line with the findings presented in the literature for sucrose gradients for HDV (Rizzetto *et al.* 1980b).

The plasma was derived from a patient, chronically infected with HDV and HBV, but HBV DNA was neither detected in the CsCl-gradient nor in the sucrose-gradient. It is known that HDV represses the HBV replication and secretion in chronically infected patients (Williams et al. 2009; Gordien et al. 2001). The concentration of HBV genomes in the fractions after centrifugation was probably under the detection limit of the qPCR (detection limit: 10 GE).

A successful infection of PTHs with the purified fractions of HDV indicates that PTHs are susceptible for HDV. Using the established methods, these results of the present work are in line with the findings of other groups which also showed that PTHs can be infected with HDV *in vitro* and *in vivo* (Li et al. 1995; Yan et al. 1996, Yan et al. 2012). The infection with HDV can be neutralized with monoclonal antibodies especially against the SHBs and LHBs, and the infection can be blocked by using myr preS1-peptide. These findings are completely conform to the literature (Yan et al. 2012; Lütgehetmann et al. 2012, Lamas Longarela et al. 2013). In the present work, it was also demonstrated that PTHs are susceptible for HDV on day two to day four after isolation, as it is already known from HBV (Çağ 2004). Due to the fact that HDV is dependent on the envelope proteins of HBV for virion assembly and infectivity, the results support the findings that the specific receptor for HBV and HDV, the NTCP, is present on the plasma membrane, only a short period of time after isolation of primary hepatocytes (Liang et al. 1993).

When comparing the infectivity of serum derived HBV to plasma derived HDV for PTHs in the present study, it was observed that more hepatitis B virions (calculated as genome equivalents) are needed for an effective infection (1×10^8 GE) than hepatitis D virus particles (1×10^6 GE) in the specific setting used here. A possible reason for the differences in infectivity could be the different up-take mechanism and, therefore, the different endocytotic pathway of HBV and HDV. It was speculated that these differences could probably be caused by their different proportion of HBsAg and, therefore, by their different use of other co-receptors (Bonino et al. 1984, 1986; Sureau et al. 1991). Bonino *et al.* (1986) showed that the surface protein composition of HDV particles is more related to that of subviral particles than to hepatitis B virions because the HDV envelope exhibits only 1 % or less of the LHBs (Bonino et al. 1986). Normally, HBV particles from genotype D exhibit approximately 16 % LHBs. Furthermore, the interaction of SHBs with the HDV RNP could induce conformational changes in the SHBs, which may expose other domains of the surface proteins on the viral envelope, leading to the binding of additional receptors, which then mediate other uptake mechanisms. Another possible reason for the different amounts of HBV and HDV required for an effective infection of PTHs might be the different quality of the human serum and plasma that was used. For infection with another HBV preparation a smaller amount of purified HBV was sufficient (1×10^6 GE) for a successful infection (Saniewski 2009). The discrepancy of the infection efficiency between these two human HBV positive sera may be explained by a different efficiency of the purification procedure and is also dependent on the quality of the serum itself. Due to their buoyant density of approx. 1.18 g/cm^3 in CsCl, subviral particles, especially filaments,

cannot be separated completely from virions. A large number of subviral particles produced in HBV infected patients can interfere with the infection process and lead to a less efficient infection outcome.

Furthermore, it could be shown that co-infection of HBV and HDV and super-infection of HBV infected primary hepatocytes with HDV were possible. In the past, co- and super-infection studies were first done with susceptible chimpanzees, which were infected with HBV and HDV to examine and compare the clinical manifestation of a co- or super-infection to that in humans (Purcell et al. 1987). Because of the ethical concerns, the limited availability, and the high costs, these experiments were stopped. Until today, only a few co-transfection analyses in hepatoma cell lines with replication-competent HBV and HDV expressing plasmids (Wu et al. 1991), and some co- and super-infection assays in humanized mice (Lütgehetmann et al. 2012; Giersch et al. 2014) were done to analyze the intracellular interaction of HBV and HDV. In fact, infection assays on primary *Tupaia* hepatocytes *in vitro* with naturally occurring HDV and HBV derived from infected patients, to analyze co- and super-infection were never done before. Although it was possible to infect PTHs with both viruses, no differences were observed between HBV/HDV co- or super-infections in the present study. A RT-qPCR was used for the detection of the HDV infection. Therefore, it is not sure if single PTHs are co-infected with both viruses simultaneously or if mono-infections occur as well. Mono- and co-infections can be analyzed in future projects with immunofluorescence. Normally, in patients who are super-infected with HBV and HDV, the infection course tends to result in a chronic HDV infection over months, leading to the suppression of HBV replication and antigen expression. This was not observed in the present study because of the limited time scale of the *in vitro* experiments. Co- as well as super-infection with HBV and HDV resulted in equal amounts of newly secreted HBsAg and newly transcribed HDV RNA. The reason might be that PTHs are susceptible for HBV and HDV only in a short time period after isolation (Yan et al. 2012). It is conceivable that a different *in vitro* infection system would be more appropriate for further co- and super-infection studies, for example a stably transfected cell line that constitutively expresses the hepadnaviral high affinity receptor NTCP to study the HBV/HDV co- and super-infection *in vitro*. It might be that in such a system the co- and super-infection develops similarly to the naturally occurring infection course and, therefore, adequate information about the entry, the used endocytotic pathways of both viruses, and their interaction within the cell can be provided. Because of the lack of time, this experiment was carried out only once. Therefore, variances cannot be excluded and this experimental setting has to be repeated to verify the results presented in this work.

4.6. Production and Detection of Recombinant HDV Enveloped with Different Combinations of HBsAg

Virion formation, the release of mature virions, and the infectivity for HBV and HDV is often compromised by mutations within the viral genome that frequently arise during antiviral therapy as well as under the pressure of the immune-system, for example during occult hepatitis B infection. In order to

study the effects of the mutations in the relevant surface proteins, a transfection system was established to generate HDV like-particles enveloped with defined mutants of HBV surface proteins. In conformity with the literature, the Huh7 cell line was used to generate these HDV pseudo-particles (Sureau et al. 1991; Wu et al. 1991; Gudima et al. 2007). The present study shows that the transiently transfected cells secrete recombinant HDV after three days, indicating that the transfected cells readily synthesize the mutated HBV surface proteins, leading to the assembly of HDV (Gudima et al. 2007). As expected, HDV pseudo-particles were generated and secreted when HDV was covered with all three surface proteins, the LHBS and the SHBs or the SHBs, only. These findings are conform to the literature and indicate that the SHBs alone is sufficient for HDV-secretion, too (Chang et al. 1991; Sureau et al. 1993). In previous studies conducted by Sureau and coworkers, it could be shown that the C-terminus of the SHBs, especially one amino acid in the internal loop of the SHBs, is the crucial region for the binding of HBsAg and HDV RNP. This interaction mediates the envelopment and secretion of mature hepatitis D virions (Jenna and Sureau 1999; Komla-Soukha and Sureau 2006). In contrast to HDV, the assembly and secretion of mature hepatitis B virions do not depend on SHBs, solely, but also on the LHBS-isoform that is exposed on the internal site of the viral envelope. The internal loop of the SHBs as well as a domain in the preS1/preS2 region are necessary for the encapsidation of mature core particles of the hepatitis B virus (Bruss 1997). The MHBs does not seem to be necessary for virion assembly or infectivity for HBV (Bruss and Ganem 1991; Le Seyec et al. 1998) as well as HDV (Sureau et al. 1994), and its function in the viral life cycle of both viruses still remains unclear. However, some studies postulate that the MHBs facilitates the secretion of hepatitis B virions and subviral particles (Garcia et al. 2009). Nevertheless, the present work shows that a transfection system to generate HDV pseudo-particles was successfully established.

After transient transfection, the cells were cultivated up to 12 days. Because of the rapid growth of the cells, they had to be split within a very short period of time, which made handling difficult. Probably, HepG2 cells could be used, not only to avoid some difficulties in handling, but also because they are more related to differentiated liver cells than Huh7 cells. Another particular feature is that they can be arrested in their cell cycle by adding DMSO (Kost and Michalopoulos 1991) while cultivating. For reasons that are still unknown, this treatment slows down the cell proliferation and is known to promote the production of virus particles. This cell line could be an appropriate alternative to the Huh7 cells but it has to be mentioned that the transfection efficiency of HepG2 is lower than that of Huh7 cells (transfection efficiency of HepG2: 10 %; transfection efficiency Huh7: 50-75 %) (Chang et al. 1987). Moreover, this cell line has not yet been used to produce HDV pseudo-particles, so it still has to be tested, if these cells are really qualified to generate recombinant HDV.

After transient transfection, there was a high amount of DNA-background that was caused by plasmids that might be bound to the plasma membrane or on the cell culture plate. Those plasmids are not taken-up into the cells after transfection and can be detected subsequently by qPCR. A. Geipel (2011) showed that the application of several washing steps and the transfer of the cells to a new cell culture plate reduced the

plasmid-background after transient transfection. Barrera *et al.* (2004) included a DNase I digestion before running the PCR. These improvements were also used in this work to decrease the DNA-background. Nevertheless, there is still plasmid-DNA detectable. Probably the plasmid background is not fully reduced by washing steps as shown by A. Geipel (2011). An additional explanation could be an incomplete DNase digestion because of the huge amount of plasmids in the supernatant. One idea would be to extend the time of DNase digestion or to use higher amounts of DNase, like Barrera *et al.* (2004) did in their work. They used 4 U DNase to digest the plasmid-DNA, whereas 1 U of DNase was taken in this study.

To optimize the system, the ratio of the HDV plasmid and the plasmid encoding the HBV surface protein mutants could be titrated. Several distinct plasmid-concentrations were used in the literature to produce HDV pseudo-particles. Gudima and Taylor *et al.* (2007), for example, use a ratio of 1:4 HDV to HBV envelope protein expressing plasmids. In this study a ratio of 1:1.3 was used according to the ratio taken by Sureau and colleagues (1:1, 1:2) (Jenna and Sureau 1999; Abou-Jaoudé *et al.* 2007). It has to be mentioned that the direct comparison of these different transfection assays is difficult because different transfection reagents and HBV surface protein plasmids, which are regulated by different promoters, were used. Taylor and colleagues, for example, used HBV surface protein expressing plasmids derived from genotype A under the control of an SV40 promoter known to lead to a high constitutive expression rate of the protein (Gudima *et al.* 2007). In contrast, Sureau and colleagues utilized HBV envelope encoding plasmids, derived from genotype D, which was under the control of the natural HBV promoter (Jenna and Sureau 1999). The subgenomic HBV envelope protein expressing plasmids that were used in this work were under the control of the natural HBV promoter, too, and, therefore, they provide a more related HBsAg-expression in cell culture compared to naturally occurring infections in hepatocytes. The improvement of the plasmid ratio between HDV and HBV could be helpful to find out the optimal ratio that leads to a maximized yield of HDV pseudo-particles and minimized cell stress.

4.7. Infection of PTHs with Recombinant HDV in Comparison with Purified HDV

Secreted HDV like-particles enveloped with all three HBV surface proteins, with the LHBs and SHBs or covered with only the SHBs, were tested in the infection assay to prove their ability to infect PTHs. Supernatant from transiently transfected cells with the HDV-plasmid and an HBsAg deficient plasmid was used as negative control. PTHs were also infected with HDV, purified from a chronically infected patient that served as positive control. This work shows that HDV pseudo-particles possessing the LHBs are able to infect PTHs, confirming the observations that have already been made by other groups (Sureau *et al.* 1991, 1991; Jaoudé and Sureau 2005; Abou-Jaoude and Sureau 2007). PTHs were not infected when they were treated with either the supernatant of cells transfected with the HDV-plasmid and an HBsAg lacking plasmid or HDV like-particles covered with the SHBs, only. It can be summarized that HDV like-

particles derived from cell culture, are able to infect PTHs, demonstrating that an infection system for recombinant HDV pseudo-particles was successfully established.

If the efficiency of the infection of recombinant HDV and purified wt HDV (derived from human plasma) is compared, it is important to highlight that the infectivity of recombinant HDV is lower than the infectivity of purified HDV derived from human plasma. This observation has already been made by Sureau and colleagues (Sureau et al. 1992). These differences in the infectivity can be explained with the generation procedure because it must be considered that the production of HDV pseudo-particles covered with different HBV surface protein variants was performed in immortalized hepatoma cell lines that do not necessarily have the same features like primary cells. It might be that cell culture derived HDV pseudo-particles are not totally similar in their surface protein composition and, therefore, the efficiency of infection cannot totally be compared to plasma-derived HDV. Further experiments, for example western blot analyses of cell culture derived HDV compared to plasma-derived virus, would give an indication of the amount of the HBsAg. A further explanation for the differences in the infectivity of HDV derived from human plasma and cell culture could be the purification procedure and the production process of the recombinant HDV like-particles. Because of apoptotic processes, a lot of cell debris and unfinished virus-like particles probably are released into the supernatant of transfected cells. This cell debris and unfinished virus-like particles could be concentrated, too, when HDV pseudo-particles derived from cell culture were enriched during the concentration procedure. These particles may reduce the infection efficiency by interfering and preventing the binding of the LHBs with the preS1 region of the NTCP. In this context, it may also be that a contamination with plasmid-DNA is another possible reason for the low infectivity rate. Because of the concentration process, in that the plasmid-DNA was also concentrated, one could assume that it binds to the viral surface membrane during infection procedure and then can be detected in the qPCR, too. This disagreement would be wiped out by performing an additional DNase digestion. A better possibility to purify and concentrate the HDV pseudo-particles from cell culture could be the utilization of a continuous sucrose gradient. This method provides better and clearer purification of the hepatitis D virus-like particles and was also used by Sureau *et al.* (1991) before starting infection assays on primary hepatocytes. Nevertheless, the data of the present work show that cell culture derived HDV pseudo-particles are infectious in PTHs, too.

4.8. Influence of Mutations within the HBV S-ORF that Arise During Antiviral Therapy on the Viral Life Cycle of the Hepatitis D Virus

The mutation rtM204V in the viral polymerase of HBV is crucial not only for the development of HBV resistance mutants and, therefore, antiviral treatment but also influences the viral life cycle of its satellite virus: the hepatitis delta virus. The present work has shown that a stop mutation at position sW172 or sW196 as well as an amino acid change at position sW196 in the SHBs leads to a block in the secretion of HDV pseudo-particles (summarized in Table 6, page 77). It could be assumed, that these stop mutations

lead to the loss of the transmembrane domain III and IV and, therefore, also to the loss of the third internal loop of the SHBs. The internal loop region is crucial for the interaction of the HDV RNP with the HBsAg during envelopment and secretion of HDV. Sureau and coworkers have shown that especially the internal loop between transmembrane III and IV is the HDV packaging-domain and essential for an effective secretion (Jenna and Sureau 1998, 1999). In 2006, Komla-Soukha and Sureau detected the position 196 in the SHBs (sW196) as an essential position for the interaction of the HDV RNP with the small HBV surface protein. In contrast to HBV, the present data show that the release of enveloped virions was not rescued if an amino acid change to serine or leucine took place at position 196, and thus highlight the important function of the position sW196 in the SHBs for HDV secretion, too (Wang et al. 1991; Komla-Soukha and Sureau 2006). Mutants carrying the functional SHBs (wt, M1T, 172L) were encapsidated and secreted similarly to the wild type (summarized in Table 6). In consequence, an HDV particle infecting hepatocytes that carries the HBV surface variant sW196* only, would result in a dead end for HDV infection cycle. Both, HBV and HDV would still be able to replicate in these hepatocytes, but the sW196* variant of the HBV S-ORF would inhibit the envelopment and secretion of both viruses. Furthermore, no subviral particles could be secreted. This situation could only be changed, if either the cell would be infected by a wild type HBV again providing non-mutated surface proteins, or a mutation within the cccDNA pool of the infected hepatocytes restored the sW196* mutation into wild type.

A stop mutation in the SHBs does not only significantly affect the life cycle of HBV and HDV, but also has strong clinical consequences for the antiviral treatment and diagnostic. The HDV infection is a rarely occurring disease in the western countries and seems to be restricted to HBsAg-positive intravenous drug addicts, mostly (Kucirka et al. 2010). However, chronic HDV infection is still a significant health problem in Europe, especially caused by the immigration of individuals from highly endemic regions. These immigrants often carry a chronic HBV/HDV co-infection (Farci 2003b). If a co-infection is not diagnosed, this will be strongly detrimental for the patients if they are treated with nucleos(t)ide analogs because it has been proven that the treatment with these inhibitors does not affect HDV (Niro et al. 2005; Mansour et al. 2010; Brichtler et al. 2013). The treatment with nucleos(t)ide analogs would decrease the viral load of HBV but it would not affect the secretion of infectious HDV particles. As already mentioned, a typical resistance mutation emerging during lamivudine treatment is the mutation pattern rtM204I sW196S/L/stop. If this mutation pattern was selected, it would inhibit the secretion of hepatitis delta virions, but an amino acid change at position 196 from tryptophan to serine or leucine would rescue the HBV variants resulting in resistance mutants which then cause an antiviral breakthrough. The change from lamivudine to another nucleos(t)ide analog would then decrease the viral load of HBV again, but could promote a re-mutation of the rtM204I sW196S/L/stop leading to a rebound of HDV particles once again. The sequential treatment with nucleos(t)ide analogs can lead to another complication in the HBV therapy and probably in the HDV therapy, too. Nucleos(t)ide analogs that exhibit similar characteristics, for example lamivudine and entecavir, can promote the selection for multidrug resistant mutants of HBV. These HBV mutants do not only cause a therapy failure of HBV but also can mediate HBV and HDV

variants that exhibit mutations in the antigenic loop of the HBsAg, for example the mutation pattern in the S-ORF sE164D /sI195M with the corresponding P-ORF mutations rtV519L/rtL526M/rtM550V (Torresi et al. 2002b). These mutations could induce a misdetection of HBsAg-diagnostic methods and could lead to the misdetection of anti-HBs antibodies in HBV diagnostics. To avoid such multidrug resistant HBV and HDV variants, HBsAg-positive carriers should be tested carefully before the onset of an antiviral therapy for circulating antiviral resistant HBV variants and in parallel for an HDV co-infection. Patients with an HBV/HDV co-infection are treated with a combination of interferon - the only therapeutic recommendation for HDV treatment to the present day - in combination with nucleos(t)ide analogs trying to decrease the viral load of HBV as well as HDV (Brichler et al. 2013). Unfortunately, the treatment with IFN- α and nucleos(t)ide analogs is associated with several side effects and high costs.

It can be concluded that our current knowledge about the consequences of an antiviral treatment on the life cycles of HBV and HDV needs improvement. Further investigations are needed to analyze and characterize 1) further HBsAg mutations occurring during antiviral therapy 2) their secretion capacity and 3) their competence to infect new hepatocytes. These results should lead to a better understanding of the viral life cycle of both, HBV and HDV and hopefully also to new treatment options for the co-infected patients.

5. Perspectives

The detailed investigation and description of resistance patterns in the viral polymerase induced by the antiviral therapy of a chronic HBV infection could be helpful to find out new resistance mutations and, therefore, to improve the antiviral therapy. Moreover, the characterization of HBV surface protein mutations induced by the long term treatment with nucleos(t)ide analogs could be helpful to optimize the sensitivity of several diagnostic methods to detect HBV resistance variants.

Furthermore, the finding of NTCP as the high affinity receptor for HBV and HDV opens up new opportunities to examine the HBV and HDV life cycle. Because of the limited time scale in which PTHs are susceptible for HBV and HDV, a stably transfected cell line, which constitutively expresses the hepadnaviral high affinity receptor NTCP, would be a more appropriate infection model. Such an infection system could be used to study the uptake mechanism and the used endocytotic pathway of both viruses. The obtained results could be used to develop new pharmaceuticals that block key proteins or enzymes of the HBV and/or HDV entry process and thereby specifically inhibit infection. Additionally, with the help of such an infection system, HBV/HDV co- and super-infection assays could be established. Due to the fact that a chronic HBV/HDV co-infection leads to a higher prevalence for developing HCC or liver cirrhosis, such an infection system would allow a better understanding of the viral life cycle of HBV and HDV, and could improve our knowledge of the interaction of both viruses within the cells. In contrast to HBV, a specific antiviral drug is not available, but urgently needed. A better understanding of the viral life cycle would probably lead to the development of specific antiviral drugs that inhibit HDV replication. The clarification of the interaction-machinery and the knowledge of how HDV represses the HBV replication in chronically co-infected patients will possibly lead to the development of new antiviral pharmaceuticals that probably are able to inhibit the transcription of HBV mRNA. A better understanding of the interaction between both viruses could hopefully lead to the development of new therapy strategies in HBV/HDV co-infection.

6. References

- Abou-Jaoudé G, Molina S, Maurel P, Sureau C. 2007. Myristoylation signal transfer from the large to the middle or the small HBV envelope protein leads to a loss of HDV particles infectivity. *Virology* **365**: 204–209.
- Abou-Jaoude G, Sureau C. 2007. Entry of Hepatitis Delta Virus Requires the Conserved Cysteine Residues of the Hepatitis B Virus Envelope Protein Antigenic Loop and Is Blocked by Inhibitors of Thiol-Disulfide Exchange. *J Virol* **81**: 13057–13066.
- Aden DP, Fogel A, Plotkin S, Damjanov I, Knowles BB. 1979. Controlled synthesis of HBsAg in a differentiated human liver carcinoma-derived cell line. *Nature* **282**: 615–616.
- Almeida JD, Rubenstein D, Stott EJ. 1971. New antigen-antibody system in Australia-antigen-positive hepatitis. *Lancet* **2**: 1225–1227.
- Angus P, Vaughan R, Xiong S, Yang H, Delaney W, Gibbs C, Brosgart C, Colledge D, Edwards R, Ayres A, et al. 2003. Resistance to adefovir dipivoxil therapy associated with the selection of a novel mutation in the HBV polymerase. *Gastroenterology* **125**: 292–297.
- Avellón A, Echevarría JM, Weber B, Weik M, Schobel U, Willems WR, Gerlich WH. 2011. European collaborative evaluation of the Enzygnost HBsAg 6.0 assay: performance on hepatitis B virus surface antigen variants. *J Med Virol* **83**: 95–100.
- Bardens A, Döring T, Stieler J, Prange R. 2011. Alix regulates egress of hepatitis B virus naked capsid particles in an ESCRT-independent manner. *Cell Microbiol* **13**: 602–619.
- Barker LF, Chisari FV, McGrath PP, Dalgard DW, Kirschstein RL, Almeida JD, Edington TS, Sharp DG, Peterson MR. 1973. Transmission of type B viral hepatitis to chimpanzees. *J Infect Dis* **127**: 648–662.
- Barrera A, Guerra B, Lee H, Lanford RE. 2004. Analysis of host range phenotypes of primate hepadnaviruses by in vitro infections of hepatitis D virus pseudotypes. *J Virol* **78**: 5233–5243.
- Bartenschlager R, Schaller H. 1992. Hepadnaviral assembly is initiated by polymerase binding to the encapsidation signal in the viral RNA genome. *EMBO J* **11**: 3413–3420.
- Bartenschlager R, Schaller H. 1988. The amino-terminal domain of the hepadnaviral P-gene encodes the terminal protein (genome-linked protein) believed to prime reverse transcription. *EMBO J* **7**: 4185–4192.
- Bartholomeusz A, Locarnini S. 2006. Hepatitis B virus mutations associated with antiviral therapy. *J Med Virol* **78 Suppl 1**: S52–55.
- Bartholomeusz A, Schaefer S. 2004. Hepatitis B virus genotypes: comparison of genotyping methods. *Rev Med Virol* **14**: 3–16.
- Beasley RP, Hwang LY, Lin CC, Chien CS. 1981. Hepatocellular carcinoma and hepatitis B virus. A prospective study of 22 707 men in Taiwan. *Lancet* **2**: 1129–1133.
- Berger J, Hauber J, Hauber R, Geiger R, Cullen BR. 1988. Secreted placental alkaline phosphatase: a powerful new quantitative indicator of gene expression in eukaryotic cells. *Gene* **66**: 1–10.
- Bernas T, Dobrucki J. 2002. Mitochondrial and nonmitochondrial reduction of MTT: Interaction of MTT with TMRE, JC-1, and NAO mitochondrial fluorescent probes. *Cytometry* **47**: 236–242.

- Berting A, Fischer C, Schaefer S, Garten W, Klenk HD, Gerlich WH. 2000. Hemifusion activity of a chimeric influenza virus hemagglutinin with a putative fusion peptide from hepatitis B virus. *Virus Res* **68**: 35–49.
- Billioud G, Pichoud C, Parent R, Zoulim F. 2012. Decreased infectivity of nucleoside analogs-resistant hepatitis B virus mutants. *J Hepatol* **56**: 1269–1275.
- Block GD, Locker J, Bowen WC, Petersen BE, Katyal S, Strom SC, Riley T, Howard TA, Michalopoulos GK. 1996. Population expansion, clonal growth, and specific differentiation patterns in primary cultures of hepatocytes induced by HGF/SF, EGF and TGF alpha in a chemically defined (HGM) medium. *J Cell Biol* **132**: 1133–1149.
- Block TM, Lu X, Platt FM, Foster GR, Gerlich WH, Blumberg BS, Dwek RA. 1994. Secretion of human hepatitis B virus is inhibited by the imino sugar N-butyldeoxynojirimycin. *Proc Natl Acad Sci U S A* **91**: 2235–2239.
- Bonino F, Heermann KH, Rizzetto M, Gerlich WH. 1986. Hepatitis delta virus: protein composition of delta antigen and its hepatitis B virus-derived envelope. *J Virol* **58**: 945–950.
- Bonino F, Hoyer B, Shih JW, Rizzetto M, Purcell RH, Gerin JL. 1984. Delta hepatitis agent: structural and antigenic properties of the delta-associated particle. *Infect Immun* **43**: 1000–1005.
- Bordier BB, Ohkanda J, Liu P, Lee S-Y, Salazar FH, Marion PL, Ohashi K, Meuse L, Kay MA, Casey JL, et al. 2003. In vivo antiviral efficacy of prenylation inhibitors against hepatitis delta virus. *J Clin Invest* **112**: 407–414.
- Branch AD, Benenfeld BJ, Baroudy BM, Wells FV, Gerin JL, Robertson HD. 1989. An ultraviolet-sensitive RNA structural element in a viroid-like domain of the hepatitis delta virus. *Science* **243**: 649–652.
- Bremer CM, Bung C, Kott N, Hardt M, Glebe D. 2009a. Hepatitis B virus infection is dependent on cholesterol in the viral envelope. *Cell Microbiol* **11**: 249–260.
- Bremer CM, Saniewski M, Wend UC, Torres P, Lelie N, Gerlich WH, Glebe D. 2009b. Transient occult hepatitis B virus infection in a blood donor with high viremia. *Transfusion (Paris)* **49**: 1621–1629.
- Brichler S, Setshedi M, Renou C. 2013. Resolution of chronic hepatitis delta infection after five years of peginterferon-adefovir: lessons from a case report. *Clin Res Hepatol Gastroenterol* **37**: e81–84.
- Bruss V. 1997. A short linear sequence in the pre-S domain of the large hepatitis B virus envelope protein required for virion formation. *J Virol* **71**: 9350–9357.
- Bruss V, Ganem D. 1991. The role of envelope proteins in hepatitis B virus assembly. *Proc Natl Acad Sci U S A* **88**: 1059–1063.
- Bruss V, Lu X, Thomssen R, Gerlich WH. 1994. Post-translational alterations in transmembrane topology of the hepatitis B virus large envelope protein. *EMBO J* **13**: 2273–2279.
- Çağ N. 2004. Suszeptibilität von Tupaia Hepatozyten für das hepatitis B Virus in Abhängigkeit vom Differenzierungszustand der zellkultur. Justus-Liebig-Universität, Gießen.
- Carman WF, Zanetti AR, Karayiannis P, Waters J, Manzillo G, Tanzi E, Zuckerman AJ, Thomas HC. 1990. Vaccine-induced escape mutant of hepatitis B virus. *Lancet* **336**: 325–329.
- Casey JL, Brown TL, Colan EJ, Wignall FS, Gerin JL. 1993. A genotype of hepatitis D virus that occurs in northern South America. *Proc Natl Acad Sci U S A* **90**: 9016–9020.

- Casey JL, Gerin JL. 1995. Hepatitis D virus RNA editing: specific modification of adenosine in the antigenomic RNA. *J Virol* **69**: 7593–7600.
- Chang CM, Jeng KS, Hu CP, Lo SJ, Su TS, Ting LP, Chou CK, Han SH, Pfaff E, Salfeld J. 1987. Production of hepatitis B virus in vitro by transient expression of cloned HBV DNA in a hepatoma cell line. *EMBO J* **6**: 675–680.
- Chang FL, Chen PJ, Tu SJ, Wang CJ, Chen DS. 1991. The large form of hepatitis delta antigen is crucial for assembly of hepatitis delta virus. *Proc Natl Acad Sci U S A* **88**: 8490–8494.
- Chao M, Hsieh SY, Taylor J. 1990. Role of two forms of hepatitis delta virus antigen: evidence for a mechanism of self-limiting genome replication. *J Virol* **64**: 5066–5069.
- Chen PJ, Kalpana G, Goldberg J, Mason W, Werner B, Gerin J, Taylor J. 1986. Structure and replication of the genome of the hepatitis delta virus. *Proc Natl Acad Sci U S A* **83**: 8774–8778.
- Chisari FV, Ferrari C. 1995. Hepatitis B virus immunopathology. *Springer Semin Immunopathol* **17**: 261–281.
- Cooreman MP, Leroux-Roels G, Paulij WP. 2001. Vaccine- and hepatitis B immune globulin-induced escape mutations of hepatitis B virus surface antigen. *J Biomed Sci* **8**: 237–247.
- Cross TJS, Rizzi P, Horner M, Jolly A, Hussain MJ, Smith HM, Vergani D, Harrison PM. 2008. The increasing prevalence of hepatitis delta virus (HDV) infection in South London. *J Med Virol* **80**: 277–282.
- Crowther RA, Kiselev NA, Böttcher B, Berriman JA, Borisova GP, Ose V, Pumpens P. 1994. Three-dimensional structure of hepatitis B virus core particles determined by electron cryomicroscopy. *Cell* **77**: 943–950.
- Dane DS, Cameron CH, Briggs M. 1970. Virus-like particles in serum of patients with Australia-antigen-associated hepatitis. *Lancet* **1**: 695–698.
- Dejean A, Sonigo P, Wain-Hobson S, Tiollais P. 1984. Specific hepatitis B virus integration in hepatocellular carcinoma DNA through a viral 11-base-pair direct repeat. *Proc Natl Acad Sci U S A* **81**: 5350–5354.
- Dény P. 2006. Hepatitis delta virus genetic variability: from genotypes I, II, III to eight major clades? *Curr Top Microbiol Immunol* **307**: 151–171.
- Dienstag JL. 2009. Benefits and risks of nucleoside analog therapy for hepatitis B. *Hepatology* **49**: S112–121.
- Dienstag JL. 2008. Hepatitis B virus infection. *N Engl J Med* **359**: 1486–1500.
- Doerr HW. 2008. *Medizinische Virologie: Grundlage, Diagnostik und Therapie virologischer Erkrankungen*. Thieme, Stuttgart.
- Drexler JF, Geipel A, König A, Corman VM, van Riel D, Leijten LM, Bremer CM, Rasche A, Cottontail VM, Maganga GD, et al. 2013. Bats carry pathogenic hepadnaviruses antigenically related to hepatitis B virus and capable of infecting human hepatocytes. *Proc Natl Acad Sci U S A* **110**: 16151–16156.
- Dryden KA, Wieland SF, Whitten-Bauer C, Gerin JL, Chisari FV, Yeager M. 2006. Native hepatitis B virions and capsids visualized by electron cryomicroscopy. *Mol Cell* **22**: 843–850.

- Emini EA, Ellis RW, Miller WJ, McAleer WJ, Scolnick EM, Gerety RJ. 1986. Production and immunological analysis of recombinant hepatitis B vaccine. *J Infect* **13 Suppl A**: 3–9.
- Engelke M, Mills K, Seitz S, Simon P, Gripon P, Schnölzer M, Urban S. 2006. Characterization of a hepatitis B and hepatitis delta virus receptor binding site. *Hepatology* **43**: 750–760.
- De Falco S, Ruvoletto MG, Verdoliva A, Ruvo M, Raucci A, Marino M, Senatore S, Cassani G, Alberti A, Pontisso P, et al. 2001. Cloning and expression of a novel hepatitis B virus-binding protein from HepG2 cells. *J Biol Chem* **276**: 36613–36623.
- Farci P. 2003a. Delta hepatitis: an update. *J Hepatology* **39 Suppl 1**: S212–219.
- Farci P. 2003b. Delta hepatitis: an update. *J Hepatology* **39 Suppl 1**: S212–219.
- Fattovich G, Boscaro S, Noventa F, Pornaro E, Stenico D, Alberti A, Ruol A, Realdi G. 1987. Influence of hepatitis delta virus infection on progression to cirrhosis in chronic hepatitis type B. *J Infect Dis* **155**: 931–935.
- Fattovich G, Giustina G, Christensen E, Pantalena M, Zagni I, Realdi G, Schalm SW. 2000. Influence of hepatitis delta virus infection on morbidity and mortality in compensated cirrhosis type B. The European Concerted Action on Viral Hepatitis (Eurohep). *Gut* **46**: 420–426.
- Ferns RB, Nastouli E, Garson JA. 2012. Quantitation of hepatitis delta virus using a single-step internally controlled real-time RT-qPCR and a full-length genomic RNA calibration standard. *J Virol Methods* **179**: 189–194.
- Filipovska J, Konarska MM. 2000. Specific HDV RNA-templated transcription by pol II in vitro. *RNA* **6**: 41–54.
- Fu TB, Taylor J. 1993. The RNAs of hepatitis delta virus are copied by RNA polymerase II in nuclear homogenates. *J Virol* **67**: 6965–6972.
- Le Gal F, Gault E, Ripault M-P, Serpaggi J, Trinchet J-C, Gordien E, Dény P. 2006. Eighth major clade for hepatitis delta virus. *Emerg Infect Dis* **12**: 1447–1450.
- Ganem D. 1991. Assembly of hepadnaviral virions and subviral particles. *Curr Top Microbiol Immunol* **168**: 61–83.
- Ganem D, Prince AM. 2004. Hepatitis B virus infection--natural history and clinical consequences. *N Engl J Med* **350**: 1118–1129.
- Ganem D, Varmus HE. 1987. The molecular biology of the hepatitis B viruses. *Annu Rev Biochem* **56**: 651–693.
- Garcia T, Li J, Sureau C, Ito K, Qin Y, Wands J, Tong S. 2009. Drastic Reduction in the Production of Subviral Particles Does Not Impair Hepatitis B Virus Virion Secretion. *J Virol* **83**: 11152–11165.
- Gavilanes F, Gonzalez-Ros JM, Peterson DL. 1982. Structure of hepatitis B surface antigen. Characterization of the lipid components and their association with the viral proteins. *J Biol Chem* **257**: 7770–7777.
- Geipel A. 2011. Phänotypische Charakterisierung klinisch relevanter Hepatitis-B-Virus-Mutanten. Justus-Liebig-Universität, Gießen.
- Geipel DA. poster presented at International Meeting on Molecular Biology of Hepatitis B Virus, Oxford, UK, 2012. UK, 2012.

- Gerelsaikhon T, Tavis JE, Bruss V. 1996. Hepatitis B virus nucleocapsid envelopment does not occur without genomic DNA synthesis. *J Virol* **70**: 4269–4274.
- Gerlich WH. 2013. Medical virology of hepatitis B: how it began and where we are now. *Virology* **10**: 239.
- Gerlich WH, Bremer C, Saniewski M, Schüttler CG, Wend UC, Willems WR, Glebe D. 2010. Occult hepatitis B virus infection: detection and significance. *Dig Dis Basel Switz* **28**: 116–125.
- Gerlich WH, Glebe D, Schüttler CG. 2007. Deficiencies in the standardization and sensitivity of diagnostic tests for hepatitis B virus. *J Viral Hepat* **14 Suppl 1**: 16–21.
- Gerlich WH, Robinson WS. 1980. Hepatitis B virus contains protein attached to the 5' terminus of its complete DNA strand. *Cell* **21**: 801–809.
- Ghany M, Liang TJ. 2007. Drug targets and molecular mechanisms of drug resistance in chronic hepatitis B. *Gastroenterology* **132**: 1574–1585.
- Giersch K, Helbig M, Volz T, Allweiss L, Mancke LV, Lohse AW, Polywka S, Pollok JM, Petersen J, Taylor J, et al. Persistent Hepatitis D Virus mono-infection in humanized mice is efficiently converted by Hepatitis B Virus to a productive co-infection. *J Hepatol*. [http://www.journal-of-hepatology.eu/article/S0168-8278\(13\)00811-8/abstract](http://www.journal-of-hepatology.eu/article/S0168-8278(13)00811-8/abstract) (Accessed January 4, 2014).
- Gish RG. 2009. Hepatitis B treatment: Current best practices, avoiding resistance. *Cleve Clin J Med* **76 Suppl 3**: S14–19.
- Glebe D. 2006. Attachment sites and neutralising epitopes of hepatitis B virus. *Minerva Gastroenterol Dietol* **52**: 3–21.
- Glebe D, Aliakbari M, Krass P, Knoop EV, Valerius KP, Gerlich WH. 2003. Pre-s1 antigen-dependent infection of Tupaia hepatocyte cultures with human hepatitis B virus. *J Virol* **77**: 9511–9521.
- Glebe D, Bremer CM. 2013. The molecular virology of hepatitis B virus. *Semin Liver Dis* **33**: 103–112.
- Glebe D, Gerlich WH. 2004. Study of the Endocytosis and Intracellular Localization of Subviral Particles of Hepatitis B Virus in Primary Hepatocytes. In *Hepatitis B and D Protocols* (eds. R.K. Hamatake and J.Y.N.L. MD), *Methods in Molecular Medicine*TM, pp. 143–152, Humana Press <http://link.springer.com/protocol/10.1385/1-59259-670-3%3A143> (Accessed November 19, 2013).
- Glebe D, Urban S. 2007. Viral and cellular determinants involved in hepadnaviral entry. *World J Gastroenterol WJG* **13**: 22–38.
- Glebe D, Urban S, Knoop EV, Cag N, Krass P, Grün S, Bulavaite A, Sasnauskas K, Gerlich WH. 2005. Mapping of the hepatitis B virus attachment site by use of infection-inhibiting preS1 lipopeptides and tupaia hepatocytes. *Gastroenterology* **129**: 234–245.
- Glenn JS, Watson JA, Havel CM, White JM. 1992. Identification of a prenylation site in delta virus large antigen. *Science* **256**: 1331–1333.
- Gomes-Gouvêa MS, Soares MCP, Bensabath G, de Carvalho-Mello IMVG, Brito EMF, Souza OSC, Queiroz ATL, Carrilho FJ, Pinho JRR. 2009. Hepatitis B virus and hepatitis delta virus genotypes in outbreaks of fulminant hepatitis (Labrea black fever) in the western Brazilian Amazon region. *J Gen Virol* **90**: 2638–2643.
- Gordien E, Rosmorduc O, Peltekian C, Garreau F, Bréchet C, Kremsdorf D. 2001. Inhibition of hepatitis B virus replication by the interferon-inducible MxA protein. *J Virol* **75**: 2684–2691.

- Greco-Stewart VS, Miron P, Abraham A, Pelchat M. 2007. The human RNA polymerase II interacts with the terminal stem-loop regions of the hepatitis delta virus RNA genome. *Virology* **357**: 68–78.
- Greco-Stewart VS, Schissel E, Pelchat M. 2009. The hepatitis delta virus RNA genome interacts with the human RNA polymerases I and III. *Virology* **386**: 12–15.
- Gripon P, Diot C, Thézé N, Fourel I, Loreal O, Brechot C, Guguen-Guillouzo C. 1988. Hepatitis B virus infection of adult human hepatocytes cultured in the presence of dimethyl sulfoxide. *J Virol* **62**: 4136–4143.
- Gripon P, Rumin S, Urban S, Le Seyec J, Glaise D, Cannie I, Guyomard C, Lucas J, Trepo C, Guguen-Guillouzo C. 2002. Infection of a human hepatoma cell line by hepatitis B virus. *Proc Natl Acad Sci U S A* **99**: 15655–15660.
- Gudima S, Chang J, Moraleda G, Azvolinsky A, Taylor J. 2002. Parameters of human hepatitis delta virus genome replication: the quantity, quality, and intracellular distribution of viral proteins and RNA. *J Virol* **76**: 3709–3719.
- Gudima S, Dingle K, Wu TT, Moraleda G, Taylor J. 1999. Characterization of the 5' ends for polyadenylated RNAs synthesized during the replication of hepatitis delta virus. *J Virol* **73**: 6533–6539.
- Gudima S, He Y, Chai N, Bruss V, Urban S, Mason W, Taylor J. 2008. Primary human hepatocytes are susceptible to infection by hepatitis delta virus assembled with envelope proteins of woodchuck hepatitis virus. *J Virol* **82**: 7276–7283.
- Gudima S, He Y, Meier A, Chang J, Chen R, Jarnik M, Nicolas E, Bruss V, Taylor J. 2007. Assembly of Hepatitis Delta Virus: Particle Characterization, Including the Ability To Infect Primary Human Hepatocytes. *J Virol* **81**: 3608–3617.
- Heermann KH, Goldmann U, Schwartz W, Seyffarth T, Baumgarten H, Gerlich WH. 1984. Large surface proteins of hepatitis B virus containing the pre-s sequence. *J Virol* **52**: 396–402.
- Heger J. 2012. Charakterisierung eines heterogenen Plasmid-Expressionssystems zur Generierung von hepatitis-B-Viren in vitro. Justus-Liebig-Universität, Gießen.
- Heid CA, Stevens J, Livak KJ, Williams PM. 1996. Real time quantitative PCR. *Genome Res* **6**: 986–994.
- Heidrich B, Deterding K, Tillmann HL, Raupach R, Manns MP, Wedemeyer H. 2009. Virological and clinical characteristics of delta hepatitis in Central Europe. *J Viral Hepat* **16**: 883–894.
- Hirsch RC, Lavine JE, Chang LJ, Varmus HE, Ganem D. 1990. Polymerase gene products of hepatitis B viruses are required for genomic RNA packaging as well as for reverse transcription. *Nature* **344**: 552–555.
- Hruska JF, Clayton DA, Rubenstein JL, Robinson WS. 1977. Structure of hepatitis B Dane particle DNA before and after the Dane particle DNA polymerase reaction. *J Virol* **21**: 666–672.
- Hu J, Seeger C. 1996. Hsp90 is required for the activity of a hepatitis B virus reverse transcriptase. *Proc Natl Acad Sci U S A* **93**: 1060–1064.
- Hu J, Toft DO, Seeger C. 1997. Hepadnavirus assembly and reverse transcription require a multi-component chaperone complex which is incorporated into nucleocapsids. *EMBO J* **16**: 59–68.
- Huang J, Liang TJ. 1993. A novel hepatitis B virus (HBV) genetic element with Rev response element-like properties that is essential for expression of HBV gene products. *Mol Cell Biol* **13**: 7476–7486.

- Huovila AP, Eder AM, Fuller SD. 1992. Hepatitis B surface antigen assembles in a post-ER, pre-Golgi compartment. *J Cell Biol* **118**: 1305–1320.
- Imazeki F, Omata M, Ohto M. 1990. Heterogeneity and evolution rates of delta virus RNA sequences. *J Virol* **64**: 5594–5599.
- Ivaniushina V, Radjef N, Alexeeva M, Gault E, Semenov S, Salhi M, Kiselev O, Dény P. 2001. Hepatitis delta virus genotypes I and II cocirculate in an endemic area of Yakutia, Russia. *J Gen Virol* **82**: 2709–2718.
- Jaoudé GA, Sureau C. 2005. Role of the antigenic loop of the hepatitis B virus envelope proteins in infectivity of hepatitis delta virus. *J Virol* **79**: 10460–10466.
- Jenna S, Sureau C. 1998. Effect of Mutations in the Small Envelope Protein of Hepatitis B Virus on Assembly and Secretion of Hepatitis Delta Virus. *Virology* **251**: 176–186.
- Jenna S, Sureau C. 1999. Mutations in the Carboxyl-Terminal Domain of the Small Hepatitis B Virus Envelope Protein Impair the Assembly of Hepatitis Delta Virus Particles. *J Virol* **73**: 3351–3358.
- Junker-Niepmann M, Bartenschlager R, Schaller H. 1990. A short cis-acting sequence is required for hepatitis B virus pregenome encapsidation and sufficient for packaging of foreign RNA. *EMBO J* **9**: 3389–3396.
- Jursch CA, Gerlich WH, Glebe D, Schaefer S, Marie O, Thraenhart O. 2002. Molecular approaches to validate disinfectants against human hepatitis B virus. *Med Microbiol Immunol (Berl)* **190**: 189–197.
- Kamili S, Sozzi V, Thompson G, Campbell K, Walker CM, Locarnini S, Krawczynski K. 2009. Efficacy of hepatitis B vaccine against antiviral drug-resistant hepatitis B virus mutants in the chimpanzee model. *Hepatology* **49**: 1483–1491.
- Kaneko S, Miller RH. 1988. X-region-specific transcript in mammalian hepatitis B virus-infected liver. *J Virol* **62**: 3979–3984.
- Kann M, Sodeik B, Vlachou A, Gerlich WH, Helenius A. 1999. Phosphorylation-dependent binding of hepatitis B virus core particles to the nuclear pore complex. *J Cell Biol* **145**: 45–55.
- Katsoulidou A, Manesis E, Rokka C, Issaris C, Pagoni A, Sypsa V, Hatzakis A. 2013. Development and assessment of a novel real-time PCR assay for quantitation of hepatitis D virus RNA to study viral kinetics in chronic hepatitis D. *J Viral Hepat* **20**: 256–262.
- Kazim SN, Sarin SK, Sharma BC, Khan LA, Hasnain SE. 2006. Characterization of naturally occurring and Lamivudine-induced surface gene mutants of hepatitis B virus in patients with chronic hepatitis B in India. *Intervirology* **49**: 152–160.
- Kenney JM, von Bonsdorff CH, Nassal M, Fuller SD. 1995. Evolutionary conservation in the hepatitis B virus core structure: comparison of human and duck cores. *Struct Lond Engl* **3**: 1009–1019.
- King AMQ, Adams MJ, Lefkowitz E, Carstens EB. 2012. *Virus Taxonomy: Classification and Nomenclature of Viruses: Ninth Report of the International Committee on Taxonomy of Viruses*. Elsevier.
- Köck J, Nassal M, MacNelly S, Baumert TF, Blum HE, von Weizsäcker F. 2001. Efficient infection of primary tupaia hepatocytes with purified human and woolly monkey hepatitis B virus. *J Virol* **75**: 5084–5089.

- Köck J, Schlicht HJ. 1993. Analysis of the earliest steps of hepadnavirus replication: genome repair after infectious entry into hepatocytes does not depend on viral polymerase activity. *J Virol* **67**: 4867–4874.
- Köhler W, Schachtel GA, Voleske P. 2007. *Biostatistik: [eine Einführung für Biologen und Agrarwissenschaftler] ; mit 50 Tabellen*. Springer, Berlin; Heidelberg; New York.
- Komla-Soukha I, Sureau C. 2006. A tryptophan-rich motif in the carboxyl terminus of the small envelope protein of hepatitis B virus is central to the assembly of hepatitis delta virus particles. *J Virol* **80**: 4648–4655.
- Kost DP, Michalopoulos GK. 1991. Effect of 2% dimethyl sulfoxide on the mitogenic properties of epidermal growth factor and hepatocyte growth factor in primary hepatocyte culture. *J Cell Physiol* **147**: 274–280.
- Kucirka LM, Farzadegan H, Feld JJ, Mehta SH, Winters M, Glenn JS, Kirk GD, Segev DL, Nelson KE, Marks M, et al. 2010. Prevalence, correlates, and viral dynamics of hepatitis delta among injection drug users. *J Infect Dis* **202**: 845–852.
- Kuo MY, Chao M, Taylor J. 1989. Initiation of replication of the human hepatitis delta virus genome from cloned DNA: role of delta antigen. *J Virol* **63**: 1945–1950.
- Kuo MY, Sharmeen L, Dinter-Gottlieb G, Taylor J. 1988. Characterization of self-cleaving RNA sequences on the genome and antigenome of human hepatitis delta virus. *J Virol* **62**: 4439–4444.
- Lai MM. 1995. The molecular biology of hepatitis delta virus. *Annu Rev Biochem* **64**: 259–286.
- Lamas Longarela O, Schmidt TT, Schöneweis K, Romeo R, Wedemeyer H, Urban S, Schulze A. 2013. Proteoglycans act as cellular hepatitis delta virus attachment receptors. *PLoS One* **8**: e58340.
- Lambert C, Döring T, Prange R. 2007. Hepatitis B virus maturation is sensitive to functional inhibition of ESCRT-III, Vps4, and gamma 2-adaptin. *J Virol* **81**: 9050–9060.
- Lambert C, Prange R. 2003. Chaperone action in the posttranslational topological reorientation of the hepatitis B virus large envelope protein: Implications for translocational regulation. *Proc Natl Acad Sci U S A* **100**: 5199–5204.
- Landers TA, Greenberg HB, Robinson WS. 1977. Structure of hepatitis B Dane particle DNA and nature of the endogenous DNA polymerase reaction. *J Virol* **23**: 368–376.
- Lavanchy D. 2004. Hepatitis B virus epidemiology, disease burden, treatment, and current and emerging prevention and control measures. *J Viral Hepat* **11**: 97–107.
- Lavanchy D. 2005. Worldwide epidemiology of HBV infection, disease burden, and vaccine prevention. *J Clin Virol Off Publ Pan Am Soc Clin Virol* **34 Suppl 1**: S1–3.
- Lazinski DW, Taylor JM. 1994. Expression of hepatitis delta virus RNA deletions: cis and trans requirements for self-cleavage, ligation, and RNA packaging. *J Virol* **68**: 2879–2888.
- Lee CH, Chang SC, Wu CH, Chang MF. 2001. A novel chromosome region maintenance 1-independent nuclear export signal of the large form of hepatitis delta antigen that is required for the viral assembly. *J Biol Chem* **276**: 8142–8148.
- Lee CM, Bih FY, Chao YC, Govindarajan S, Lai MM. 1992. Evolution of hepatitis delta virus RNA during chronic infection. *Virology* **188**: 265–273.

- Lee CZ, Chen PJ, Chen DS. 1995. Large hepatitis delta antigen in packaging and replication inhibition: role of the carboxyl-terminal 19 amino acids and amino-terminal sequences. *J Virol* **69**: 5332–5336.
- Leistner CM, Gruen-Bernhard S, Glebe D. 2008. Role of glycosaminoglycans for binding and infection of hepatitis B virus. *Cell Microbiol* **10**: 122–133.
- Li Q, Ding M, Wang H. 1995. [The infection of hepatitis D virus in adult tupaia]. *Zhonghua Yi Xue Za Zhi* **75**: 611–613, 639–640.
- Li Y-J, Stallcup MR, Lai MMC. 2004. Hepatitis delta virus antigen is methylated at arginine residues, and methylation regulates subcellular localization and RNA replication. *J Virol* **78**: 13325–13334.
- Liang D, Hagenbuch B, Stieger B, Meier PJ. 1993. Parallel decrease of Na(+)-taurocholate cotransport and its encoding mRNA in primary cultures of rat hepatocytes. *Hepatology* **18**: 1162–1166.
- Lien JM, Aldrich CE, Mason WS. 1986. Evidence that a capped oligoribonucleotide is the primer for duck hepatitis B virus plus-strand DNA synthesis. *J Virol* **57**: 229–236.
- Locarnini S. 2005. Molecular virology and the development of resistant mutants: implications for therapy. *Semin Liver Dis* **25 Suppl 1**: 9–19.
- Lu X, Block TM, Gerlich WH. 1996. Protease-induced infectivity of hepatitis B virus for a human hepatoblastoma cell line. *J Virol* **70**: 2277–2285.
- Lu X, Mehta A, Dwek R, Butters T, Block T. 1995. Evidence that N-linked glycosylation is necessary for hepatitis B virus secretion. *Virology* **213**: 660–665.
- Lütgehetmann M, Mancke LV, Volz T, Helbig M, Allweiss L, Bornscheuer T, Pollok JM, Lohse AW, Petersen J, Urban S, et al. 2012. Humanized chimeric uPA mouse model for the study of hepatitis B and D virus interactions and preclinical drug evaluation. *Hepatology* **55**: 685–694.
- Macnaughton TB, Shi ST, Modahl LE, Lai MMC. 2002. Rolling circle replication of hepatitis delta virus RNA is carried out by two different cellular RNA polymerases. *J Virol* **76**: 3920–3927.
- Mangold CM, Streeck RE. 1993. Mutational analysis of the cysteine residues in the hepatitis B virus small envelope protein. *J Virol* **67**: 4588–4597.
- Mangold CM, Unckell F, Werr M, Streeck RE. 1995. Secretion and antigenicity of hepatitis B virus small envelope proteins lacking cysteines in the major antigenic region. *Virology* **211**: 535–543.
- Manock SR, Kelley PM, Hyams KC, Douce R, Smalligan RD, Watts DM, Sharp TW, Casey JL, Gerin JL, Engle R, et al. 2000. An outbreak of fulminant hepatitis delta in the Waorani, an indigenous people of the Amazon basin of Ecuador. *Am J Trop Med Hyg* **63**: 209–213.
- Mansour W, Ducancelle A, Le Gal F, Le Guillou-Guillemette H, Abgueuen P, Pivert A, Calès P, Gordien E, Lunel F. 2010. Resolution of chronic hepatitis Delta after 1 year of combined therapy with pegylated interferon, tenofovir and emtricitabine. *J Clin Virol Off Publ Pan Am Soc Clin Virol* **47**: 97–99.
- Menne S, Cote PJ. 2007. The woodchuck as an animal model for pathogenesis and therapy of chronic hepatitis B virus infection. *World J Gastroenterol WJG* **13**: 104–124.
- MHV van Regenmortel, Fauquet C, Bishop D, Carstens E, Estes M, Lemon S, Maniloff J, Mayo M, McGeoch D, Pringle C, et al. 2000. *Virus Taxonomy. The Classification and Nomenclature of*

- Viruses. The Seventh Annual report of the International Committee on Taxonomy of Viruses.* Academic Press, San Diego.
- Miller RH, Marion PL, Robinson WS. 1984. Hepatitis B viral DNA-RNA hybrid molecules in particles from infected liver are converted to viral DNA molecules during an endogenous DNA polymerase reaction. *Virology* **139**: 64–72.
- Mu J, Chen D, Chen P. 2001. The conserved serine 177 in the delta antigen of hepatitis delta virus is one putative phosphorylation site and is required for efficient viral RNA replication. *J Virol* **75**: 9087–95.
- Mu J-J, Tsay Y-G, Juan L-J, Fu T-F, Huang W-H, Chen D-S, Chen P-J. 2004. The small delta antigen of hepatitis delta virus is an acetylated protein and acetylation of lysine 72 may influence its cellular localization and viral RNA synthesis. *Virology* **319**: 60–70.
- Nakabayashi H, Taketa K, Miyano K, Yamane T, Sato J. 1982. Growth of human hepatoma cells lines with differentiated functions in chemically defined medium. *Cancer Res* **42**: 3858–3863.
- Nassal M. 1992. The arginine-rich domain of the hepatitis B virus core protein is required for pregenome encapsidation and productive viral positive-strand DNA synthesis but not for virus assembly. *J Virol* **66**: 4107–4116.
- Neurath AR, Kent SB, Parker K, Prince AM, Strick N, Brotman B, Sproul P. 1986a. Antibodies to a synthetic peptide from the preS 120-145 region of the hepatitis B virus envelope are virus neutralizing. *Vaccine* **4**: 35–37.
- Neurath AR, Kent SB, Strick N, Parker K. 1986b. Identification and chemical synthesis of a host cell receptor binding site on hepatitis B virus. *Cell* **46**: 429–436.
- Niekamp H. 2013. Charakterisierung der phänotypischen Resistenz von Hepatitis B Virus Mutanten gegenüber antiviralen Nukleosid- und Nukleotidanaloga. Justus-Liebig-Universität, Gießen.
- Niro GA, Ciancio A, Tillman HL, Lagget M, Olivero A, Perri F, Fontana R, Little N, Campbell F, Smedile A, et al. 2005. Lamivudine therapy in chronic delta hepatitis: a multicentre randomized-controlled pilot study. *Aliment Pharmacol Ther* **22**: 227–232.
- Niro GA, Smedile A, Andriulli A, Rizzetto M, Gerin JL, Casey JL. 1997. The predominance of hepatitis delta virus genotype I among chronically infected Italian patients. *Hepatology* **25**: 728–734.
- Norder H, Couroucé A-M, Coursaget P, Echevarria JM, Lee S-D, Mushahwar IK, Robertson BH, Locarnini S, Magnius LO. 2004. Genetic diversity of hepatitis B virus strains derived worldwide: genotypes, subgenotypes, and HBsAg subtypes. *Intervirology* **47**: 289–309.
- Olivero A, Smedile A. 2012. Hepatitis Delta Virus Diagnosis. *Semin Liver Dis* **32**: 220–227.
- Ostapchuk P, Hearing P, Ganem D. 1994. A dramatic shift in the transmembrane topology of a viral envelope glycoprotein accompanies hepatitis B viral morphogenesis. *EMBO J* **13**: 1048–1057.
- Pardo M, Marriott E, Moliner MC, Quiroga JA, Carreño V. 1995. Risks and benefits of interferon-alpha in the treatment of hepatitis. *Drug Saf Int J Med Toxicol Drug Exp* **13**: 304–316.
- Pascarella S, Negro F. 2011. Hepatitis D virus: an update. *Liver Int Off J Int Assoc Study Liver* **31**: 7–21.
- Patzer EJ, Nakamura GR, Simonsen CC, Levinson AD, Brands R. 1986. Intracellular assembly and packaging of hepatitis B surface antigen particles occur in the endoplasmic reticulum. *J Virol* **58**: 884–892.

- Perrillo RP, Schiff ER, Davis GL, Bodenheimer HC Jr, Lindsay K, Payne J, Dienstag JL, O'Brien C, Tamburro C, Jacobson IM. 1990. A randomized, controlled trial of interferon alfa-2b alone and after prednisone withdrawal for the treatment of chronic hepatitis B. The Hepatitis Interventional Therapy Group. *N Engl J Med* **323**: 295–301.
- Persing DH, Varmus HE, Ganem D. 1987. The preS1 protein of hepatitis B virus is acylated at its amino terminus with myristic acid. *J Virol* **61**: 1672–1677.
- Peterson DL. 1981. Isolation and characterization of the major protein and glycoprotein of hepatitis B surface antigen. *J Biol Chem* **256**: 6975–6983.
- Peterson DL, Paul DA, Lam J, Tribby II, Achord DT. 1984. Antigenic structure of hepatitis B surface antigen: identification of the “d” subtype determinant by chemical modification and use of monoclonal antibodies. *J Immunol Baltim Md 1950* **132**: 920–927.
- Polson AG, Bass BL, Casey JL. 1996. RNA editing of hepatitis delta virus antigenome by dsRNA-adenosine deaminase. *Nature* **380**: 454–456.
- Pontisso P, Petit MA, Bankowski MJ, Peeples ME. 1989. Human liver plasma membranes contain receptors for the hepatitis B virus pre-S1 region and, via polymerized human serum albumin, for the pre-S2 region. *J Virol* **63**: 1981–1988.
- Prange R, Streeck RE. 1995. Novel transmembrane topology of the hepatitis B virus envelope proteins. *EMBO J* **14**: 247–256.
- Purcell RH, Satterfield WC, Bergmann KF, Smedile A, Ponzetto A, Gerin JL. 1987. Experimental hepatitis delta virus infection in the chimpanzee. *Prog Clin Biol Res* **234**: 27–36.
- Qiao M, Macnaughton TB, Gowans EJ. 1994. Adsorption and penetration of hepatitis B virus in a nonpermissive cell line. *Virology* **201**: 356–363.
- Rabe B, Glebe D, Kann M. 2006. Lipid-mediated introduction of hepatitis B virus capsids into nonsusceptible cells allows highly efficient replication and facilitates the study of early infection events. *J Virol* **80**: 5465–5473.
- Rabe B, Vlachou A, Panté N, Helenius A, Kann M. 2003. Nuclear import of hepatitis B virus capsids and release of the viral genome. *Proc Natl Acad Sci U S A* **100**: 9849–9854.
- Radjef N, Gordien E, Ivaniushina V, Gault E, Anaïs P, Drugan T, Trinchet J-C, Roulot D, Tamby M, Milinkovitch MC, et al. 2004. Molecular phylogenetic analyses indicate a wide and ancient radiation of African hepatitis delta virus, suggesting a deltavirus genus of at least seven major clades. *J Virol* **78**: 2537–2544.
- Rall LB, Standring DN, Laub O, Rutter WJ. 1983. Transcription of hepatitis B virus by RNA polymerase II. *Mol Cell Biol* **3**: 1766–1773.
- Rizzetto M, Canese MG, Aricò S, Crivelli O, Trepo C, Bonino F, Verme G. 1977. Immunofluorescence detection of new antigen-antibody system (delta/anti-delta) associated to hepatitis B virus in liver and in serum of HBsAg carriers. *Gut* **18**: 997–1003.
- Rizzetto M, Canese MG, Gerin JL, London WT, Sly DL, Purcell RH. 1980a. Transmission of the hepatitis B virus-associated delta antigen to chimpanzees. *J Infect Dis* **141**: 590–602.
- Rizzetto M, Hoyer B, Canese MG, Shih JW, Purcell RH, Gerin JL. 1980b. delta Agent: association of delta antigen with hepatitis B surface antigen and RNA in serum of delta-infected chimpanzees. *Proc Natl Acad Sci U S A* **77**: 6124–6128.

- Rizzetto M, Verme G, Recchia S, Bonino F, Farci P, Aricò S, Calzia R, Picciotto A, Colombo M, Popper H. 1983. Chronic hepatitis in carriers of hepatitis B surface antigen, with intrahepatic expression of the delta antigen. An active and progressive disease unresponsive to immunosuppressive treatment. *Ann Intern Med* **98**: 437–441.
- Robinson WS, Marion PL, Miller RH. 1984. The hepadna viruses of animals. *Semin Liver Dis* **4**: 347–360.
- Roggendorf M, Pahlke C, Böhm B, Rasshofer R. 1987a. Characterization of proteins associated with hepatitis delta virus. *J Gen Virol* **68** (Pt 11): 2953–2959.
- Roggendorf M, Pahlke C, Böhm B, Rasshofer R. 1987b. Characterization of Proteins Associated with Hepatitis Delta Virus. *J Gen Virol* **68**: 2953–2959.
- Romeo R, Del Ninno E, Rumi M, Russo A, Sangiovanni A, de Franchis R, Ronchi G, Colombo M. 2009. A 28-year study of the course of hepatitis Delta infection: a risk factor for cirrhosis and hepatocellular carcinoma. *Gastroenterology* **136**: 1629–1638.
- Ryu WS, Bayer M, Taylor J. 1992. Assembly of hepatitis delta virus particles. *J Virol* **66**: 2310–2315.
- Sagnelli E, Coppola N, Scolastico C, Filippini P, Santantonio T, Stroffolini T, Piccinino F. 2000. Virologic and clinical expressions of reciprocal inhibitory effect of hepatitis B, C, and delta viruses in patients with chronic hepatitis. *Hepatology* **32**: 1106–1110.
- Sakugawa H, Nakasone H, Nakayoshi T, Kawakami Y, Miyazato S, Kinjo F, Saito A, Ma SP, Hotta H, Kinoshita M. 1999. Hepatitis delta virus genotype IIb predominates in an endemic area, Okinawa, Japan. *J Med Virol* **58**: 366–372.
- Saniewski M. 2009. Struktur und Funktion der Oberflächenproteine von ungewöhnlichen Hepatitis B Virus-Varianten. Justus-Liebig-Universität, Gießen.
- Schaper M, Rodriguez-Frias F, Jardi R, Tabernero D, Homs M, Ruiz G, Quer J, Esteban R, Buti M. 2010. Quantitative longitudinal evaluations of hepatitis delta virus RNA and hepatitis B virus DNA shows a dynamic, complex replicative profile in chronic hepatitis B and D. *J Hepatology* **52**: 658–664.
- Schlicht HJ, Schaller H. 1989. Analysis of hepatitis B virus gene functions in tissue culture and in vivo. *Curr Top Microbiol Immunol* **144**: 253–263.
- Schmitt S, Glebe D, Alving K, Tolle TK, Linder M, Geyer H, Linder D, Peter-Katalinic J, Gerlich WH, Geyer R. 1999. Analysis of the pre-S2 N- and O-linked glycans of the M surface protein from human hepatitis B virus. *J Biol Chem* **274**: 11945–11957.
- Schmitt S, Glebe D, Tolle TK, Lochnit G, Linder D, Geyer R, Gerlich WH. 2004. Structure of pre-S2 N- and O-linked glycans in surface proteins from different genotypes of hepatitis B virus. *J Gen Virol* **85**: 2045–2053.
- Schmitz J, Ohme M, Zischler H. 2000. The complete mitochondrial genome of *Tupaia belangeri* and the phylogenetic affiliation of scandentia to other eutherian orders. *Mol Biol Evol* **17**: 1334–1343.
- Scholtes C, Icard V, Amiri M, Chevallier-Queyron P, Trabaud M-A, Ramière C, Zoulim F, André P, Dény P. 2012. Standardized one-step real-time reverse transcription-PCR assay for universal detection and quantification of hepatitis delta virus from clinical samples in the presence of a heterologous internal-control RNA. *J Clin Microbiol* **50**: 2126–2128.
- Schulze A, Gripon P, Urban S. 2007. Hepatitis B virus infection initiates with a large surface protein-dependent binding to heparan sulfate proteoglycans. *Hepatology* **46**: 1759–1768.

- Seeger C, Maragos J. 1989. Molecular analysis of the function of direct repeats and a polypurine tract for plus-strand DNA priming in woodchuck hepatitis virus. *J Virol* **63**: 1907–1915.
- Seeger C, Mason WS. 2000. Hepatitis B virus biology. *Microbiol Mol Biol Rev MMBR* **64**: 51–68.
- Seitz S, Urban S, Antoni C, Böttcher B. 2007. Cryo-electron microscopy of hepatitis B virions reveals variability in envelope capsid interactions. *EMBO J* **26**: 4160–4167.
- Le Seyec J, Chouteau P, Cannie I, Guguen-Guillouzo C, Gripon P. 1998. Role of the pre-S2 domain of the large envelope protein in hepatitis B virus assembly and infectivity. *J Virol* **72**: 5573–5578.
- Sheldon J, Rodès B, Zoulim F, Bartholomeusz A, Soriano V. 2006. Mutations affecting the replication capacity of the hepatitis B virus. *J Viral Hepat* **13**: 427–434.
- Sheu SY, Lo SJ. 1994. Biogenesis of the hepatitis B viral middle (M) surface protein in a human hepatoma cell line: demonstration of an alternative secretion pathway. *J Gen Virol* **75** (Pt 11): 3031–3039.
- Shih CH, Li LS, Roychoudhury S, Ho MH. 1989. In vitro propagation of human hepatitis B virus in a rat hepatoma cell line. *Proc Natl Acad Sci U S A* **86**: 6323–6327.
- Siddiqui A, Sattler F, Robinson WS. 1979. Restriction endonuclease cleavage map and location of unique features of the DNA of hepatitis B virus, subtype adw2. *Proc Natl Acad Sci U S A* **76**: 4664–4668.
- Smedile A, Dentico P, Zanetti A, Sagnelli E, Nordenfelt E, Actis GC, Rizzetto M. 1981. Infection with the delta agent in chronic HBsAg carriers. *Gastroenterology* **81**: 992–997.
- Smedile A, Farci P, Verme G, Caredda F, Cargnel A, Caporaso N, Dentico P, Trepo C, Opolon P, Gimson A, et al. 1982. Influence of delta infection on severity of hepatitis B. *Lancet* **2**: 945–947.
- Stibbe W, Gerlich WH. 1982. Variable protein composition of hepatitis B surface antigen from different donors. *Virology* **123**: 436–442.
- Stuyver LJ, Locarnini SA, Lok A, Richman DD, Carman WF, Dienstag JL, Schinazi RF. 2001. Nomenclature for antiviral-resistant human hepatitis B virus mutations in the polymerase region. *Hepatology* **33**: 751–757.
- Su C-W, Huang Y-H, Huo T-I, Shih HH, Sheen I-J, Chen S-W, Lee P-C, Lee S-D, Wu J-C. 2006. Genotypes and viremia of hepatitis B and D viruses are associated with outcomes of chronic hepatitis D patients. *Gastroenterology* **130**: 1625–1635.
- Su JJ. 1987. [Experimental infection of human hepatitis B virus (HBV) in adult tree shrews]. *Zhonghua Bing Li Xue Za Zhi* **16**: 103–106, 22.
- Summers J, Mason WS. 1982. Replication of the genome of a hepatitis B--like virus by reverse transcription of an RNA intermediate. *Cell* **29**: 403–415.
- Sun D, Nassal M. 2006. Stable HepG2- and Huh7-based human hepatoma cell lines for efficient regulated expression of infectious hepatitis B virus. *J Hepatol* **45**: 636–645.
- Sureau C. 2006. The role of the HBV envelope proteins in the HDV replication cycle. *Curr Top Microbiol Immunol* **307**: 113–131.
- Sureau C, Fournier-Wirth C, Maurel P. 2003. Role of N glycosylation of hepatitis B virus envelope proteins in morphogenesis and infectivity of hepatitis delta virus. *J Virol* **77**: 5519–5523.

- Sureau C, Guerra B, Lanford RE. 1993. Role of the large hepatitis B virus envelope protein in infectivity of the hepatitis delta virion. *J Virol* **67**: 366–372.
- Sureau C, Guerra B, Lee H. 1994. The middle hepatitis B virus envelope protein is not necessary for infectivity of hepatitis delta virus. *J Virol* **68**: 4063–4066.
- Sureau C, Jacob JR, Eichberg JW, Lanford RE. 1991. Tissue culture system for infection with human hepatitis delta virus. *J Virol* **65**: 3443–3450.
- Sureau C, Moriarty AM, Thornton GB, Lanford RE. 1992. Production of infectious hepatitis delta virus in vitro and neutralization with antibodies directed against hepatitis B virus pre-S antigens. *J Virol* **66**: 1241–1245.
- Sureau C, Romet-Lemonne JL, Mullins JI, Essex M. 1986. Production of hepatitis B virus by a differentiated human hepatoma cell line after transfection with cloned circular HBV DNA. *Cell* **47**: 37–47.
- Sureau C, Salisse J. 2013. A conformational heparan sulfate binding site essential to infectivity overlaps with the conserved hepatitis B virus a-determinant. *Hepatology* **57**: 985–994.
- Szmunes W, Stevens CE, Harley EJ, Zang EA, Oleszko WR, William DC, Sadovsky R, Morrison JM, Kellner A. 1980. Hepatitis B vaccine: demonstration of efficacy in a controlled clinical trial in a high-risk population in the United States. *N Engl J Med* **303**: 833–841.
- Tang H, Banks KE, Anderson AL, McLachlan A. 2001. Hepatitis B virus transcription and replication. *Drug News Perspect* **14**: 325–334.
- Tavanez JP, Cunha C, Silva MCA, David E, Monjardino J, Carmo-Fonseca M. 2002. Hepatitis delta virus ribonucleoproteins shuttle between the nucleus and the cytoplasm. *RNA* **8**: 637–646.
- Taylor JM. 2006. Structure and replication of hepatitis delta virus RNA. *Curr Top Microbiol Immunol* **307**: 1–23.
- Taylor JM. 1992. The structure and replication of hepatitis delta virus. *Annu Rev Microbiol* **46**: 253–276.
- Tiollais P, Pourcel C, Dejean A. 1985. The hepatitis B virus. *Nature* **317**: 489–495.
- Torresi J, Earnest-Silveira L, Civitico G, Walters TE, Lewin SR, Fyfe J, Locarnini SA, Manns M, Trautwein C, Bock TC. 2002a. Restoration of replication phenotype of lamivudine-resistant hepatitis B virus mutants by compensatory changes in the “fingers” subdomain of the viral polymerase selected as a consequence of mutations in the overlapping S gene. *Virology* **299**: 88–99.
- Torresi J, Earnest-Silveira L, Deliyannis G, Edgton K, Zhuang H, Locarnini SA, Fyfe J, Sozzi T, Jackson DC. 2002b. Reduced antigenicity of the hepatitis B virus HBsAg protein arising as a consequence of sequence changes in the overlapping polymerase gene that are selected by lamivudine therapy. *Virology* **293**: 305–313.
- Tseng C-H, Cheng T-S, Shu C-Y, Jeng K-S, Lai MMC. 2010. Modification of small hepatitis delta virus antigen by SUMO protein. *J Virol* **84**: 918–927.
- van Regenmortel MHV, Fauquet CM, Bishop DHL, Carstens EN, Estes MK, Lemon SM, Maniloff J, Mayo MA, McGeoch DJ, Pringle CR, Wickner RB, eds. 2000. Virus Taxonomy: The Classification and Nomenclature of Viruses. *The Seventh Annual Report of the International Committee on Taxonomy of Viruses*. San Diego: Academic Press.

- Villet S, Pichoud C, Billioud G, Barraud L, Durantel S, Trépo C, Zoulim F. 2008. Impact of hepatitis B virus rtA181V/T mutants on hepatitis B treatment failure. *J Hepatol* **48**: 747–755.
- Volz T, Allweiss L, M Berek MB, Warlich M, Lohse AW, Pollok JM, Alexandrov A, Urban S, Petersen J, Lütgehetmann M, et al. 2013. The entry inhibitor Myrcludex-B efficiently blocks intrahepatic virus spreading in humanized mice previously infected with hepatitis B virus. *J Hepatol* **58**: 861–867.
- Wakil SM, Kazim SN, Khan LA, Raisuddin S, Parvez MK, Guptan RC, Thakur V, Hasnain SE, Sarin SK. 2002. Prevalence and profile of mutations associated with lamivudine therapy in Indian patients with chronic hepatitis B in the surface and polymerase genes of hepatitis B virus. *J Med Virol* **68**: 311–318.
- Walter E, Keist R, Niederöst B, Pult I, Blum HE. 1996. Hepatitis B virus infection of tupaia hepatocytes in vitro and in vivo. *Hepatol Baltim Md* **24**: 1–5.
- Wang CJ, Chen PJ, Wu JC, Patel D, Chen DS. 1991. Small-form hepatitis B surface antigen is sufficient to help in the assembly of hepatitis delta virus-like particles. *J Virol* **65**: 6630–6636.
- Wang HW, Chen PJ, Lee CZ, Wu HL, Chen DS. 1994. Packaging of hepatitis delta virus RNA via the RNA-binding domain of hepatitis delta antigens: different roles for the small and large delta antigens. *J Virol* **68**: 6363–6371.
- Wang KS, Choo QL, Weiner AJ, Ou JH, Najarian RC, Thayer RM, Mullenbach GT, Denniston KJ, Gerin JL, Houghton M. 1986. Structure, sequence and expression of the hepatitis delta (delta) viral genome. *Nature* **323**: 508–514.
- Wang Y-H, Chang SC, Huang C, Li Y-P, Lee C-H, Chang M-F. 2005. Novel nuclear export signal-interacting protein, NESI, critical for the assembly of hepatitis delta virus. *J Virol* **79**: 8113–8120.
- Warner N, Locarnini S. 2008. The antiviral drug selected hepatitis B virus rtA181T/sW172* mutant has a dominant negative secretion defect and alters the typical profile of viral rebound. *Hepatol Baltim Md* **48**: 88–98.
- Weiner AJ, Choo QL, Wang KS, Govindarajan S, Redeker AG, Gerin JL, Houghton M. 1988. A single antigenomic open reading frame of the hepatitis delta virus encodes the epitope(s) of both hepatitis delta antigen polypeptides p24 delta and p27 delta. *J Virol* **62**: 594–599.
- Will H, Reiser W, Weimer T, Pfaff E, Büscher M, Sprengel R, Cattaneo R, Schaller H. 1987. Replication strategy of human hepatitis B virus. *J Virol* **61**: 904–911.
- Williams V, Brichtler S, Radjef N, Lebon P, Goffard A, Hober D, Fagard R, Kremsdorf D, Dény P, Gordien E. 2009. Hepatitis delta virus proteins repress hepatitis B virus enhancers and activate the alpha/beta interferon-inducible MxA gene. *J Gen Virol* **90**: 2759–2767.
- Wong SK, Lazinski DW. 2002. Replicating hepatitis delta virus RNA is edited in the nucleus by the small form of ADAR1. *Proc Natl Acad Sci U S A* **99**: 15118–15123.
- Wu JC. 2006. Functional and clinical significance of hepatitis D virus genotype II infection. *Curr Top Microbiol Immunol* **307**: 173–186.
- Wu JC, Chen PJ, Kuo MY, Lee SD, Chen DS, Ting LP. 1991. Production of hepatitis delta virus and suppression of helper hepatitis B virus in a human hepatoma cell line. *J Virol* **65**: 1099–1104.
- Wu JC, Chiang TY, Sheen IJ. 1998. Characterization and phylogenetic analysis of a novel hepatitis D virus strain discovered by restriction fragment length polymorphism analysis. *J Gen Virol* **79** (Pt 5): 1105–1113.

- Wu JC, Huang IA, Huang YH, Chen JY, Sheen IJ. 1999. Mixed genotypes infection with hepatitis D virus. *J Med Virol* **57**: 64–67.
- Wu JC, Merlino G, Fausto N. 1994. Establishment and characterization of differentiated, nontransformed hepatocyte cell lines derived from mice transgenic for transforming growth factor alpha. *Proc Natl Acad Sci U S A* **91**: 674–678.
- Xia YP, Yeh CT, Ou JH, Lai MM. 1992. Characterization of nuclear targeting signal of hepatitis delta antigen: nuclear transport as a protein complex. *J Virol* **66**: 914–921.
- Yan H, Zhong G, Xu G, He W, Jing Z, Gao Z, Huang Y, Qi Y, Peng B, Wang H, et al. 2012. Sodium taurocholate cotransporting polypeptide is a functional receptor for human hepatitis B and D virus. *eLife* **1**: e00049.
- Yan RQ, Su JJ, Huang DR, Gan YC, Yang C, Huang GH. 1996. Human hepatitis B virus and hepatocellular carcinoma. I. Experimental infection of tree shrews with hepatitis B virus. *J Cancer Res Clin Oncol* **122**: 283–288.
- Yatsuji H, Noguchi C, Hiraga N, Mori N, Tsuge M, Imamura M, Takahashi S, Iwao E, Fujimoto Y, Ochi H, et al. 2006. Emergence of a novel lamivudine-resistant hepatitis B virus variant with a substitution outside the YMDD motif. *Antimicrob Agents Chemother* **50**: 3867–3874.
- Zoulim F, Locarnini S. 2009. Hepatitis B virus resistance to nucleos(t)ide analogues. *Gastroenterology* **137**: 1593–1608.e1–2.
- Zoulim F, Locarnini S. 2013. Optimal management of chronic hepatitis B patients with treatment failure and antiviral drug resistance. *Liver Int Off J Int Assoc Study Liver* **33 Suppl 1**: 116–124.
2013. WHO | Hepatitis B. WHO. <http://www.who.int/mediacentre/factsheets/fs204/en/index.html> (Accessed November 20, 2013).

7. List of figures

Figure 1: Structure of HBV and subviral particles.....	6
Figure 2: Genome structure of HBV.....	7
Figure 3: Hypothetical membrane topologies of HBsAg.....	10
Figure 4: Schematic overview of viral life cycle.....	12
Figure 5: A) Schematic model of HDV covered with HBsAg (dark green, red, and yellow).....	14
Figure 6: Replication cycle of HDV after the rolling cycle mechanism.....	16
Figure 7: A) Regression model for calculation of IC ₅₀ and IC ₉₀	36
Figure 8: Overview of the generated HBV surface protein variants.....	45
Figure 9: Detected genome equivalents in the supernatant of Huh7 cells transiently transfected with HBV expression plasmids encoding stop mutants within their S-ORF.....	46
Figure 10: Results of the ELISA against all three HBV surface proteins and HBV core.....	47
Figure 11: Immunohistochemical analysis of HBV proteins of wt or MIT transfected Huh7 cells.....	49
Figure 12: Immunohistochemical analysis of HBV proteins of HBV-variants with mutations at position 172 of the SHBs.....	50
Figure 13: Immunohistochemical analysis of HBV proteins of HBV-variants with mutations at position 196 of the SHBs.....	51
Figure 14: Immunohistochemical analysis of HBV proteins of HBV-variants with mutations at position 196 in the SHBs.....	52
Figure 15: CsCl-gradient of serum derived HBV compared to cell culture derived HBV.....	53
Figure 16: CsCl-gradient of mutant with amino acid change in the start codon of LHBs.....	54
Figure 17: CsCl-gradient of mutants with changes at position 172 of the SHBs.....	55
Figure 18: CsCl-gradient of mutants with mutations at position 196 into the SHBs.....	56
Figure 19: Formaldehyde gel of <i>in vitro</i> generated HDV RNA-standard.....	58
Figure 20: Titration of control plasmid (pSVLD3, <i>EcoRI</i> digested) and <i>in vitro</i> generated RNA-standard.....	58
Figure 21: RNA-standard with and without RNase A and DNase I digestion.....	59
Figure 22: CsCl-gradient of a human plasma chronically infected with HDV and HBV. Human plasma (5x10 ⁶ GE/ml HDV) was treated with or without NP40/TCEP (1 h, RT).....	60
Figure 23: Sucrose gradient of a human plasma from a patient chronically infected with HDV/HBV.....	61
Figure 24: Infection of PTHs with patient derived HDV purified by sucrose gradient centrifugation.....	62
Figure 25: Kinetic of HBV and HDV susceptibility of PTHs.....	63
Figure 26: HBV/HDV co- and super-infection of PTHs.....	64
Figure 27: Kinetic of generated recombinant HDV pseudo-particles with several combinations of HBV surface proteins.....	65
Figure 28: Infection of PTHs with recombinant HDV from cell culture.....	66
Figure 29: Infection of PTHs with recombinant HDV pseudo-particles and purified HDV derived from human plasma neutralized with mABs against HBV surface proteins.....	67
Figure 30: Kinetic of HDV-production with stop mutants.....	68
Figure 31: Regression profile of patient isolate KW 6a-6.....	104
Figure 32: Regression profile of patient isolate KW 11a-1.....	104
Figure 33: Regression profile of patient isolate KW 14-8.....	105
Figure 34: Regression profile of patient isolate RK 172-2.....	105
Figure 35: Regression profile of patient isolate RK 172-4.....	106
Figure 36: Analysis of stop mutants transiently transfected in the murine hepatoma cell line AML12.....	106
Figure 37: Analysis of stop mutants transiently transfected in the human hepatoma cell line HepG2.....	107
Figure 38: Immunohistochemical staining of control experiments.....	107
Figure 39: CsCl-gradient of tested mutants with mutations at position 176 and 182 into the SHBs.....	109
Figure 40: CsCl-gradient of tested mutants with mutations at position 199 and 216 into the SHBs.....	110
Figure 41 Purified HDV from sucrose-gradient of a human plasma chronically infected with HDV.....	112

8. List of tables

Table 1 Schematic overview of pipetted nucleos(t)ide analogs with different concentrations.	34
Table 2: Light Cycler program for HOPE-PCR.....	38
Table 3: Light Cycler Program for X-PCR	39
Table 4: Light Cycler Program for HDV-PCR	39
Table 5: Results of the phenotypic resistance test of five patient isolates against four clinical used nucleos(t)ide analogs adefovir (ADV), tenofovir (TDV), entecavir (ETV) and lamivudine (LMV).....	43
Table 6: Summary of expressed and secreted HBV surface proteins variants, subviral particles, uncoated HBV capsids and secreted HDV pseudo-particles enveloped with different HBV surface protein variants.....	75
Table 7: Table of measured density and genome equivalents for serum derived and cell culture derived HBV	108
Table 8: Table of measured density and genome equivalents for mutant M1T.	108
Table 9: Table of measured density and genome equivalents for mutants 172* and 172L.....	108
Table 10: Table of measured density and genome equivalents for mutants 196*, 196S and 196L.....	109
Table 11: Table of measured density and genome equivalents for mutants 176* and 182*.	110
Table 12: Table of measured density and genome equivalents for mutant 199*.	111
Table 13: Table of measured density and genome equivalents for mutants 216TAA and 216TGA.....	111
Table 14: CsCl-gradient of HDV-positive serum derived from a chronically infected patient.....	111
Table 15: Sucrose gradient of a HDV-positive plasma derived from a chronically infected patient.	112

9. Appendix

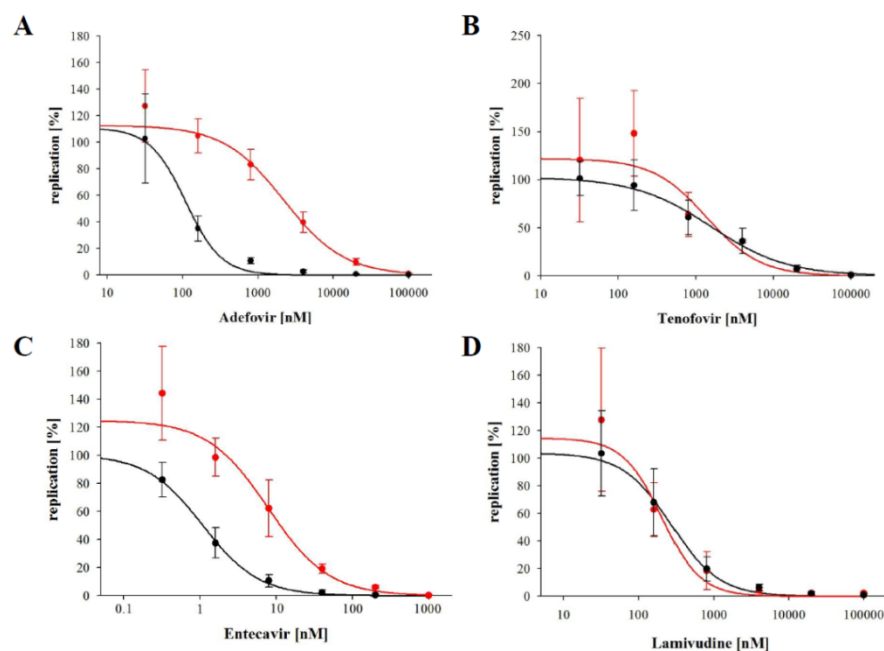


Figure 31: Regression profile of patient isolate KW 6a-6. Patient isolate KW 6a-6 was tested in phenotypic resistance assay against the four common nucleos(t)ide analogs. **Black** line shows consensus curve of the wt. **Red** line shows resistance profile of tested patient isolate KW 6a-6.

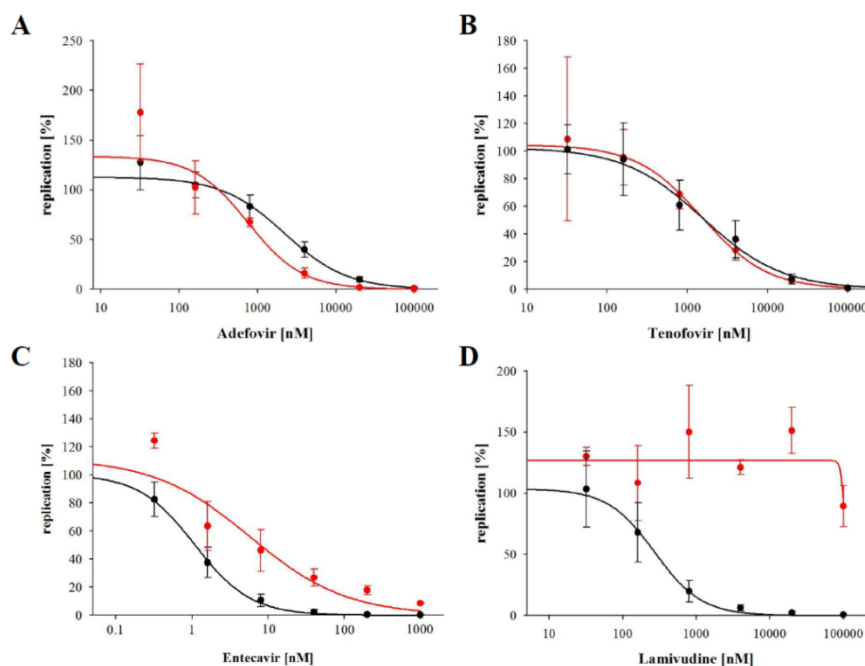


Figure 32: Regression profile of patient isolate KW 11a-1. Patient isolate KW 11a-1 was tested in phenotypic resistance assay against the four common nucleos(t)ide analogs. **Black** line shows consensus curve of the wt. **Red** line shows resistance profile of tested patient isolate KW 11a-1.

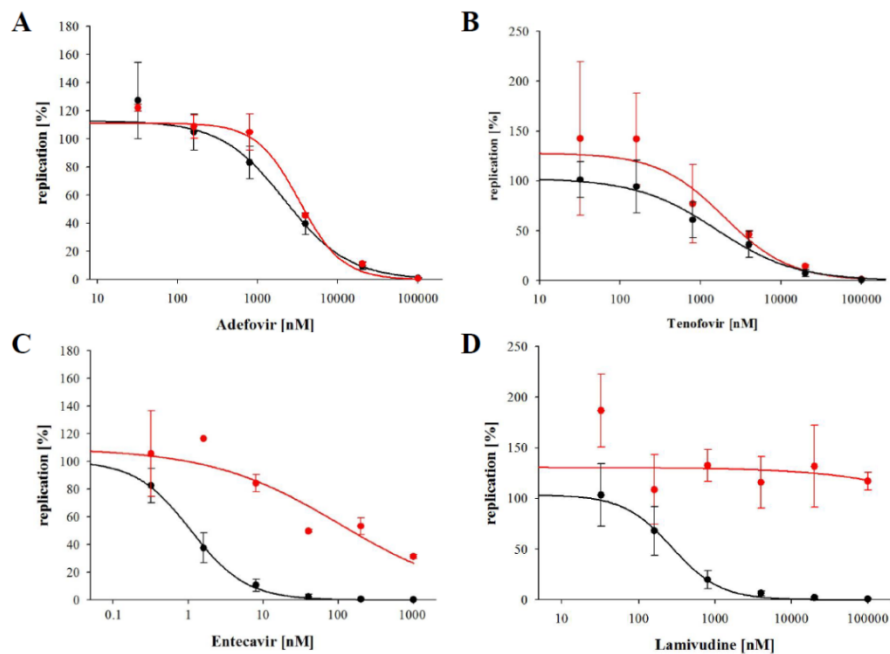


Figure 33: Regression profile of patient isolate KW 14-8. Patient isolate KW 14-8 was tested in phenotypic resistance assay against the four common nucleos(t)ide analogs. **Black** line shows consensus curve of the wt. **Red** line shows resistance profile of tested patient isolate KW 14-8.

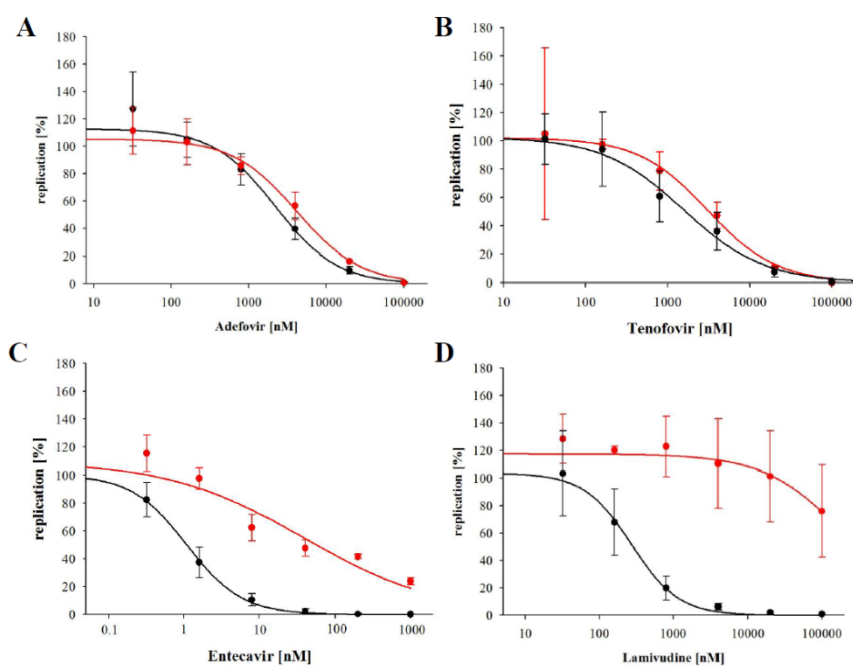


Figure 34: Regression profile of patient isolate RK 172-2. Patient isolate RK 172-2 was tested in phenotypic resistance assay against the four common nucleos(t)ide analogs. **Black** line shows consensus curve of the wt. **Red** line shows resistance profile of tested patient isolate RK 172-2.

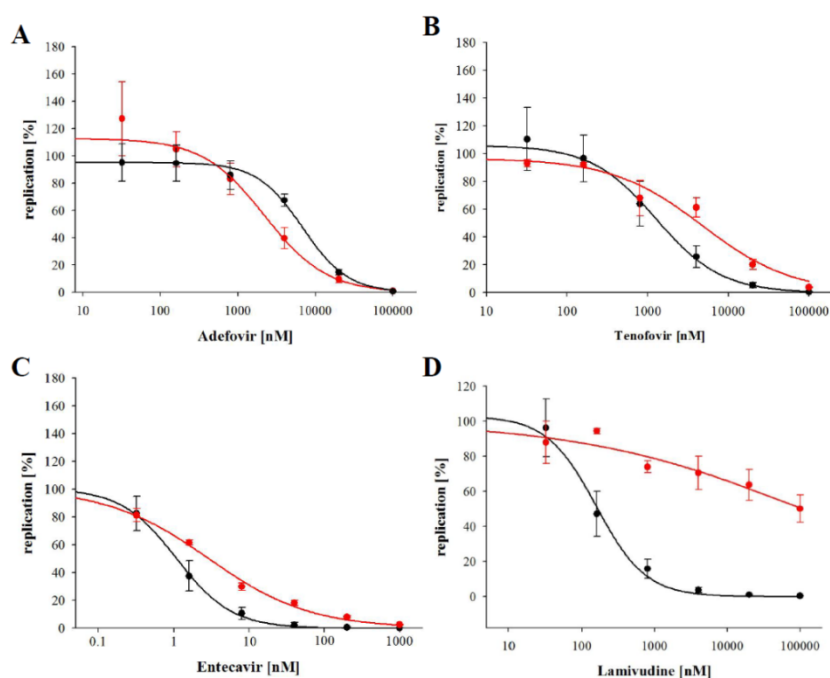


Figure 35: Regression profile of patient isolate RK 172-4. Patient isolate RK 172-4 was tested in phenotypic resistance assay against the four common nucleos(t)ide analogs. **Black** line shows consensus curve of the wt. **Red** line shows resistance profile of tested patient isolate RK 172-4.

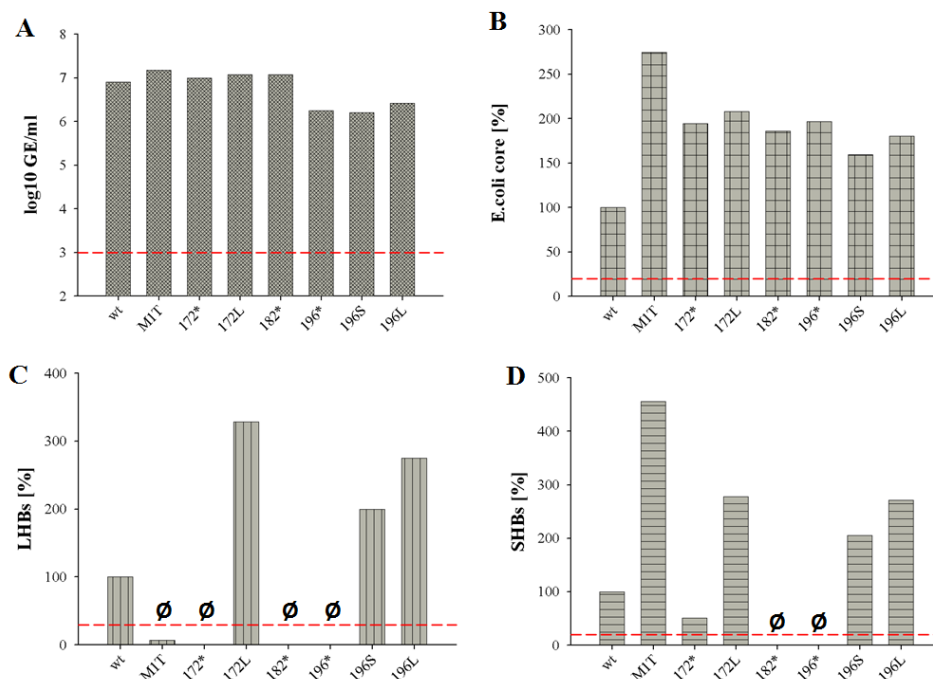


Figure 36: Analysis of stop mutants transiently transfected in the murine hepatoma cell line AML12. Supernatant of AML12 cells transiently transfected with HBV surface protein variants was tested for newly secreted HBsAg and HBV core-particles, three days after transfection. **A)** Detected Genome equivalents in the supernatant of stop mutants. **B)** Results of the ELISA against HBV core using a polyclonal antibody against the core antigen derived from rabbit (DAKO). **C)** Results of the ELISA against LHBs using the monoclonal antibody MA18/7. **D)** Results of the ELISA against SHBs using the monoclonal antibody C20/02. Cut-off for each test is presented with **red** dotted line.

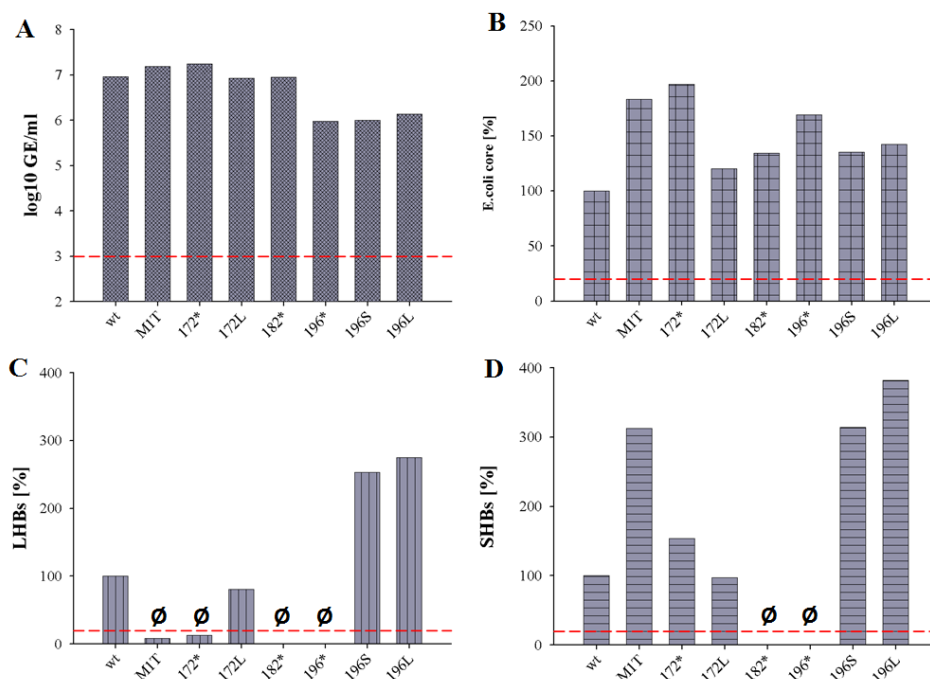


Figure 37: Analysis of stop mutants transiently transfected in the human hepatoma cell line HepG2. Supernatant of HepG2 cells transiently transfected with HBV surface protein variants was tested for newly secreted HBsAg and HBV core-particles, three days after transfection. **A)** Detected genome equivalents in the supernatant of stop mutants. **B)** Results of the ELISA against HBV core using a polyclonal antibody against the core antigen derived from rabbit (DAKO). **C)** Results of the ELISA against LHBs using the monoclonal antibody MA18/7. **D)** Results of the ELISA against SHBs using the monoclonal antibody C20/02. Cut-off for each test is presented with red dotted line.

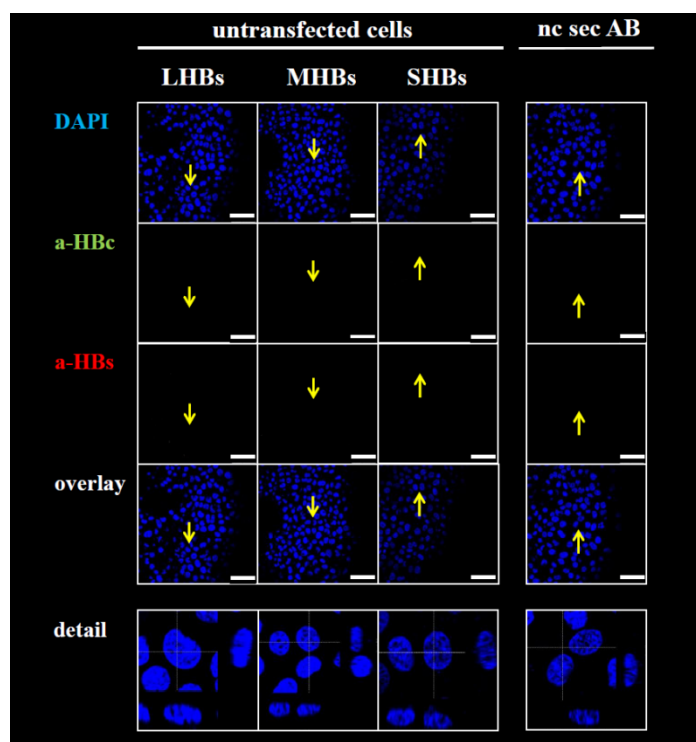


Figure 38: Immunohistochemical staining of control experiments. As control for primary antibodies, untransfected Huh7 cells were treated as transfected cells and stained for HBsAg (LHBs: MA18/7, MHBs: Q19/10, SHBs: C20/02, red panel, Alexa-594) and HBV core (DAKO, green panel, Alexa-488). As control for secondary antibodies, HBV wt transfected cells were stained with only secondary antibodies (right section). Cells marked with the yellow arrow are shown in more detail with a cut view through z-stack-images of single cells. Scale bars: 50 μ m

Table 7: Table of measured density and genome equivalents for serum derived and cell culture derived HBV.

treatment fractions	serum derived HBV				cell culture derived HBV (wt)			
	- NP40/TCEP		+ NP40/TCEP		- NP40/TCEP		+ NP40/TCEP	
	density [g/ml]	GE/ml	density [g/ml]	GE/ml	density [g/ml]	GE/ml	density [g/ml]	GE/ml
1	1.47	1.66x10 ³	1.43	1.55x10 ³	1.46	3.40x10 ⁴	1.45	3.85x10 ⁴
2	1.43	1.24x10 ³	1.43	1.85x10 ³	1.43	8.40x10 ³	1.45	5.05x10 ⁴
3	1.38	1.24x10 ³	1.40	3.58x10 ³	1.39	1.74x10 ⁵	1.40	3.78x10 ⁵
4	1.34	3.35x10 ³	1.36	1.65x10 ⁵	1.35	3.83x10 ⁵	1.35	7.85x10 ⁵
5	1.29	2.03x10 ⁵	1.32	1.23x10 ⁵	1.30	6.88x10 ⁴	1.32	2.55x10 ⁵
6	1.26	4.10x10 ⁵	1.28	2.43x10 ⁴	1.27	2.39x10 ⁶	1.28	1.27x10 ⁵
7	1.21	7.95x10 ⁴	1.25	8.20x10 ³	1.22	2.58x10 ⁶	1.24	6.85x10 ⁴
8	1.18	1.46x10 ⁴	1.20	4.70x10 ³	1.18	3.35x10 ⁵	1.19	4.13x10 ⁴
9	1.15	4.55x10 ³	1.16	5.25x10 ³	1.15	8.70x10 ⁴	1.16	4.53x10 ⁴
10	1.12	4.69x10 ³	1.14	5.55x10 ³	1.12	7.25x10 ⁴	1.13	4.85x10 ⁴
11	1.10	3.75x10 ³	1.12	9.18x10 ³	1.10	1.06x10 ⁵	1.11	1.09x10 ⁵
12	1.10	5.00x10 ³	1.09	7.63x10 ⁴	1.09	2.12x10 ⁵	1.08	2.37x10 ⁶

Table 8: Table of measured density and genome equivalents for mutant MIT.

treatment fractions	MIT			
	- NP40/TCP		+ NP40/TCEP	
	density [g/ml]	GE/ml	density [g/ml]	GE/ml
1	1.46	1.84x10 ⁵	1.42	1.12x10 ⁵
2	1.39	3.53x10 ⁴	1.43	5.80x10 ⁴
3	1.37	1.75x10 ⁶	1.35	1.08x10 ⁶
4	1.33	2.39x10 ⁶	1.31	1.16x10 ⁶
5	1.29	1.12x10 ⁶	1.28	1.33x10 ⁶
6	1.25	6.38x10 ⁵	1.22	4.38x10 ⁵
7	1.20	3.80x10 ⁵	1.19	2.25x10 ⁵
8	1.16	1.91x10 ⁵	1.13	1.31x10 ⁵
9	1.13	9.08x10 ⁴	1.14	1.08x10 ⁵
10	1.11	5.55x10 ⁴	1.11	2.19x10 ⁵
11	1.08	1.08x10 ⁵	1.09	5.38x10 ⁶
12	1.08	5.53x10 ⁴		

Table 9: Table of measured density and genome equivalents for mutants 172* and 172L.

treatment fractions	172*				172L			
	- NP40/TCP		+ NP40/TCEP		- NP40/TCP		+ NP40/TCEP	
	density [g/ml]	GE/ml	density [g/ml]	GE/ml	density [g/ml]	GE/ml	density [g/ml]	GE/ml
1	1.46	1.10x10 ⁵	1.45	6.08x10 ⁴	1.45	4.20x10 ⁵	1.45	2.58x10 ⁶
2	1.45	3.38x10 ⁴	1.45	2.95x10 ⁴	1.45	3.45x10 ⁴	1.45	1.36x10 ⁵
3	1.40	2.75x10 ⁵	1.40	6.78x10 ⁵	1.39	2.88x10 ⁴	1.40	1.75x10 ⁵
4	1.36	1.65x10 ⁶	1.36	3.00x10 ⁶	1.35	7.88x10 ⁴	1.35	2.73x10 ⁵
5	1.32	5.60x10 ⁵	1.31	8.30x10 ⁵	1.32	1.64x10 ⁵	1.33	2.04x10 ⁵
6	1.28	8.45x10 ⁵	1.27	3.45x10 ⁵	1.27	8.05x10 ⁶	1.28	1.85x10 ⁵
7	1.24	5.45x10 ⁶	1.22	1.42x10 ⁵	1.24	5.23x10 ⁶	1.24	8.90x10 ⁴
8	1.19	3.28x10 ⁶	1.18	9.13x10 ⁴	1.19	6.98x10 ⁵	1.19	3.93x10 ⁴
9	1.16	5.73x10 ⁵	1.15	1.12x10 ⁵	1.16	2.63x10 ⁵	1.17	8.78x10 ⁴
10	1.13	2.58x10 ⁵	1.14	1.73x10 ⁵	1.13	1.35x10 ⁵	1.15	1.70x10 ⁵
11	1.11	2.27x10 ⁵	1.11	5.83x10 ⁵	1.11	2.25x10 ⁵	1.13	7.53x10 ⁵
12	1.10	4.98x10 ⁵	1.10	4.70x10 ⁶	1.10	5.09x10 ⁵	1.11	3.18x10 ⁶

Table 10: Table of measured density and genome equivalents for mutants 196*, 196S and 196L.

treatment	196*				196S			
	- NP40/TCP		+ NP40/TCEP		- NP40/TCP		+ NP40/TCEP	
	fractions	density [g/ml]	GE/ml	density [g/ml]	GE/ml	density [g/ml]	GE/ml	
1	1.47	9.65x10 ⁴	1.46	7.93x10 ⁴	1.45	9.50x10 ⁴	1.39	1.17x10 ⁵
2	1.46	3.25x10 ⁴	1.42	2.40x10 ⁴	1.43	2.70x10 ⁴	1.45	5.55x10 ⁴
3	1.41	4.20x10 ⁵	1.41	3.30x10 ⁵	1.40	1.08x10 ⁵	1.41	3.80x10 ⁵
4	1.37	2.13x10 ⁶	1.35	1.47x10 ⁶	1.36	1.39x10 ⁶	1.34	2.35x10 ⁶
5	1.33	9.68x10 ⁵	1.32	6.78x10 ⁵	1.33	6.13x10 ⁵	1.33	2.29x10 ⁶
6	1.30	3.55x10 ⁵	1.27	3.88x10 ⁵	1.27	1.79x10 ⁶	1.29	1.21x10 ⁶
7	1.26	3.05x10 ⁵	1.25	1.50x10 ⁵	1.25	3.80x10 ⁶	1.25	3.33x10 ⁵
8	1.19	1.50x10 ⁵	1.19	6.20x10 ⁴	1.19	6.60x10 ⁵	1.21	1.54x10 ⁵
9	1.16	9.70x10 ⁴	1.16	6.23x10 ⁴	1.16	2.32x10 ⁵	1.19	9.13x10 ⁴
10	1.14	4.93x10 ⁴	1.14	9.73x10 ⁴	1.13	1.11x10 ⁵	1.15	1.11x10 ⁵
11	1.10	3.63x10 ⁴	1.12	6.50x10 ⁵	1.12	1.09x10 ⁵	1.14	1.35x10 ⁵
12	1.10	6.88x10 ⁴	1.10	2.88x10 ⁶	1.10	3.00x10 ⁵	1.10	1.54x10 ⁶

treatment	196L			
	- NP40/TCP		+ NP40/TCEP	
	fractions	density [g/ml]	GE/ml	density [g/ml]
1	1.45	3.88x10 ⁴	1.43	4.48x10 ⁴
2	1.43	1.35x10 ⁴	1.45	1.94x10 ⁴
3	1.37	6.45x10 ⁴	1.38	1.28x10 ⁵
4	1.37	8.15x10 ⁵	1.35	1.07x10 ⁶
5	1.32	3.95x10 ⁵	1.32	1.14x10 ⁶
6	1.28	8.68x10 ⁵	1.27	6.50x10 ⁵
7	1.26	4.73x10 ⁶	1.26	1.88x10 ⁵
8	1.20	1.13x10 ⁶	1.20	1.14x10 ⁵
9	1.17	2.85x10 ⁵	1.18	9.70x10 ⁴
10	1.14	1.40x10 ⁵	1.14	8.08x10 ⁴
11	1.12	8.03x10 ⁴	1.13	3.48x10 ⁵
12	1.10	2.22x10 ⁵	1.13	2.73x10 ⁶

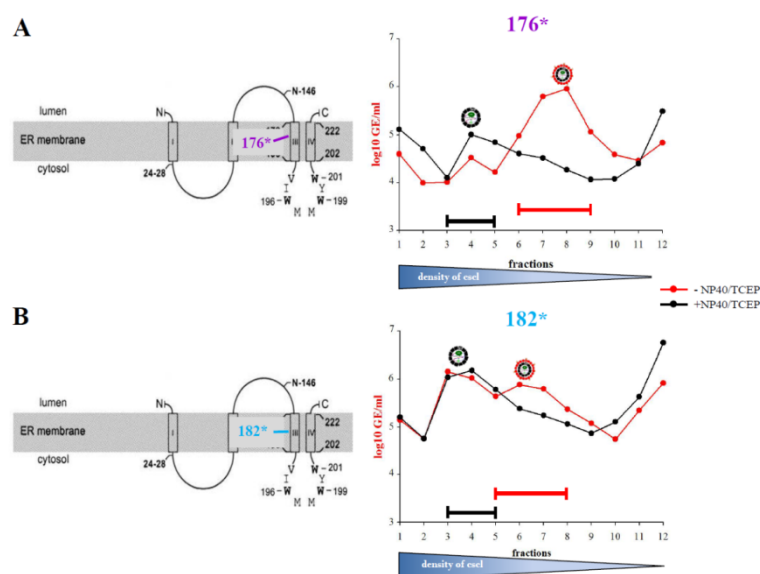


Figure 39: CsCl-gradient of tested mutants with mutations at position 176 and 182 into the SHBs. Supernatant of transiently transfected cells with HBV surface protein variants 176* and 182* were treated with NP40 and TCEP (1h, RT), layered on a linear CsCl-gradient and ultracentrifuged. 1×10^6 GE/ml for both HBV surface protein variants were used. The gradient was fractionated from the bottom to the top. **A**) On the left site presented schematic depiction of localization of stop mutation at position 176 into the SHBs (modified after Komla-Soukha and Sureau 2006). CsCl-gradient for stop mutant 176 is presented on the right site. **B**) On the left site, presented schematic description of localization of stop mutation at position 182 into the SHBs. CsCl-gradient for stop mutant 182 is picketed on the right site. **Red bars** indicate the fractions where enveloped virions are expected. **Black bars** indicate the fractions where uncoated capsids are expected. Representative data of three independent experiments are depicted.

Table 11: Table of measured density and genome equivalents for mutants 176* and 182*.

treatment	176*				182*			
	- NP40/TCEP		+ NP40/TCEP		- NP40/TCEP		+ NP40/TCEP	
	density [g/ml]	GE/ml	density [g/ml]	GE/ml	density [g/ml]	GE/ml	density [g/ml]	GE/ml
1	1.43	3.98×10^4	1.42	1.31×10^5	1.47	1.40×10^5	1.45	1.60×10^5
2	1.43	9.93×10^3	1.45	5.08×10^4	1.42	5.65×10^4	1.43	5.70×10^4
3	1.39	1.02×10^4	1.41	1.26×10^4	1.38	1.44×10^6	1.39	1.10×10^6
4	1.36	3.30×10^4	1.37	1.01×10^5	1.33	1.06×10^6	1.35	1.54×10^6
5	1.32	1.65×10^4	1.33	6.95×10^4	1.30	4.35×10^5	1.31	6.10×10^5
6	1.28	9.55×10^4	1.30	4.05×10^4	1.25	7.73×10^5	1.27	2.43×10^5
7	1.25	6.15×10^5	1.27	3.28×10^4	1.20	6.28×10^5	1.22	1.74×10^5
8	1.20	8.98×10^5	1.22	1.86×10^4	1.16	2.35×10^5	1.18	1.15×10^5
9	1.17	1.16×10^5	1.19	1.16×10^4	1.13	1.19×10^5	1.15	7.35×10^4
10	1.14	3.88×10^4	1.16	1.19×10^4	1.11	5.55×10^4	1.14	1.27×10^5
11	1.12	2.90×10^4	1.10	2.49×10^4	1.09	2.23×10^5	1.11	4.28×10^5
12	1.10	6.88×10^4	1.12	3.05×10^5	1.08	8.33×10^5	1.10	5.70×10^6

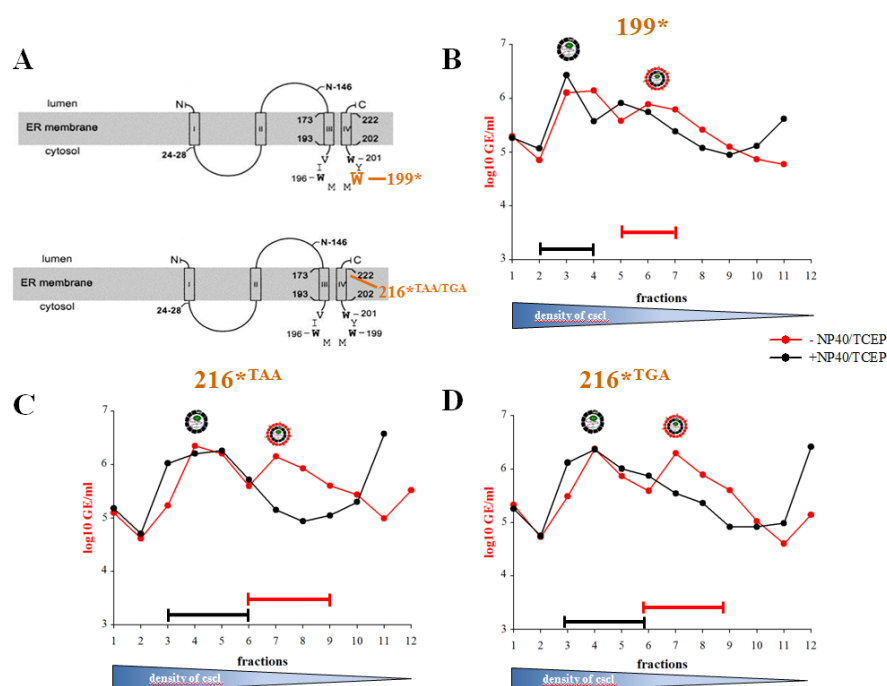


Figure 40: CsCl-gradient of tested mutants with mutations at position 199 and 216 into the SHBs. Supernatant of transiently transfected cells with HBV surface protein variants 199*, 216*^{TAA} and 216*^{TGA} were treated with NP40 and TCEP (1h, RT), layered on a linear CsCl-gradient and ultracentrifuged. 1×10^6 GE/ml for all three HBV surface protein variants were used. The gradient was fractionated from the bottom to the top. **A)** Schematic depiction of localization of stop mutations at positions 199 (upper panel) and 216 (lower panel) (modified after Komla-Soukha and Sureau 2006) **B)** CsCl-gradient of tested mutant 199*. **C)** CsCl-gradient of tested mutant 216TAA. **D)** CsCl-gradient of tested mutant 216TGA. **Red bars** indicate the fractions where enveloped virions are expected. **Black bars** indicate the fractions where uncoated capsids are expected. Representative data of three independent experiments are depicted.

Table 12: Table of measured density and genome equivalents for mutant 199*.

treatment fractions	199*			
	- NP40/TCEP		+ NP40/TCEP	
	density[g/ml]	GE/ml	density[g/ml]	GE/ml
1	1.42	1.95x10 ⁵	1.42	1.84x10 ⁵
2	1.43	7.10x10 ⁴	1.42	1.17x10 ⁵
3	1.39	1.27x10 ⁶	1.38	2.70x10 ⁶
4	1.35	1.39x10 ⁶	1.34	3.73x10 ⁵
5	1.31	3.83x10 ⁵	1.30	8.20x10 ⁵
6	1.26	7.80x10 ⁵	1.26	5.55x10 ⁵
7	1.22	6.15x10 ⁵	1.22	2.44x10 ⁵
8	1.18	2.60x10 ⁵	1.19	1.20x10 ⁵
9	1.15	1.26x10 ⁵	1.16	8.93x10 ⁴
10	1.12	7.35x10 ⁴	1.14	1.31x10 ⁵
11	1.10	5.95x10 ⁴	1.11	4.15x10 ⁵
12	1.09	2.49x10 ⁵	1.10	4.28x10 ⁶

Table 13: Table of measured density and genome equivalents for mutants 216TAA and 216TGA.

treatment fractions	216TAA				216TGA			
	- NP40/TCEP		+ NP40/TCEP		- NP40/TCEP		+ NP40/TCEP	
	density [g/ml]	GE/ml	density [g/ml]	GE/ml	density [g/ml]	GE/ml	density [g/ml]	GE/ml
1	1.40	1.26x10 ⁵	1.42	1.51x10 ⁵	1.42	2.15x10 ⁵	1.38	1.81x10 ⁵
2	1.41	4.18x10 ⁴	1.38	5.10x10 ⁴	1.43	5.35x10 ⁴	1.39	5.60x10 ⁴
3	1.40	1.72x10 ⁵	1.38	1.06x10 ⁶	1.36	3.08x10 ⁵	1.38	1.32x10 ⁶
4	1.36	2.24x10 ⁶	1.32	1.59x10 ⁶	1.36	2.39x10 ⁶	1.33	2.33x10 ⁶
5	1.30	1.60x10 ⁶	1.26	1.82x10 ⁶	1.30	7.33x10 ⁵	1.29	1.02x10 ⁶
6	1.25	3.98x10 ⁵	1.21	5.23x10 ⁵	1.27	3.90x10 ⁵	1.27	7.48x10 ⁵
7	1.22	1.42x10 ⁶	1.17	1.43x10 ⁵	1.21	1.98x10 ⁶	1.21	3.50x10 ⁵
8	1.19	8.50x10 ⁵	1.15	8.68x10 ⁴	1.18	7.83x10 ⁵	1.19	2.31x10 ⁵
9	1.16	4.03x10 ⁵	1.15	1.11x10 ⁵	1.15	4.03x10 ⁵	1.14	8.30x10 ⁴
10	1.15	2.73x10 ⁵	1.11	1.99x10 ⁵	1.13	1.06x10 ⁵	1.12	8.33x10 ⁴
11	1.11	9.78x10 ⁴	1.07	3.75x10 ⁶	1.10	4.03x10 ⁴	1.12	9.70x10 ⁴
12	1.08	3.30x10 ⁵			1.07	1.40x10 ⁵	1.09	2.60x10 ⁶

Table 14: CsCl-gradient of HDV-positive serum derived from a chronically infected patient.

fractions	- NP40/TCEP		+ NP40/TCEP	
	density [g/ml]	GE/ml	density [g/ml]	GE/ml
1	1.45	2.38x10 ⁶	1.42	3.36x10 ³
2	1.45	1.09x10 ⁶	1.42	4.44x10 ³
3	1.39	3.94x10 ⁵	1.39	7.00x10 ³
4	1.35	1.65x10 ⁵	1.35	2.36x10 ³
5	1.32	8.20x10 ⁵	1.32	5.60x10 ³
6	1.30	1.04x10 ⁹	1.29	3.18x10 ³
7	1.29	1.69x10 ⁹	1.28	3.33x10 ³
8	1.27	5.50x10 ⁷	1.25	0
9	1.19	4.83x10 ⁷	1.17	0
10	1.14	1.36x10 ⁷	1.14	0
11	1.11	6.45x10 ⁶	1.12	0
12	1.11	2.77x10 ⁷	1.10	0

Table 15: Sucrose gradient of a HDV-positive plasma derived from a chronically infected patient.

fractions	density sucrose [%]	protein concentration [mg/ml]	GE/ml
1	58.00	0.50	1.92x10 ⁷
2	57.50	0.00	1.12x10 ⁷
3	55.50	0.20	8.65x10 ⁶
4	52.00	0.30	1.12x10 ⁷
5	49.00	0.20	1.10x10 ⁸
6	46.50	0.20	9.13x10 ⁸
7	44.50	0.90	8.65x10 ⁹
8	42.00	2.10	9.23x10 ⁹
9	39.50	4.10	1.49x10 ⁹
10	37.50	6.10	1.38x10 ⁸
11	35.00	8.70	1.17x10 ⁸
12	33.00	10.10	3.08x10 ⁷
13	31.00	12.30	7.13x10 ⁶
14	29.00	15.10	4.73x10 ⁶
15	27.25	18.00	3.13x10 ⁶
16	25.50	18.00	1.60x10 ⁶
17	23.50	18.70	9.73x10 ⁵
18	21.50	18.90	1.47x10 ⁶
19	20.00	18.90	1.78x10 ⁶
20	18.50	0.00	1.30x10 ⁶
21	17.00	23.10	7.40x10 ⁵
22	15.00	23.10	7.30x10 ⁵
23	12.50	14.10	8.95x10 ⁵
24	10.00	6.30	6.35x10 ⁵
25	8.00	3.20	1.37x10 ⁶
26	6.50	1.10	1.36x10 ⁶
27	6.00	0.30	1.01x10 ⁶
28	5.00	0.20	7.20x10 ⁵
29	4.50	0.00	3.58x10 ⁵
30	4.50	0.10	3.58x10 ⁵
31	4.00	0.70	5.33x10 ⁶

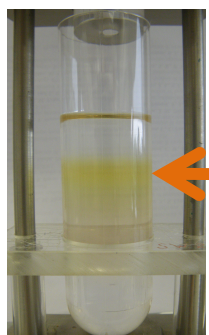


Figure 41 Purified HDV from sucrose-gradient of a human plasma chronically infected with HDV. Orange arrow showed accumulation of plasma proteins.

10. Publications

A. König; B. Döring; **C. Mohr**; J. Geyer; D. Glebe. "Hepatitis B virus and bile acids compete for binding to the Na⁺/taurocholate cotransporting polypeptide (NTCP) to enter hepatocytes. " (in revision).

11. Danksagung

An dieser Stelle möchte ich mich bei allen bedanken, die mich während meines Studium und der Promotion begleitet und unterstützt und zum Gelingen dieser Arbeit beigetragen haben:

Besonderen Dank gilt an dieser Stelle auch **HDoz. Dr. Dieter Glebe**, der mir nicht die Möglichkeit gegeben hat meine Dissertation am Institut für Medizinische Virologie in Gießen schreiben zu dürfen, sondern auch für meine spannenden Themen und das Vertrauen, für die kompetente und gute Betreuung während meiner Dissertation und die Begutachtung meiner Arbeit.

Ein großer Dank gilt auch **Prof. Dr. M. Martin**, nicht nur für die Begutachtung meiner Dissertation und der Vertretung vor dem Fachbereich 08 Biologie und Chemie, sondern auch für die jahrelange Betreuung im Bachelor- und Masterstudium mit viel Kompetenz und Engagement. Vielen herzlichen Dank!

Des Weiteren danke ich ganz herzlich **Prof. Dr. Dr. h.c. W. H. Gerlich**, für viele informative Gespräche und Diskussionen und natürlich für die Bereitschaft als Prüfer an meiner Disputation teil zu nehmen.

Ein weiter Dank gilt **Prof. Dr. Ulrike Protzer** vom Institut für Virologie, München, die die ersten beiden Jahre meiner Promotion finanziert hat, wodurch ich die Möglichkeit hatte am spannenden HOPE-Projekt mitwirken zu dürfen.

Auch **Prof. Dr. A. Bindereif** möchte ich danken, für die Bereitschaft als Prüfer an meiner Disputation teil zu nehmen.

Ein weiterer großer Dank gilt der Arbeitsgruppe: **Corinna Bremer, Andi** (ganz wichtig mit i) **Geipel, Alex König, Siggie Broehl, Franzi Rinker, Tine Müller, Pia Seiz** und **Hauke Niekamp**. Vielen Dank euch allen für ein sehr familiäres Arbeitsklima, für viele Diskussionen, für viel Spaß bei der Arbeit, für viele wichtige und unwichtige Ratschläge und Tipps, die immer sehr lehrreichen und lustigen Mittagspausen und für tolle Freundschaften. Es hat sehr viel Spaß gemacht mit euch zu Arbeiten!

Außerdem möchte ich an dieser Stelle ganz besonders meinem Freund **Philipp** danken, für den Rückhalt, die Motivation, viel Durchhaltevermögen in Bezug auf meine Launen und einfach dafür, dass du da warst und bist, wenn mal wieder alles schief lief und läuft. Danke!

Ein weiterer besonders großer Dank gilt an dieser Stelle **meiner Familie**, die immer für mich da sind, mich tatkräftig unterstützen und immer an mich geglaubt haben. Danke für euer Vertrauen in mich, dass ich alles schaffen kann, wenn ich nur will. Danke!

12. Erklärung

Ich erkläre, dass ich die vorgelegte Dissertation selbständig, ohne unerlaubte fremde Hilfe und nur mit den Hilfen angefertigt habe, die ich in der Dissertation angegeben habe. Alle Textstellen, die wörtlich oder sinngemäß aus veröffentlichten Schriften entnommen sind, und alle Angaben, die auf mündlichen Auskünften beruhen, sind als solche kenntlich gemacht. Bei den von mir durchgeführten und in der Dissertation erwähnten Untersuchungen habe ich die Grundsätze guter wissenschaftlicher Praxis, wie sie in der „Satzung der Justus-Liebig-Universität Gießen zur Sicherung guter wissenschaftlicher Praxis“ niedergelegt sind, eingehalten.

Christina Mohr